Theoretical Computer Science 407 (2008) 29–84

Contents lists available at ScienceDirect

Theoretical Computer Science

journal homepage: www.elsevier.com/locate/tcs

The domino problem of the hyperbolic plane is undecidable

Maurice Margenstern *

Laboratoire d'Informatique Théorique et Appliquée, EA 3097, Université de Metz, I.U.T. de Metz, Département d'Informatique, Île du Saulcy, 57045 Metz Cedex, France

ARTICLE INFO

Article history:
Received 26 July 2007
Received in revised form 14 April 2008
Accepted 17 April 2008
Communicated by F. Cucker

Keywords:
Tilings
Hyperbolic geometry
Undecidability

ABSTRACT

In this paper, we prove that the general tiling problem of the hyperbolic plane is undecidable by proving a slightly stronger version using only a regular polygon as the basic shape of the tiles. The problem was raised by a paper of Raphael Robinson in 1971, in his famous simplified proof that the general tiling problem is undecidable for the Euclidean plane, initially proved by Robert Berger in 1966.

1. Introduction

Whether it is possible to tile the plane with copies of a fixed set of tiles was a question raised by Hao Wang, [32] in the late 50s of the previous century. Wang solved the *origin-constrained* problem, which consists in fixing an initial tile in the above finite set of tiles. Indeed, fixing one tile is enough to entail the undecidability of the problem. Also called the **general tiling problem** further in this paper, the general case, free of any condition, in particular with no fixed initial tile, was proved undecidable by Robert Berger in 1966, [1]. Both Wang's and Berger's proofs deal with the problem in the Euclidean plane. In 1971, Raphael Robinson found an alternative, simpler proof of the undecidability of the general problem in the Euclidean plane, see [29]. In this 1971 paper, he raised the question of the general problem for the hyperbolic plane. Seven years later, in 1978, he proved that in the hyperbolic plane, the origin-constrained problem is undecidable, see [30]. Since then, the problem had remained open.

In 2006, a step forward was made with a technical report, see [17], whose new version was recently published, see [26]. This step consists in generalizing the origin-constrained problem. Later, in 2007, I deposited several improvements of a first version of the proof that the domino problem of the hyperbolic plane is undecidable on *arXiv*, see[16,21] and also on my web-page [18]. In [22], I give a synthetic presentation of the techniques contained in these different technical papers, whose very close version can be seen in [25]. Here, I provide the complementary material to fully understand [22]. In particular, full proofs with auxiliary lemmas, tables and more illustrations are given in order to make the proof as complete as possible.

In this introduction, we remind the reader the general strategy to attack the tiling problem, as already established in the famous proofs dealing with the Euclidean case. We also indicate the basic properties we need about hyperbolic geometry and of the tiling {7, 3}, whose frame our solution of the problem lies in. The reader familiar with hyperbolic geometry can skip this part of the paper. We also refer the reader to [24] and to [13] for a more detailed introduction and for other bibliographical references. Also, in order that the paper be self-contained, we sketch the notion of space–time diagram of a Turing machine.

In the second section, we establish the properties of the particular tiling which we consider within the tiling {7, 3}, the **mantilla**. There, we recall the properties already established in [17,15] and we append the new properties established in [18,16].

* Tel.: +33 3 87 31 55 44; fax: +33 3 87 54 73 04.
E-mail address: margens@univ-metz.fr.

0304-3975/$ – see front matter © 2008 Elsevier B.V. All rights reserved.
doi:10.1016/j.tcs.2008.04.038

In the third section, we present a needed interlude, a parenthesis on brackets, which is a basic ingredient of the proof. In the fourth section, we lift up this line construction to a planar Euclidean one. In the fifth section, we show how to implement the Euclidean construction in the hyperbolic plane, using the specific properties indicated in the second section. In the sixth section, we complete the proof of the main result:

Theorem 1.1. *The domino problem of the hyperbolic plane is undecidable.*

From Theorem 1.1, we immediately conclude that the general tiling problem is undecidable in the hyperbolic plane.

Still in the sixth section, we give a detailed description and a counting of the tiles.

In the seventh section, we give several corollaries of the construction and we conclude in two directions. The first one wonders whether it is possible to simplify the construction. The second direction tries to see what might be learned from the construction leading to Theorem 1.1.

Before turning to Section 1.1, let us remark that an alternative proof of the general tiling problem is claimed by Jarkko Kari, see [8,9]. His proof is completely different from this one. It is completely combinatoric and it makes use of a non-effective argument. It is not the place, here, to discuss this latter point.

1.1. The general strategy

In the proofs of the general tiling problem in the Euclidean plane by Berger and by Robinson, there is an assumption which is implicit and which was, most probably, considered as obvious at that time.

Consider a finite set S of **prototiles**. We call **solution** of the tiling of the plane by S a partition $\mathcal{P}$ such that the closure of any element of $\mathcal{P}$ is a copy of an element of S. We notice that this definition contains the traditional condition on matching signs in the case when the elements of S possess signs. We also notice that a copy means an isometrical image. In this problem, we assume that only even products of reflections in a line are considered. In the Euclidean case, rotations are also ruled out. Here this cannot be the case as the shifts leaving the tiling globally invariant also generate the rotations which leave the tiling globally invariant.

Note that the general tiling problem can be formalized as follows:

$$\forall S \ \ (\exists\, \mathcal{P}\ sol(\mathcal{P}, S) \vee \neg(\exists\, \mathcal{P}\ sol(\mathcal{P}, S))),$$

where $sol(\mathcal{P}, S)$ means that $\mathcal{P}$ is a solution of S and where $\vee$ is interpreted in a constructive way: there is an algorithm which, applied to S provides us with 'yes' if there is a solution and 'no' if there is none.

The origin-constrained problem can be formalized in a similar way by:

$$\forall(S, a) \ \ (\exists\, \mathcal{P}\ sol(\mathcal{P}, S, a) \vee \neg(\exists\, \mathcal{P}\ sol(\mathcal{P}, S, a))),$$

where $a \in S$, with the same algorithmic interpretation of $\vee$ and where the formula $sol(\mathcal{P}, S, a)$ means that $\mathcal{P}$ is a solution of S which starts with a.

Now, note that if we have a solution of the general tiling problem for the considered instance, we also have a solution of the origin-constrained problem, with the facility that we may choose the first tile. However, to prove that the general tiling problem, in the considered instance, has no solution, we have to prove that, whatever the initial tile, the corresponding origin-constrained problem has no solution either.

However, in Berger's and Robinson's proofs the construction starts with a special tile, called the **origin**. There is no contradiction with what we have just said, because they force the tiling to have a dense subset of origins. In the construction, the origins start the simulation of the space–time diagram of the computation of a Turing machine M. All origins compute the same machine M which can be assumed to start from an empty tape. The origins define infinitely many domains of computation of infinitely many sizes. If the machine does not halt, starting from an origin, it is possible to tile the plane. If the machine halts, whatever the initial tile, we find an origin nearby and, from this one, we shall eventually fall into a domain which contains the halting of the machine: at this point, it is easy to prevent the tiling from going on.

The present construction aims at the same goal.

1.2. The tiling {7, 3}

In this sub-section, we very sketchily remember the minimal data about hyperbolic geometry and about the tiling which constitutes the general frame of our construction.

The hyperbolic plane

Hyperbolic geometry appeared in the first half of the 19th century, as the conclusion of the very long quest to prove the famous axiom of parallels of Euclid's *Elements* from the other axioms. As presently known, the axiom on parallels is independent from the others. The discovery of hyperbolic geometry also raised the notion of independence in an axiomatic theory. In the second half of the 19th century, several models were devised in which the axioms of hyperbolic geometry are satisfied. Among these models, Poincaré's models became very popular. One model makes use of the half-plane in the Euclidean plane, the other makes use of a disc, also in the Euclidean plane. Each time we shall need to refer to a model, especially for illustrations, we shall use Poincaré's disc model, if not otherwise specified.

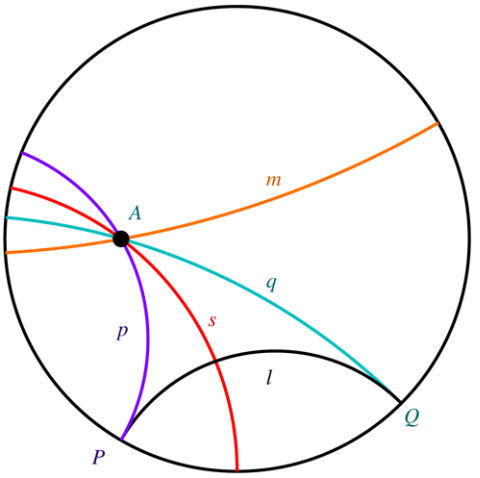

Fig. 1. An illustration of Poincaré's model.

Let us fix an open disc U of the Euclidean plane. Its points constitute the points of the hyperbolic plane $\mathbb{H}^2$. The border of U, ∂U, is called the set of **points at infinity**. Lines are the trace in U of its diameters or the trace in U of circles which are orthogonal to ∂U. The model has a very remarkable property, which it shares with the half-plane model: hyperbolic angles between lines are the Euclidean angles between the corresponding circles. The model is easily generalized to higher dimension, see [24] for definitions and properties of such generalizations as well as references for further reading.

In Fig. 1, the lines p and q pass through the point A and they are parallel to the line ℓ. We notice that each of them has a common point at infinity with ℓ: P in the case of p and Q in the case of q. The line s which also passes through A cuts the line ℓ: it is a **secant** to this line. However, the line m, which also passes through A meets ℓ, neither in U, nor at infinity, *i.e.* on ∂U. Such a line is called **non-secant** with ℓ. Non-secant lines have a nice characteristic property: two lines are non-secant if and only if they have a common perpendicular which is unique.

A tiling of the hyperbolic plane: the ternary heptagrid

Regular tessellations are a particular case of tilings. They are generated from a regular polygon by reflection in its sides and, recursively, of the images in their sides. In the Euclidean case, there are, up to isomorphism and up to similarities, three tessellations, respectively based on the square, the equilateral triangle and on the regular hexagon. Later on we say **tessellation**, for short.

In the hyperbolic plane, there are infinitely many tessellations. They are based on the regular polygons with p sides and with $\frac{2\pi}{q}$ as vertex angle and they are denoted by $\{p, q\}$. This is a consequence of a famous theorem by Poincaré which characterizes the triangles starting from which a tiling can be generated by the recursive reflection process which we already mentioned. Any triangle tiles the hyperbolic plane if its vertex angles are of the forms $\frac{\pi}{p}$, $\frac{\pi}{q}$ and $\frac{\pi}{r}$ with the condition that $\frac{1}{p} + \frac{1}{q} + \frac{1}{r} < 1$.

Among these tilings, we choose the tiling $\{7, 3\}$ which we called the **ternary heptagrid** in [2]. It is illustrated below by Fig. 2.

In [2,24], many properties of the ternary heptagrid are described. An important tool to establish them is the splitting method, prefigured in [12] and for which we refer to [24]. Here, we just suggest the use of this method which allows us to exhibit a tree, spanning the tiling: the **Fibonacci tree**. Below, the left-hand side of Fig. 3 illustrates the splitting of $\mathbb{H}^2$ into a central tile T and seven sectors dispatched around T. Each sector is spanned by a Fibonacci tree. The right-hand side of Fig. 3 illustrates how the sector can be split into sub-regions. Now, we notice that two of these regions are copies of the same sector and that the third region S can be split into a tile and then a copy of a sector and a copy of S. Such a process gives rise to a tree whose nodes are in bijection with the tiles of the sector. The tree structure will be used in the sequence and other illustrations will allow the reader to understand better the process.

Another important tool to study the tiling $\{7, 3\}$ is given by the **mid-point** lines, which are illustrated by Fig. 4. The lines have this name because they join the mid-points of contiguous edges of tiles. We can see in the figure how such lines allow to delimit a sector, a property which is proved in [2,24].

The space–time diagram of a Turing machine

As our proof of Theorem 1.1 makes use of the simulation of a Turing machine, we sketchily remind a few features of the Turing machines, see [31,7]. We shall specifically remind the use of space–time diagrams.

A Turing machine is a device which consists of an infinite **tape** and of a **head**. The tape is constituted of adjacent **squares**, each one containing a symbol belonging to a finite alphabet A. The head looks at a square, the **scanned square** and it is in a given **state**. Depending on its state and on the symbol read in the scanned square, the machine performs an action specified

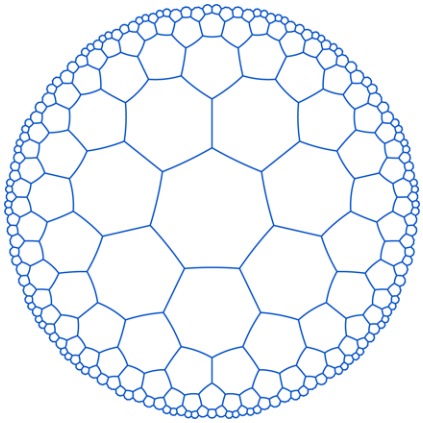

Fig. 2. The tiling {7, 3} of the hyperbolic plane in Poincaré's disc model.

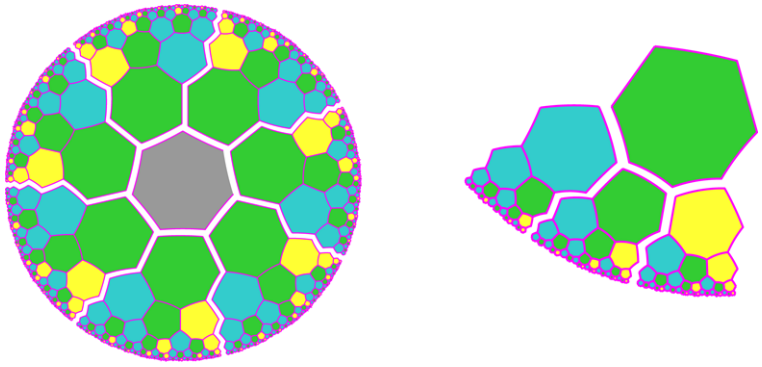

Fig. 3. Left-hand side: the standard Fibonacci trees which span the tiling {7, 3} of the hyperbolic plane. Right-hand side: the splitting of a sector, spanned by a Fibonacci tree.

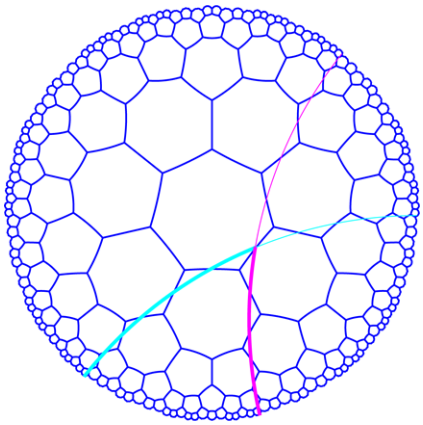

Fig. 4. The mid-point lines.

by an **instruction**: replace the read letter by a new letter, possibly the same one, turn to a new state, possibly the same one, and go to the next scanned square which is either the right-hand side neighbour of the scanned square, or its left-hand side neighbour or again, the same scanned square. There are finitely many instructions whose set constitutes the **program** of the machine. One symbol of A plays a special role. It is called the **blank** and a square containing the blank is called **empty**.

The configuration of a Turing machine is defined by two squares: the leftmost and the rightmost ones, called the **borders** of the configuration. For the initial configuration, these borders define the smallest finite interval of the tape which contains both the square scanned by the head of the machine and all the non-empty squares. It is assumed that at the initial time, there are finitely non-empty squares in the tape. When the borders of the current configuration are defined, the borders of the next configuration are either the same or one of them is moved by one square further: this is the case when the head scans a border and when its action moves outside the current configuration.

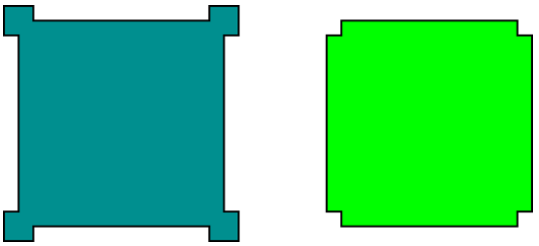

Fig. 5. Robinson's basic tiles for the undecidability of the tiling problem in the Euclidean case.

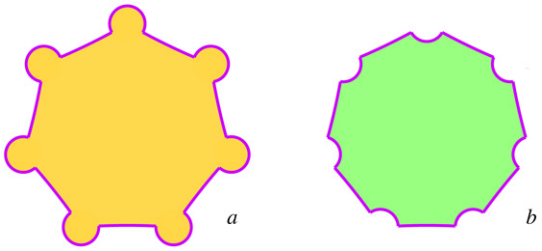

Fig. 6. A 'literal' translation of Robinson's basic tiles to the situation of the ternary heptagrid.

Now, a **space–time diagram** of the execution of a Turing machine M consists in placing successive configurations of the computation of M on the Euclidean plane. The initial configuration C_0 is put along the x-axis with the origin at a fixed position of the tape: it corresponds to the abscissa 0. The configuration i which is obtained after i steps of computation is placed on the parallel to the x-axis which has the abscissa i.

As can immediately be seen, the important feature is not that we have strictly parallel lines, and that squares are aligned along lines which are perpendicular to the tapes. What is important is that we have a **grid**, which may be a more or less distorted image of the just described representation.

2. The mantilla

In this section, we remind the construction of the tiling which will be the frame in which our proof of the main theorem takes place. We start with the motivation of this special tiling which we call the **mantilla**.

2.1. The flowers

In this setting, we define a **ball** to be the set of tiles which are within a fixed distance from a fixed tile which we call its **centre**, where the **distance** of a tile to this centre is the number of tiles constituting the shortest path between the tile and the centre excepted. The distance which defines the ball is called its **radius**. In what follows, we denote a ball of radius n by B_n. But as we shall be very often concerned by balls of radius 1 only, we give them a special name, **flowers**.

In [24], we proved that flowers tile the hyperbolic plane.

But here, we shall use another object in which we partially **merge** flowers. This will give rise to another way of tiling the ternary heptagrid which will be at the basis of our construction.

The idea of merging the flowers comes from the following consideration. Robinson's proof of the undecidability of tiling the Euclidean plane is based upon a simple tiling consisting of two tiles represented by Fig. 5.

In the Euclidean case, this fixes the tiling immediately and we refer the reader to Robinson's paper [29] to see the very nice consequences deduced from these simple tiles.

If we try to apply the same idea to the ternary heptagrid, we get the tiles of Fig. 6.

It is not very difficult to see that these cannot tile. Indeed, the tile a requires seven copies of b around it and once we put three tiles a around a tile b, we cannot continue.

However, it is not very difficult to change a bit the tile b to make things work much better, perfectly well as will be seen later. Consider the new couple of tiles given by Fig. 7.

This time we can see that we always must put seven copies of tile c around a tile a and that we need three copies of a around a tile c. Also, we can see that three tiles c may abut around their untouched vertex.

We shall later derive a set of tiles to construct tilings of the hyperbolic plane based only on the tiles a and c of Fig. 7. We shall say that such a tiling is a **realization** of the **mantilla**. However, by contrast with the Euclidean case, here we have infinitely many such tilings, even uncountably many of them.

The seven copies of c around a tile a give immediately the idea of a flower. Also, we shall modify the representation in order to obtain strict *à la Wang* tiles. Moreover, the tiles will abut simply, only requiring that abutting edges have the same colour.

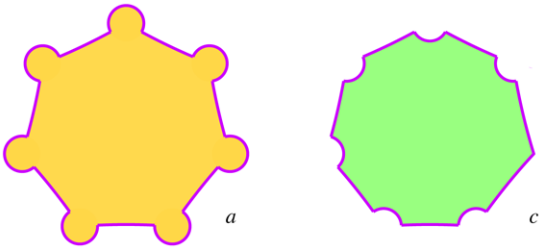

Fig. 7. An adaptation of Robinson's basic tiles to the ternary heptagrid.

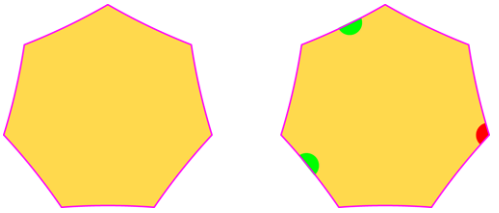

Fig. 8. The basic two kinds of tiles, translation of tiles *a* and *c* into dominoes. (For interpretation of the references to colour in this figure legend, the reader is referred to the web version of this article.)

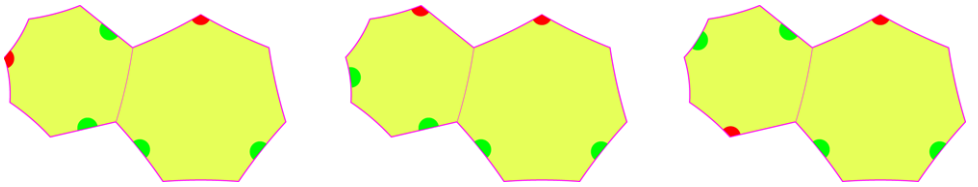

Fig. 9. The three ways of making petals abut along blank edges: in all cases, it is impossible to continue the tiling. (For interpretation of the references to colour in this figure legend, the reader is referred to the web version of this article.)

Using the notion of flower, we introduce two kind of tiles: blank ones which, later on will be called **centres**, and the others will be called the **petals**. The tiles are represented by Fig. 8. As can be more or less guessed, centres correspond to the tile *a* of Fig. 7 and petals correspond to the tile *c* of the same figure. Green and red marks indicate the edges where a petal abuts on another one, the other sides being shared with a centre.

The basic figure of the mantilla is the flower. Later, we will re-define the tiling in such a way that a condition will be put on the tiles: a centre can be surrounded by petals only; it cannot abut with another centre. A consequence of this constraint is that any petal belongs to three flowers and so, we can view petals and centres as meshes and holes of a vast crochet, whence the name *mantilla*.

It will appear that there can be infinitely many mantillas if any. Indeed, we shall find an *algorithmic way* to combine petals and centres in order to get a tiling. We shall do this a bit later.

Lemma 2.1. *A petal can abut at a blank edge only with a centre. Two petals can abut either by their red vertex and an edge of this vertex or by an edge with a green mark.*

Proof of Lemma 2.1. If we consider a petal, it cannot abut on itself or another petal by the blank edges. To check this point, we fix one petal and an edge and we make the other petal rotate three times in order to present all its blank edges to the chosen blank edge of the fixed petal. As can be seen on Fig. 9, in two cases, this would require a tile where two adjacent edges bear a green mark, which is impossible. In the remaining case, this would require a tile with an edge marked by a green side and an adjacent edge with a red vertex at the non-common vertex. This is also impossible. The conclusion of the lemma follows. ■

The possibilities to abut a petal on another one are indicated by Fig. 10.

Assuming that solutions exist, let us investigate as to what they look like. Considering a centre, it is not difficult to see that it is surrounded by centres, not immediately but at a small distance. Indeed, the first row of surrounding tiles are petals but in the second row, centres necessarily appear. Note in Fig. 11 that the red vertex of three petals must be glued together. This will define the **red vertices** of the configurations we shall study. Also, two green dots are connected by the sides of two neighbouring petals. Accordingly, we say that the corresponding side is **green**. Now, we note that red vertices are always at the end of a side where the other belongs to the border of a centre. We shall say that the considered red vertex is **at distance 1** from this centre. Note that any red vertex is always at distance 1 of exactly three distinct centres.

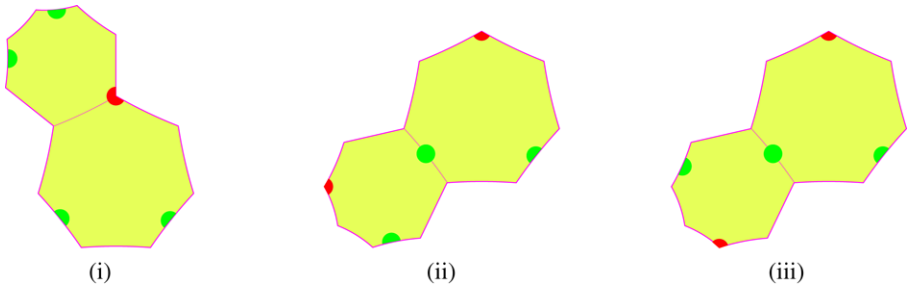

Fig. 10. Three ways to make correctly two petals abut. The two other ways are obtained as follows. First, take the reflection of (ii) in the vertical axis of the big heptagon. This gives the fourth way. The fifth way is obtained from (iii), using the same reflection.

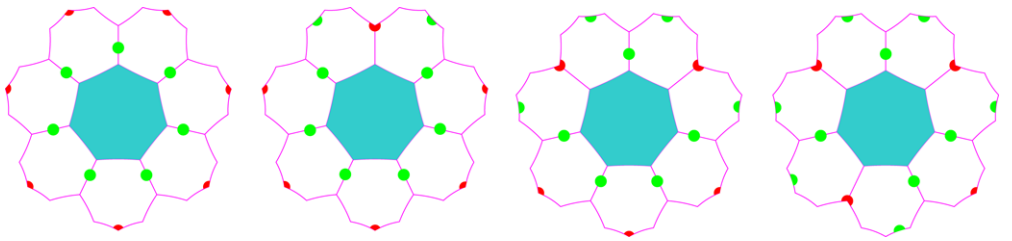

Fig. 11. Flowers with, respectively, 7, 8, 9 and 10 centres in their centre rings. (For interpretation of the references to colour in this figure legend, the reader is referred to the web version of this article.)

From Figs. 10 and 11, we can see that the number of centres of the second row ranges in the interval $\{7..10\}$. Call **centre ring** the set of centres in the second row of tiles around a given centre. The centre defining the centre ring is again called the **centre** of the centre ring or simply centre if no confusion may arise. Then, it can be noted that the number of elements in the centre ring is directly connected with the number of red vertices which are at distance 1 from the centre of the centre ring. The correspondence is given by the following formula:

$$\#centres = \#red\_vertices + 7.$$

This comes from the fact that a green side connects directly two centres, and that a red vertex is at distance 1 of three centres and for each of these three centres, both remaining centres belong to its centre ring. Accordingly, a red vertex generates 2 centres of the centre ring while a green side exactly generates one of them. Now,

$$\#red\_vertices + \#green\_sides = 7$$

and so,

$$\#centres = 2\#red\_vertices + \#green\_sides = \#red\_vertices + 7.$$

Next, it is not very difficult to see that there cannot be tilings where all centres have a centre ring of 7 elements, or of 8 elements or of 10 elements respectively. Indeed, if a centre is surrounded by seven green sides, then any element of its centre ring has at least two red vertices at distance 1 and so, the corresponding centre has a centre ring with at least 9 elements. The same remark applies also to a centre whose centre ring contains 8 elements. And so, there cannot be tilings of this kind where centres are all centres of a centre ring with 8 elements.

It remains to see that all centres cannot have a centre ring with 10 elements. Indeed, consider a centre with a centre ring of 10 elements. As a red vertex at distance 1 from a centre defines two green sides in contact with the centre, the 3 red vertices of such a flower are separated either by a single green side touching the centre of the flower, or by two such green sides. Now, consider two red vertices of a centre surrounded by 10 centres which are separated by a single green vertex. This green vertex connects the centre of the considered centre ring with another centre C. Now, from what we said, C has 3 consecutive green sides around itself and so, it cannot be the centre of a centre ring of 10 elements.

Professor Chaim Goodman-Strauss told me that the situation when all centres are surrounded by a centre ring of 9 elements is possible. He mentioned that this can be performed algorithmically, but in a more complicated way than in Section 2.2.

2.2. The mantilla

On the other side, we have the following:

Lemma 2.2. *There is a tiling of* $\{7, 3\}$ *with the petals and centres such that all flowers of the tiling have a centre ring of* 9 *elements or of* 8 *elements. Moreover, it is possible to algorithmically construct such a tiling.*

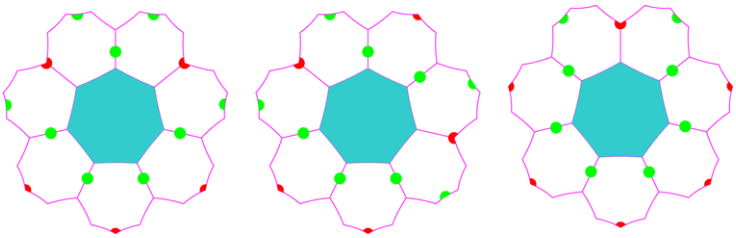

Fig. 12. The flowers of the mantilla: they consist of flowers with 8 or 9 elements in their centre rings. Note the representation of **F**- and **G-flowers** for the flowers with 9 centres. (For interpretation of the references to colour in this figure legend, the reader is referred to the web version of this article.)

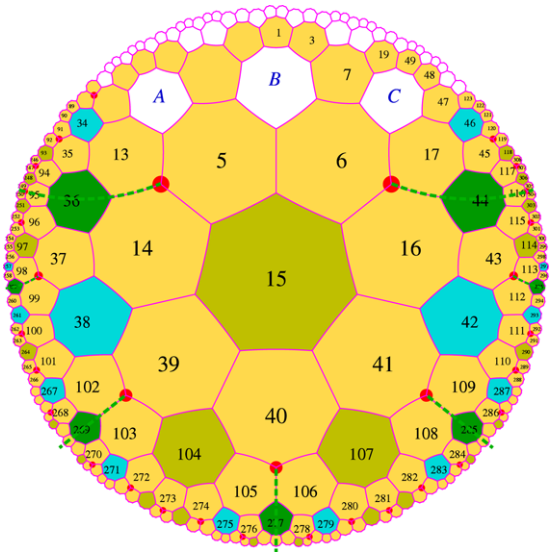

Fig. 13. Splitting the sector associated to an *F*-flower of the mantilla, whose centre is tile 15. The line β_ℓ crosses tile 36 and the line β_r crosses tile 44. (For interpretation of the references to colour in this figure legend, the reader is referred to the web version of this article.)

In this proof, we distinguish between flowers with 9 elements in a centre ring as there are two different possible patterns, see Fig. 12. Indeed, the two red vertices of the flower may be separated by one green edge or by two, considering the shortest number between them in the centre ring. We call **F-flowers** the flowers for which the two red vertices are separated by only one green edge. We call **G-flowers** the others: their red vertices are separated by two green edges. We shall call **8-flowers** the flowers with 8 elements in their centre ring.

Proof of Lemma 2.2. The proof consists in showing that the new tiling can also be generated by the splitting method, see Fig. 3. This is performed by induction.

Figs. 13–15 indicate how we split *F*-, *G*- and **8**-flowers respectively. In the case of an *F*-flower, we call **parental petals** the two petals of the flower which are between the two red vertices.

In the case of a *G*-flower, the parental petals are also taken among the three petals between the two red vertices of the flower. The central petal of this triple is a parental petal, call it *p*. The red vertex of *p* defines two centres which are in contact with the triple. By induction on the splitting, we shall show that one of these two centres defines an **8**-flower. The other non-parental petal of the *G*-flower is the petal which belongs to this **8**-flower.

In the case of an **8**-flower, the parental petals are the two petals which are in contact with the single red vertex.

Important convention: from now on, if not otherwise indicated, we shall not mention green sides, only red vertices in order to make the figures more easily readable.

In the case of *F*- and *G*-flowers, the splitting is defined as follows: let β_ℓ be the line which supports an edge of the non-parental petal sharing the left-hand red vertex and which is not in contact with the centre. We define β_r to be the reflection of β_ℓ in the bisector of the segment which joins the two red vertices of the flower. We call *F*- or *G*-**sector** the region delimited by β_ℓ, β_r and the lower border of the non-parental petals of the considered flower, see Figs. 13 and 14.

Note that we have two kinds of *G*-flowers: left-hand side and right-hand side flowers, depending on the side of the **8**-flower which is in contact with a parental flower. However, a *G*-sector is symmetric.

In the case of an **8**-flower, let *u* and *v* be the parental petals and let *p* and *q* be the non-parental neighbouring petals of *u* and *v* respectively. Denote by *A* the red vertex of *p* and by *B* the one of *q*. Note that *B* and *q* are the respective reflections of *A* and *p* in the line σ which passes through the red vertex of the **8**-flower and through the mid-point *O* of its centre.

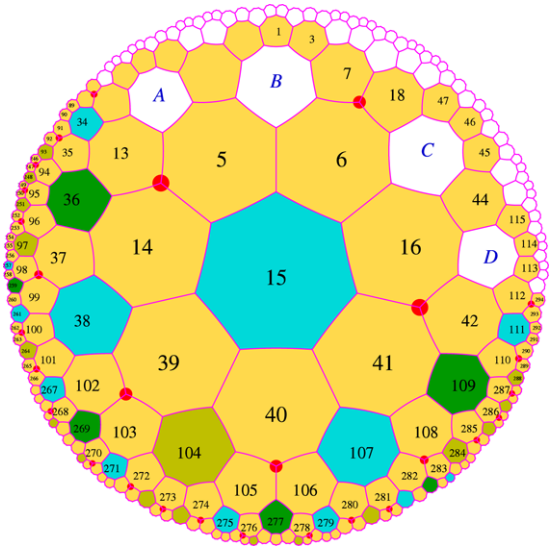

Fig. 14. Splitting the sector associated to a *G*-flower of the mantilla. Here, the line β_r crosses tile 109. (For interpretation of the references to colour in this figure legend, the reader is referred to the web version of this article.)

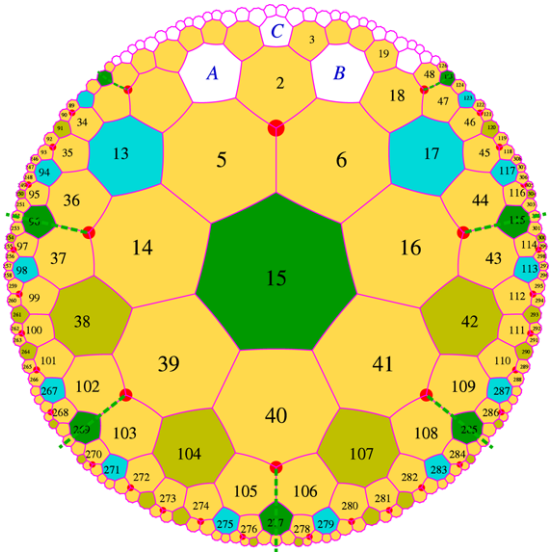

Fig. 15. Splitting the sector associated to an 8-flower of the mantilla.

Define the line which starts from *O* and which passes through *A*. Then denote by β_ℓ the ray on this line which is issued from *A* and which does not cut the centre of the flower. Symmetrically, define β_r to be the reflection of β_ℓ in σ.

The **8-sector** is defined by β_ℓ and β_r and by the part of the lower border of the non-parental petals of the flower which falls inside the angular sector defined by β_ℓ and β_r.

We note that the parental petals also belong to another flower. They both belong to the same other flower in the case of an *F*-flower. They belong to different flowers in the cases of a *G*- or an **8**-flower.

Note that the distinction between parental and non-parental petals introduces the notions of **top** and **bottom** in a flower of the tiling. In Section 2.5, we shall come back to this point by the introduction of the notion of **levels** and of **isoclines** of the mantilla. In Figs. 13–15, we say that the central tile is the **centre** of the sector.

It is not difficult to see how the splitting indicated in each case of Figs. 13–15 can go on *downwards*, from the non-parental petals of the flower. The non-parental petals of the central flower of the pictures in Figs. 13–15 induce the flowers which are the head of the sectors into which the above sectors can be split.

In the case of an **8-flower**, the splitting defines four sectors exactly. We consider that the *G*-flowers which appear outside the sector and around its head are defined by another flower: this property also belongs to the induction hypothesis. Also by induction, we will check the following property. Consider the three centres which are around a red vertex. Then, exactly

one of them is the centre of an **8**-flower. The others are either both centres of F-flowers or one centre is from a G-flower, the other from an F-flower.

In the case of F- and G-flowers, beyond the side of the G-sector which is not shared by an F-sector, we have the half of an **8**-sector: a right-hand side half on the left-hand side and a left-hand side half on the right-hand side.

Accordingly, as half- and right-hand sides are isometric, the splitting can be given by the following rules:

$$\begin{aligned} F &\longrightarrow 2F, 2G, 2 \times \frac{1}{2}\mathbf{8} \\ G &\longrightarrow F, 2G, 2 \times \frac{1}{2}\mathbf{8} \\ \mathbf{8} &\longrightarrow 4F. \end{aligned}$$

For counting the elements of the spanning tree on the same level, we may replace 2 halves of an **8**-sector by a whole sector, and so, we get the following matrix:

$$\begin{matrix} 2 & 2 & 1 \\ 1 & 2 & 1 \\ 4 & 0 & 0 \end{matrix}$$

and accordingly, the characteristic polynomial P of the splitting is:

$$P(X) = X^2 - 4X - 2.$$

We note that it is a Pisot polynomial whose greatest real root is $2 + \sqrt{6}$.

At this point, we note that we have a tiling of any sector, neglecting the fact that the borders of a sector may involve half-tiles: we know that such halves will be completed by another sector which must necessarily be present.

Now, to tile the plane, we use the argument of [14]: consider a sector whose head is a flower **F**. The parental petals of **F** are non-parental petals of another flower **H**, **higher** than **F** in the tiling. It is clear that the sector Σ defined by **H** contains the sector defined by **F** as a sub-sector in the above tiling of Σ. Call **H** a **completing** sector of **F**.

It remains to prove that, whatever the choices are for the completing sector of the head of a given sector, we obtain a sequence of sectors whose union is the hyperbolic plane.

To prove this point, define the **augmented** sector of a given sector S to be the union of the sector and its heading flower, its parental petals being ruled out. Let B_n be the greatest ball around a once for all fixed origin O, contained in an augmented sector. Then, by completing the sector, we define a new sector of the splitting which, when augmented, contains S and B_{n+1} around O.

First, consider the case of an F-flower **F**. Fig. 13 indicates three centres which share a petal with **F**. Call them A, B and C, from the left to the right in Fig. 13.

Taking into account the already realized splittings, as the red vertex shared by tiles 13, 5 and 14 is at distance 1 of the centre A and the **8**-centre situated at tile 36, A cannot be the centre of an **8**-flower. It may be the centre of a 9-flower, either F or G. The same conclusion holds for C. Now, the following chains of consequences hold as can be easily checked by the reader:

$$\begin{aligned} A = F \quad &\Rightarrow B = 8 \quad \Rightarrow C = G \\ &\qquad\qquad\ \ \Rightarrow C = F \\ &\Rightarrow B = F \quad \Rightarrow C = G \\ A = G \quad &\Rightarrow B = 8 \quad \Rightarrow C = F \\ &\Rightarrow B = F \quad \Rightarrow C = F \\ &\Rightarrow B = G \quad \Rightarrow C = G. \end{aligned}$$

We could also start with B and the above chains also indicate the possible choices: we note that B may be any kind of centre. But once it is fixed, it also fixes the choices for A and B when B is the centre of a G-flower, and we have two solutions in both cases when B is the centre of either an **8**-flower or an F-flower.

In all these situations, as tiles 5 and 6 in Fig. 13 belong to the sector headed by B, the ball obtained from B_n by appending a new level of tiles is also in the sector. And this new ball is exactly B_{n+1}. And so, our claim is proved in this case.

Next, consider the case of a G-flower which is illustrated by Fig. 14.

In this case, we have to discuss the situation of four centres denoted by respectively A, B, C and D in the figure.

It is not difficult to note that A and D are occupied by the centre of an F-flower. Indeed, A cannot be the centre of an **8**-flower, because there is already such a centre at distance 1 from the red vertex shared by tiles 13, 5 and 14 in Fig. 14. Also, A cannot be the centre of a G-flower as there cannot be two adjacent G-sectors in the splitting of any sector. And so, A must be the centre of an F-flower. By symmetry of the figure, this is also the case for D.

Now, the possible cases for B and C are indicated by the following diagram:

$$\begin{array}{lll} B = 8 & \Rightarrow C = F \\ & \quad\ C = G \\ B = F & \Rightarrow C = 8 \\ B = G & \Rightarrow C = 8. \end{array}$$

It is not difficult to check that, in all these cases, tiles 36, 13, 5, 6, 16, 42 and 109 do belong to the new appended augmented sector, either in B or in C and so, accordingly, the new augmented sector contains B_{n+1}.

At last, we remain with the case of an **8**-sector which is illustrated by Fig. 15.

Here, we have the union of the four F-sectors defined by its splitting. The augmented sectors contain tiles 14, 15 and 16, as can be easily checked.

As the red vertex shared by 5 and 6 is at distance 1 from the centre of the considered **8**-flower, A and B cannot be the centre of an **8**-flower as they are at distance 1 from this red vertex.

This leaves four cases a priori. But A and B cannot be both centres of a G-flowers, as two G-sectors cannot be adjacent. And so we are left with three cases: A and B are both centres of an F-flower, or A is the centre of a G-flower and B, that of an F-flower, or, conversely, B is the centre of a G-flower and A, that of an F-flower.

In all cases, tiles 5 and 6 also belong to the union of the new augmented sectors and so, whatever the tile appended in C, it is the centre of a flower and the considered tiles together with 36, 13, 17 and 44 are in the sector defined by C.

And so, the following property is proved:

Lemma 2.3. *Completing a sector S by any of the possible centres which will give rise to a new sector Σ in which S enters its splitting, in at most two steps of such a completion, if S contains the ball B_n around a fixed in advance tile T, Σ contains the ball B_{n+1} around T.*

With this property, the proof of Lemma 2.2 is completed. ■

2.3. The set of tiles

Now, we show that the tiling which we have described in general terms in the previous section can effectively be generated from a small finite set of tiles: we simply need 21 of them.

We have to implement the construction of F-, G- and **8**-flowers and the rules of generations of the carpet structure of the mantilla, see [24,14] for the notion of carpet.

For this aim, remember that in the flowers we have two categories of tiles: the petals and the centres. Also remember that we started with two kinds of tiles: tiles with a red vertex and two green sides and tiles with no marks. In Section 2.1, we postponed the construction of marks on the tiles which force the centres to be surrounded by petals. It is now time to indicate how to proceed.

A solution consists in labeling the edges of such a tile by numbers from 1 up to 7. It is very easy to check that with such a labeling, the domino tiles associated to the tile a of Section 2.1, see Fig. 8, cannot alone tile the plane as the labels cannot match. This property is not specific to tiling $\{7, 3\}$, indeed it is shared by any regular tiling $\{p, 2q+1\}$,[1] as long as $p \neq 2q+1$. Due to the matching condition on edges, the tiles which support the petals should be dotted with similar labels. But the labels are needed only on the edges of petals which are shared by a centre. A priori, this would give 7^3 different tiles for the initial set of tiles which, after Berger, we call the **prototiles**. As we shall soon see, we need only 21 prototiles to construct the mantilla: 17 petals and 4 centres.

To see this, let us fix where we put number 1 in a tile which is a centre. For F-flowers, it seems natural to put 1 and 7 at symmetric places with respect to the vertical axis of reflection of the flower. It is also easy to fix 1 and 7 for an **8**-flower: the red vertex is exactly on the vertical axis of reflection of the flower. We have a different situation with G-flowers. We already noted that there are left- and right-hand side flowers. Here, we shall stress on this difference by giving G-flowers a different numbering: instead of clockwise increasing around the edges of the tile, the numbers will increase while **counter-clockwise** going around the edges of the tile. Also, in order to distinguish between petals, we introduce two sets of numbers: we shall consider **marked** and **unmarked** numbers. Unmarked numbers in $\{1..7\}$ are those which we ordinarily use. Marked numbers are in $\{\overline{1}..\overline{7}\}$. The difference appears, in Table 1 and in Fig. 16.

We remark that the new numbers do not change the fact that central tiles alone, even by mixing the labels, cannot tile the plane by themselves.

From this, we derive 17 prototiles from the petals, looking at the different configurations of petals attached to edges numbered from 2 up to 6 of all possible centres. In this respect, we define such tiles as the **non-parental** tiles which will be the meaning of this expression until the end of the paper.

Fig. 17 displays the complete set of 21 tiles of the mantilla.

The non-parental petals can be grouped according to the flowers in which they occur. This is given in Table 2. In this table, the position of the red vertex in the petal is indicated by the occurrence of symbol ∘. The labels are indicated by putting in

[1] The property does not hold for $\{p, q\}$ when q is even.

Table 1
Table of the distribution of colours on the sides of the central tiles

	2	3	4	5	6
F	2	$\overline{3}$	$\overline{4}$	$\overline{5}$	6
G_ℓ	$\overline{6}$	$\overline{5}$	4	3	2
G_r	6	5	4	$\overline{3}$	$\overline{2}$
8	$\overline{2}$	3	$\overline{4}$	5	$\overline{6}$

The labels are given for sides numbered from 1 up to 7 clockwise running around the tile. For centres of G-flowers, we indicate the reverse ordering on the labels. The labels 1 and 7 are not indicated: they are the same for F- and **8**-flowers, and they are exchanged for G-flowers.

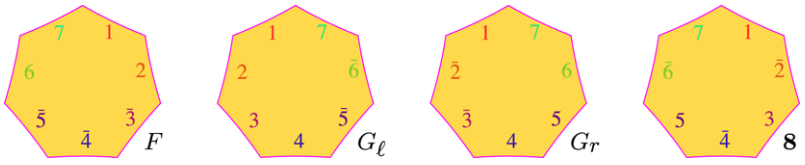

Fig. 16. The prototiles for the centres: F-, **8**-, G_ℓ- and G_r-centres.

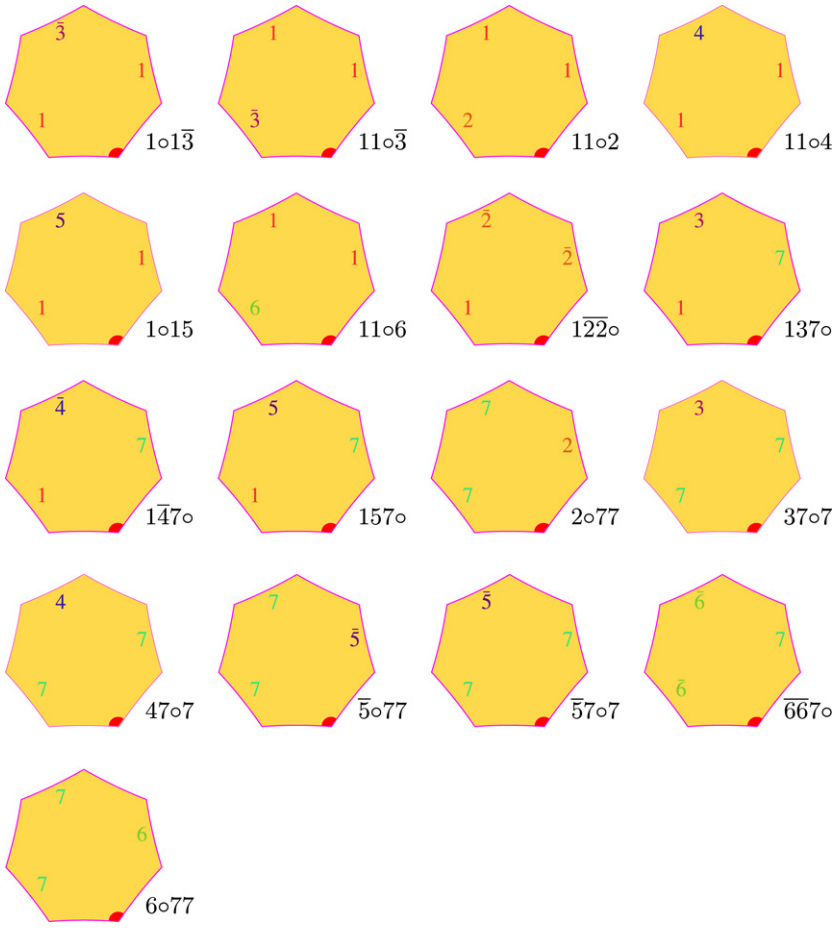

Fig. 17. The prototiles for the non-parental petals.

Table 2
Table of the non-parental petals according to their parent flowers

	2	$\overline{2}$	3	$\overline{3}$	4	$\overline{4}$	5	$\overline{5}$	6	$\overline{6}$
F	2∘77			1∘1$\overline{3}$		1$\overline{4}$7∘		$\overline{5}$7∘7	11∘6	
G_ℓ	11∘2		37∘7		1∘14			$\overline{5}$∘77		$\overline{6}\overline{6}$7∘
G_r		1$\overline{2}\overline{2}$∘		11∘$\overline{3}$	47∘7		1∘15		6∘77	
8		1$\overline{2}\overline{2}$∘	137∘			1$\overline{4}$7∘	157∘			$\overline{6}\overline{6}$7∘

Table 3
The possible values of the parental tiles of an F-flower

	F_ℓ	F_r	G_ℓ	G_r	$\mathbf{8}_1$	$\mathbf{8}_2$	$\mathbf{8}_3$	$\mathbf{8}_4$
1	$1\overline{4}7\circ$	$1\circ1\overline{3}$	$1\circ14$	$1\circ15$	$1\overline{2}\overline{2}\circ$	$137\circ$	$1\overline{4}7\circ$	$157\circ$
7	$\overline{5}7\circ7$	$1\overline{4}7\circ$	$37\circ7$	$47\circ7$	$137\circ$	$1\overline{4}7\circ$	$157\circ$	$\overline{6}\overline{6}7\circ$

first position the lowest label according to the alphabetic order and then by following the occurrence of the other labels and of the red vertex while running around the tile clockwise.

Table 2 results from a careful checking. It is not difficult to check, in each case, that the configuration of each petal is unique, even when the same tile may appear in different contexts.

In this line, we note that the following petals appear only in a fixed centre:

$2\circ77$, $1\circ1\overline{3}$, $\overline{5}7\circ7$ and $11\circ6$ for F-flowers;
$11\circ2$, $37\circ7$, $1\circ14$ and $\overline{5}\circ77$ for G_ℓ-flowers;
$11\circ\overline{3}$, $47\circ7$, $1\circ15$ and $6\circ77$ for G_r-flowers;
$137\circ$ and $157\circ$ for **8**-flowers.

For the other petals:

$1\overline{4}7\circ$ is common to F- and **8**-flowers;
$\overline{6}\overline{6}7\circ$ is common to G_ℓ- and to **8**-flowers;
$1\overline{2}\overline{2}\circ$ is common to G_r and **8**-flowers.

Now, we have to establish a converse of the table. Starting from a tile, we necessarily obtain what can be deduced from the table and nothing else.

For this aim, we first prove:

Lemma 2.4. *The set of tiles defined by Table 2 together with the four tiles for the centres generates the mantilla. Namely, starting from a tile, we precisely have the abuttings which can be derived from the table.*

In order to prove the lemma, we first note that a corollary of Lemma 2.1 is the following result:

Corollary 1. *A petal can abut at a numbered edge only with a centre, at the edge which bears the same number. If the number on the edge of the petal is marked, the same number on the edge of the centre must also be marked.*

The proof of Lemma 2.4 is long and tedious. It is written to the full extent in [17]. It consists in a careful examination of all the possible cases and in showing, in particular, that no other possibility than those dictated by the tables is possible. However, the examination of [17] is a bit simplified by the two following elementary remarks: considering the petals which have been to be put around a centre, they abut with different numbers and, also, adjacent petals abut with consecutive numbers, considering here that 1 and 7 are consecutive. The checking is rather easy for an F-flower, but it is more intricate for a G-flower and also for an **8**-flower.

Now, Tables 1 and 2 allow to construct the tiling **downwards**. Note that Fig. 18, illustrates the just indicated tables and it is a convenient way to represent them.

In order to construct it also **upwards**, we need additional information, which we also present in the form of tables. These new tables can be seen as a reversal reading of Tables 1 and 2. We again repeat that the goal of the lemma is not to establish the tables, which is rather easy, but to prove that with the set of prototiles defined by Figs. 16 and 17, we cannot obtain a combination which is not indicated by the tables. The tables indicate what is possible and only that.

In order to determine the reverse tables, see Tables 3–5, it is not difficult to see that the first thing we have to do is to determine what the parental tiles are.

Our first remark is that we should check that parental tiles do not bring in new types of tiles. Indeed, a parental tile in a given flower is also a non-parental tile in another one. Accordingly, we should have already all possible types of tiles.

In [17], a careful checking shows that this is the case and that the property is obtained from the tiles themselves.

The tables are established for each type of flower.

First, Table 3 indicates all the possible pairs of parental tiles of an F-flower.

We note that the table gives additional information about the position of the flower induced by the indicated parental petals. From what we computed, we see that there is a single case for G_ℓ- and G_r-flowers. This corresponds to the fact that in a G-flower, there is a single F-son. For an F-flower, we have two cases: this is due to the fact that an F-son has two F-sons. One is on the left-hand side, it is determined by the petals $\overline{5}7\circ7$ and $1\overline{4}7\circ$ as we can see in Fig. 18. This is why Table 3 indicates F_ℓ. The other F-son of an F-flower is determined by the petals $1\overline{4}7\circ$ at edge 7 and $1\circ1\overline{5}$ at edge 1 as we can see in Fig. 18. From this we understand the indication F_r of the table. Now, it is easy to understand the indications $\mathbf{8}_i$, $i \in \{1..4\}$ of the table. An **8**-flower has four F-sons and, numbering them from 1 to 4, going clockwise around the centre as we can see from Fig. 18 we obtain: the first F-son is determined by the petals $1\overline{2}\overline{2}\circ$ at edge 1 and $137\circ$ at edge 7, the second by $137\circ$ at edge 1 and

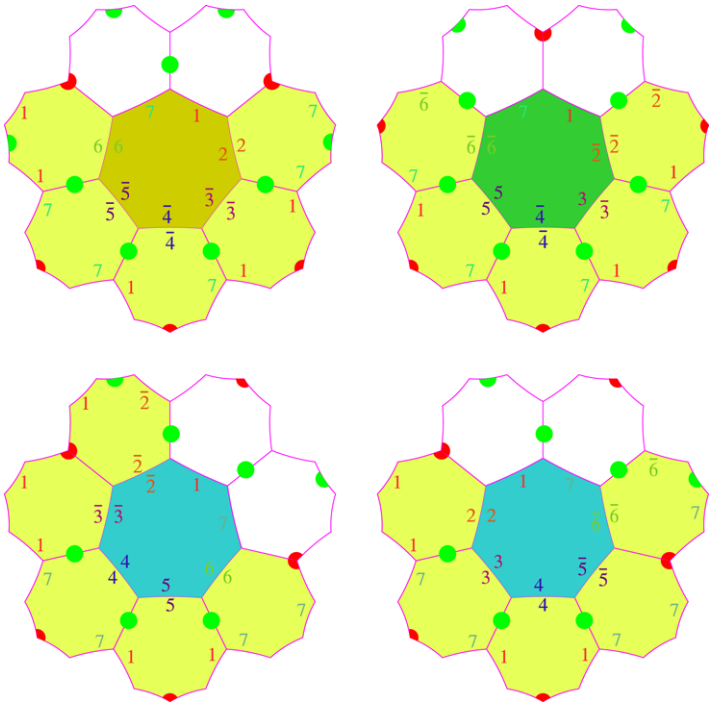

Fig. 18. All the non-parental tiles induced by the centres: above, left-hand side, an F-centre; right-hand side, an **8**-flower. Below, left-hand side, a G_r-centre; right-hand side, a G_ℓ-centre.

Table 4
The possible values of the parental tiles of a G-flower

	F	G_ℓ	G_r		F	G_ℓ	G_r
1	$1\circ1\bar{3}$	$1\circ14$	$1\circ15$	1	$11\circ6$	$11\circ2$	$11\circ\bar{3}$
7	$2\circ77$	$\bar{5}\circ77$	$6\circ77$	7	$\bar{5}7\circ7$	$37\circ7$	$47\circ7$

On the left-hand side, the case of a G_ℓ-flower. On the right-hand side, the case of a G_r-flower.

Table 5
Above: the possible values of the parental tiles of an **8**-flower

	F-F	F-G_ℓ	F-G_r	G_ℓ-F	G_r-F
1	$11\circ6$	$11\circ2$	$11\circ\bar{3}$	$11\circ6$	$11\circ6$
7	$2\circ77$	$2\circ77$	$2\circ77$	$\bar{5}\circ77$	$6\circ77$

	F-F				F-G_r	G_ℓ-F
3rd	$1\bar{4}7\circ$	$1\bar{4}7\circ$	$137\circ$	$157\circ$	$12\bar{2}\circ$	$\bar{6}\bar{6}7\circ$
	F	**8**	**8**	**8**	**8**	**8**

	F-G_ℓ			G_r-F		
3rd	$1\bar{3}1\circ$	$141\circ$	$151\circ$	$7\bar{5}7\circ$	$737\circ$	$747\circ$
	F	G_ℓ	G_r	F	G_ℓ	G_r

Below, in two tables, the third petal and the third centre.

$1\bar{4}7\circ$ at edge 7, the third by $1\bar{4}7\circ$ at edge 1 and $157\circ$ at edge 7 and the last one by $157\circ$ at edge 1 and $\bar{6}\bar{6}7\circ$ at edge 7. These are exactly the indications of Table 3.

We argue in a similar way for G-flowers, taking into account their laterality: we have G_ℓ- and G_r-flowers.

The corresponding information is given in Table 4, for both cases of G_ℓ and G_r-flowers.

Note a property which we have already noticed with the definition of a sector and that we find again from considerations on the tiles only: the parent of a G-flower is either an F-flower or a G-flower. It is never an **8**-flower.

Now, let us turn to the case of an **8**-flower.

To better understand Table 5, we refer the reader to Fig. 15, where the tiles marked A, B and C play an important role. In the second and third sub-tables, we have three rows. The first row corresponds to what we could call the two parents of the **8**-flower, A and B in Fig. 15. The second row corresponds to what is called the **third tile** in [17]: it is the tile 2 of Fig. 15, which is a petal. The third row corresponds to the third centre, the tile C of Fig. 15.

Table 6
The ultimately periodic path followed by the mid-point line of the rightmost branch of a tree of the mantilla

Rank	1	2	3	4	5	6	7	8	9	10	11
Tile	7	2	6	5	15	14	39	38	102	101	267
Pattern	$1\circ 1\alpha$	F	$2\circ 77$	$1\circ 1\overline{3}$	G_ℓ	$11\circ 2$	$37\circ 7$	G_r	$6\circ 77$	$1\circ 15$	G_ℓ
Sides	$\diamond-1$	$1-2$	$2-\diamond$	$\diamond-1$	$1-2$	$2-\diamond$	$\diamond-7$	$7-6$	$6-\diamond$	$\diamond-1$	$1-2$

The table indicates the patterns of the tiles crossed by the mid-point lines. For each tile, it also indicates the sides of the tile which are crossed. The $\diamond$ sign indicates a green side.

Note that Table 5 shows that the two centres defined by the petals at edge 7 and at edge 1 cannot be both G-centres, a situation which was already ruled out by the definition of the splitting and which can be derived from the definition of the tiles only.

Accordingly, the proof of Lemma 2.4 is completed. ■

2.4. The trees of the mantilla

First, we define what we shall from now on call a tree. Consider one of the angular sectors defined in Section 1.2, and call it the **basic sector**. It is delimited by two mid-point lines issued from the mid-point A of a tile and making a fixed angle α. Remember that the set of tiles whose centres are contained in the basic sector is spanned by a Fibonacci tree. We call **positive isometry of the tiling** an even product of reflections in lines which leaves the ternary heptagrid globally invariant.

Definition 2. We call **tree** in the tiling $\{7, 3\}$ a couple $(S, \mathcal{F})$, where S is a set of tiles which is a copy of the basic sector under a positive isometry of the tiling, and $\mathcal{F}$ is a standard Fibonacci tree. We also say that S is the **area** delimited by the tree or, simply, the **area of the tree**.

The composition φ of the bijection of $\mathcal{F}$ onto the tiles of the basic sector with the isometry ι defining a tree $(S, \mathcal{F})$ allows us to transfer the numbering of the nodes of $\mathcal{F}$ to the tiles of S, as well as the relationship between the nodes of the tree. In particular, denoting the root of $\mathcal{F}$ by ρ, we call $\varphi(\rho)$ the **root** of the tree. Similarly, a tile U of S is called the son of another one V, if and only if $\varphi^{-1}(U)$ is the son of $\varphi^{-1}(V)$. We shall often identify a tree with its area. We call $\iota(A)$ **vertex** of the tree. See Fig. 19 for a representation of a tree.

Next, we define where the trees are placed. For this aim, we use a very simple criterion:

Definition 3. In the mantilla, we call **tree of the mantilla**, a tree whose root ρ is the centre C of an F-flower which is the F-son of a G-flower and whose vertex is on the bisector of the segment joining the red vertices of C, the sons of ρ being non-parental petals of C. The root of a tree of the mantilla is called a **seed**.

We shall prove two basic properties of the trees of the mantilla: they are completely contained in the sector defined by the F-flower whose centre is their root. We also prove that two such trees have either distinct areas or the area of one contains the other area.

Lemma 2.5. *In the mantilla, a tree of the mantilla is completely contained in the sector defined by its root.*

Proof. Obvious. ■

In fact, we can say more: between the leftmost branch of the tree and the left-hand side border of the sector, new trees appear. This can be seen in Fig. 19. The configuration of tile 104 is exactly that of tile 2. Note that tile 17 plays for tile 2 the role which is played by tile 277 for tile 104. There is a shift transforming the configuration of tile 2 into that of tile 104. The same shift applied to tile 104 provides us with a new tree between the rightmost branch of the tree rooted at tile 104 and the right-hand side border of the region defined by the F-flower whose centre is tile 104.

Now, let us start from the parental petals of an F-flower which is the F-son of a G-flower. There are two possible couples of such petals: $37\circ 7$ and $1\circ 14$ in the case of a G_ℓ-flower, $47\circ 7$ and $1\circ 15$ in the case of a G_r-flower.

Consider the right-hand side border.

We successively meet the following tiles, starting from the first one, say $1\circ 1\alpha$ with $\alpha \in \{4, 5\}$:

We note that the sequence of tiles crossed by the mid-point lines is ultimately periodic. The period involves six tiles and the aperiodic part at the beginning of the sequence involves four tiles. Note that the table also indicates the sides which are crossed by the mid-point line for each tile involved by the border. In the table, a green side is represented by $\diamond$.

A similar table can be established for the left-hand side border where the first tile is $\beta 7\circ 7$ with $\beta \in \{3, 4\}$:

Taking into account that the construction of the tiling is deterministic when we go from a centre to its non-parental petals, the sequences defined by Tables 6 and 7 for the ranks, the patterns and the sides are the same for all trees. Accordingly, we proved the following result:

Lemma 2.6. *The sequence of the tiles crossed by the border of the tree is ultimately periodic. The length of the period is the same for the right-hand and for the left-hand side borders.*

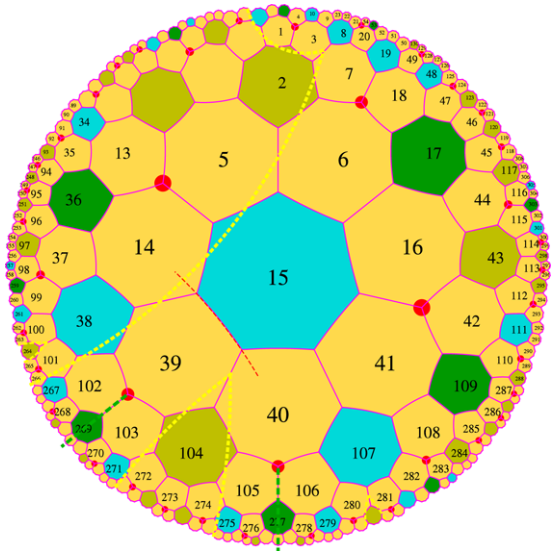

Fig. 19. The tree generated by an F-flower which is the son of a G-flower. (For interpretation of the references to colour in this figure legend, the reader is referred to the web version of this article.)

Table 7
The ultimately periodic path followed by the mid-point line of the leftmost branch of a computing tree

Rank	1	2	3	4	5	6	7	8	9	10	11
Pattern	$\beta 7 \circ 7$	F	$11 \circ 6$	$\overline{5}7 \circ 7$	G_r	$6 \circ 77$	$1 \circ 15$	G_ℓ	$11 \circ 2$	$37 \circ 7$	G_r
Sides	$\diamond - 7$	$7-6$	$6-\diamond$	$\diamond - 7$	$7-6$	$6-\diamond$	$\diamond - 1$	$1-2$	$2-\diamond$	$\diamond - 7$	$7-6$

Same conventions as in Table 6.

Let us look again at the tiles involved in the border.

The initial tiles $1 \circ 1\alpha$ and $\beta 7 \circ 7$ may occur in the period. This is the case for $\alpha = 5$ and $\beta = 3$ only. Consider a tile $1 \circ 15$. When it is the first tile of a tree, the border is the right-hand side one and it crosses sides $\diamond - 1$. We note that the concerned sides are on the left-hand side of edge 5 when the red vertex is below this edge. When it appears in the periodic part of the border, the same tile is also crossed at sides $\diamond - 1$. As we can see in Fig. 19, the crossed side is on the other side of edge 5, with the red vertex again in a position below, see tile 101 in Fig. 19. This means that another border may use this tile as indicated. A similar remark holds for a tile $37 \circ 7$. It is crossed along sides $\diamond - 7$. But the crossed sides are on the right-hand side of edge 3 when the red vertex of the tile is below this edge. When the tile $37 \circ 7$ again appears in the period of a border, it is also crossed at edges $\diamond - 7$, but on the right-hand side of the tile when the red vertex is below edge 3, as can be noted in Fig. 19 with tile 39. This means that this tile may also be crossed by another border at the same time. In Fig. 19, this is the case for tile 39.

Another tile can be crossed by two borders at the same time. It is, of course, the F-tile which is at the root of the tree. The involved edges are $1-2$ on one side and $7-6$ on the other.

Let us look at the other tiles. Using Tables 6 and 7 and Fig. 19, we have the following properties:

- tiles crossed by a right-hand side border only: $1 \circ 14$, at edges $\diamond - 1$ only; $2 \circ 77$, at edges $2-\diamond$ only; $1 \circ 1\overline{3}$, at edges $\diamond - 1$ only;
- tiles crossed by a left-hand side border only: $47 \circ 7$, at edges $\diamond - 7$ only; $11 \circ 6$, at edges $6-\diamond$ only; $\overline{5}7 \circ 7$, at edges $\diamond - 7$ only;
- tiles crossed by one border only, when the left-hand side border, when the right-hand side one: G_ℓ, at edges $1-2$ only; $11 \circ 2$, at edges $2-\diamond$ only; G_r, at edges $7-6$ only; $6 \circ 77$ at edges $6-\diamond$ only;
- tiles possibly crossed by two borders: F, always at both edges $1-2$ and $7-6$; $1 \circ 15$ at edges $\diamond - 1$, when both, when one of them; $37 \circ 7$ at edges $\diamond - 7$, when both, when one of them.

Next, we have the following property of the mid-point lines which we consider:

Lemma 2.7. *Consider two mid-point lines ℓ_1 and ℓ_2 of tiling $\{7, 3\}$. Recall that we consider lines joining the mid-points of two consecutive edges of tiles of the tiling. Then if ℓ_1 and ℓ_2 do intersect, they meet at the mid-point of an edge of a tile.*

Proof. Indeed, assume that ℓ_1 and ℓ_2 meet at a point A. On a mid-point line of the tiling, any point is between two mid-points of two consecutive edges of a tile, as can easily be seen in Fig. 19. Let A_1 and B_1 be such points for ℓ_1 with respect to A and A_2 and B_2 for ℓ_2 with respect to A too. By construction of a mid-point line of the tiling, if A is inside a tile τ, A_1 and B_1 must be vertices of τ. It is clear that A_2 and B_2 must be the same vertices as this happens also on the same tile. And so,

this is impossible if $\ell_1 \neq \ell_2$. Accordingly, A belongs to the border of a tile and, by construction of a mid-point line, it is the mid-point of an edge of a tile. ■

Now, if we look at what we observed on the tiles involved in borders, the single possible meeting of two borders is the mid-point of the common edge shared by the tiles 37∘7 and 1 ∘14, or the tiles 47∘7 and 1∘15.

Consequently:

Lemma 2.8. *The border of a tree of the mantilla does not meet the border of another tree of the mantilla.*

Proof. There is no tile which would allow to realize the meeting of two borders as the only ones which can contain the intersection of two mid-point lines are the parental petals of the root of the tree. ■

What we proved on the border of a tree and of a sector proves Lemma 2.8 too. Fig. 19 indicates that along a border, new trees appear, both outside and inside the area of the tree. They are generated by G_ℓ's and G_r's tiles which periodically occur among the tiles crossed by the border. Tiles 39 and 101 are crossed by two borders and they illustrate both situations. At the same level, other F-sons of a G-centre are further and, indeed, they belong to different sectors. They belong either to a sector which is outside the sector defined by the root of the initially considered tree, or they belong to a sector which is inside the area of the tree. In the first case, as sectors define a partition starting from a given level, the property of the lemma follows. In the second case, it is not difficult to see that the border of a sector involves **8**-centres which occur periodically along the border as we go down along it. As **8**-centres have only F-sons, these F-centres do not generate trees. This is why, trees are rather 'far' from such a border. And so, using the isoclines which we further introduce in the mantilla, independently of its trees, we can see that the trees which are generated on the same isocline always occur in sectors which have no border in common. Look at Figs. 13 and 14. Also, Fig. 19 contains two examples of the situation when borders of different trees are as close as possible. Tile 39 is crossed by the right-hand side border of the tree rooted at 2 and it is also crossed by the created left-hand side border of the tree rooted at tile 104. For tile 101, it is crossed by the right-hand side border of the tree rooted at 2 and also by the just now created right-hand side border of the tree rooted at tile 264 as the latter tree is inside the former. Note that this is the single possibility for a tree to be so closed to another one. 'Old' trees are indeed very far from each other.

Now we get an important corollary of Lemma 2.8:

Lemma 2.9. *In the mantilla, two trees of the mantilla have either disjoint areas or one area contains the other.*

Proof. Assume that we have two trees A_1 and A_2 such that their areas intersect and that none of them contains the other. Let τ_i be the root of A_i, $i \in \{1, 2\}$. Let τ be a tile of the intersection. In the tree A_1, there is a path from τ to τ_1 which consists of tiles of A_1. As $\tau_1 \notin A_2$, there is a last tile of A_1 on the path, say σ_1, which meets the border of A_2. As σ_1 is on the border of A_2, there is a last tile of A_2, among those which are on the border from σ_1 to τ_2, say σ_2 which meets the border of A_1. And so, σ_2 contains both the border of A_2 and the border of A_1. Considering the triangle defined by τ_1, τ_2 and σ_1, the border of A_2 must meet the border of A_1, a contradiction with Lemma 2.8. ■

Now, we define the following notion:

Definition 4. A **thread** is a set $\mathcal{F}$ of trees of the mantilla such that:

(i) if $A_1, A_2 \in \mathcal{F}$, then either $A_1 \subset A_2$ or $A_2 \subset A_1$;
(ii) if $A \in \mathcal{F}$, then there is $B \in \mathcal{F}$ with $B \subset A$, the inclusion being proper;
(iii) if $A_1, A_2 \in \mathcal{F}$ with $A_1 \subset A_2$ and if A is a tree of the mantilla with $A_1 \subset A$ and $A \subset A_2$, then $A \in \mathcal{F}$.

Definition 5. A thread $\mathcal{F}$ of the mantilla is called an **ultra-thread** if it possesses the following additional property:

(iv) there is no $A \in \mathcal{F}$ such that for all $B \in \mathcal{F}$, $B \subset A$.

Lemma 2.10. *A set $\mathcal{F}$ of trees of the mantilla is an ultra-tread if and only if it possesses properties* (i) *and* (ii) *of Definition 4 together with the following:*

(v) *for all $A \in \mathcal{F}$ and for all tree B of the mantilla, if $A \subset B$, then $B \in \mathcal{F}$.*

Proof. Indeed, an ultra-thread satisfies (v). Otherwise, let $A \in \mathcal{F}$ and B be a tree of the mantilla such that $A \subset B$ and $B \notin \mathcal{F}$. From (iii) we get that for any tree C of the mantilla such that $B \subset C$, then $C \notin \mathcal{F}$. From Lemma 2.9, if $A \subset B$, A is a sub-tree of B and so, considering the path leading from the root of A to the root of B, there are at most finitely many trees D of the mantilla such that $A \subset D \subset B$. Note that if two trees D_1 and D_2 of the mantilla contain A, we have $D_1 \subset D_2$ or $D_2 \subset D_1$ by Lemma 2.9. And so, considering the biggest tree D between A and B with $D \in \mathcal{F}$, we obtain an element D in $\mathcal{F}$ such that for all $A \in \mathcal{F}$, $A \subset D$. This contradicts (iv). And so, if B is a tree of the mantilla which contains A, it belongs to $\mathcal{F}$.

Conversely, if a set $\mathcal{F}$ of trees of the mantilla satisfies (i), (ii) and (v), it obviously satisfies (iii) and (iv). ■

Accordingly, an ultra-thread is a maximal thread with respect to the inclusion.

Note that the mantilla may possess ultra-threads and it may possess none of them. Indeed, consider the following construction:

- at time 0, we fix an F-son of a G_r-centre, defining a tree F_0; at level 3 of F_0, and on its right-hand side border, there is a G_r-centre whose F-son defines a tree of the mantilla F_{-1}, as a sub-tree of F_0; repeating this by induction produces a

sequence $\{F\}_{n\leq 0}$ of trees of the mantilla such the area of F_i is contained in that of F_{i+1} for all negative i; denote by C_i the root of F_i and by $\mathcal{S}_i$ the sector attached to C_i;

• at the time $2n+1$, $n \geq 0$, complete $\mathcal{S}_{2n}$ by a G_ℓ-centre C'_n; it defines a tree F_{2n+1} whose area contains that of F_{2n} and a sector $\mathcal{S}_{2n+1}$;

• at the time $2n+2$, $n \geq 0$, complete $\mathcal{S}_{2n+1}$ by an F-centre C_{n+1}; it defines a tree F_{2n+2} whose area contains that of F_{2n+1} and a sector $\mathcal{S}_{2n+2}$.

Then it is clear that the sequence constructed by C_n defines an ultra-thread.

Now, modify the just indicated construction by the following rule for a time n, $n > 0$:

• at the time $n+1$, $n \geq 0$, complete $\mathcal{S}_n$ with an **8**-centre C_{n+1}; this defines a tree F_{n+1} whose area contains that of F_n and a sector $\mathcal{S}_{n+1}$.

Then as the sectors defined by C_n are increasing sectors, all the threads existing at time n have a maximal tree at some level with respect to C_n. As the sequence of flowers above C_n do not contain the root of a tree, we have that the maximal trees we define at the time t_n are not included in a tree, by induction on the construction of the sequence $\{C_n\}$. The tree which appears at higher levels generates trees whose areas never intersect the sector defined at time n.

Here are additional properties of the ultra-threads.

Lemma 2.11. *Let $\mathcal{U}$ be an ultra-thread. Then, $\mathcal{U} = \{A_n\}_{n\in\mathbb{Z}}$, where $A_n \in \mathcal{U}$ for all $n \in \mathbb{Z}$ and $A_n \subset A_{n+1}$, the inclusion being proper. We also have that $\bigcup_{n\in\mathbb{Z}} A_n = \mathbb{H}^2$.*

Proof. By properties (ii) and (v) of the ultra-threads, there is a sequence $\{C_n\}_{n\in\mathbb{Z}}$ such that $C_n \subset C_{n+1}$ for all n in $\mathbb{Z}$, the inclusion being proper. As C_n is a sub-tree of C_{n+1}, there is a path which goes from the root of C_n to that of C_{n+1}. Along these paths, there are finitely many trees of the mantilla. By (v), these trees also belong to $\mathcal{F}$. Accordingly, we obtain $\{A_n\}$ by appending these trees to $\{C_n\}$.

From our study of trees issued from a G-centre crossed by the border of a given tree of the mantilla, we know that we have the following property. If A and B are two trees of the mantilla with $A \subset B$, the inclusion being proper, consider the set of tiles A' which is obtained by appending a layer of one tile along the borders of A and outside A. Then, we have that $A' \subseteq B$.

Now, fix a tile τ_0 in A_0. From what we just noted, we obtain that $B_1 \subset A_1$ and, by induction, that $B_n \subset A_n$ where B_h is the ball of radius h around τ_0. Accordingly, $\bigcup_{n\in\mathbb{Z}} A_n = \mathbb{H}^2$. ∎

Lemma 2.12. *Let $\mathcal{U} = \{A_n\}_{n\in\mathbb{Z}}$ and $\mathcal{V} = \{C_m\}_{m\in\mathbb{Z}}$ be two ultra-threads. Then, there are two integers n_0 and m_0 such that $A_n = C_m$ for all n and m such that $n - n_0 = m - m_0$.*

Proof. Indeed, consider A_0. Then, as $\bigcup_{n\in\mathbb{Z}} C_n = \mathbb{H}^2$, there is m_0 such that C_{m_0} contains the root of A_0. Now, by Lemma 2.9, necessarily, $A_0 \subset C_{m_0}$ and so, $C_{m_0} \in \mathcal{U}$ by property (v) of the ultra-threads. This means that there is n_0 such that $A_{n_0} = C_{m_0}$. Now, by construction of $\{A_n\}$ and $\{C_m\}$, there is no tree of the mantilla between A_n and A_{n+1} and, similarly, between C_m and C_{m+1}. Accordingly, $A_{n_0+1} = C_{m_0+1}$. By induction, we get $A_{n_0+k} = C_{m_0+k}$ for all $k \in \mathbb{N}$. ∎

2.5. Isoclines

In [18], we have a new ingredient. We define the status of a tile as **black** or **white**, defining them by the usual rules of such nodes in a Fibonacci tree. Then, we have the following property.

Lemma 2.13. *It is possible to require that **8**-centres are always black tiles. When this is the case, a seed is always a black tile.*

Proof. The argument is based on the pictures of Fig. 21. In these figures, we can see the differentiation between black and white nodes performed by arcs drawn on the tiles. One kind of arc joins the mid-points of two edges of the heptagon which are separated by one edge. The other joins the mid-points of two edges which are separated by two consecutive edges of the heptagon. The figure illustrates this definition on the tile of an F-centre. As we shall soon see, the same tile of the mantilla may occur as a black tile or as a white one.

Of course, once we define a tile as a black or a white tile, its sons are defined according to the usual rules of a standard Fibonacci tree, see [24]: a black node has two sons, a black and a white one; a white node has three sons, a black and two white ones. In both cases, the black son is also the leftmost.

Starting from the picture of an **8**-centre in Fig. 20, the last one in the first row, we can see that the sectors attached to the sons of the centre are, from the left to the right: $Fw61$, Fb, Fb, $Fw72$, where Fb is the node which is represented on the left-hand side of Fig. 21, $Fw61$ is the node which is represented on the right-hand side of the figure. The figure clearly indicates the reason of the name of the latter tile. For what is $Fw72$, it is symmetric to $Fw61$ with respect to the reflection axis of the latter tile exchanging sides 1 and 7, for instance, but renumbering the tile in the same way as previously after the reflection, as the axis of the reflection is not changed. We can see the induced sons of the new defined centres. In fact, we obtain the sons of any centre, step by step, using Table 8.

In the middle picture of Fig. 20, we can see that along a ray crossing **8**-centres along a reflection axis, if we define the **8**-centre as a black tile and its petals $1\overline{4}7\circ$ and $157\circ$ as black and white tiles respectively, then these attributes are kept by induction along the position of the tiles on the ray. From this, defining the patterns in each sector, we find out that the

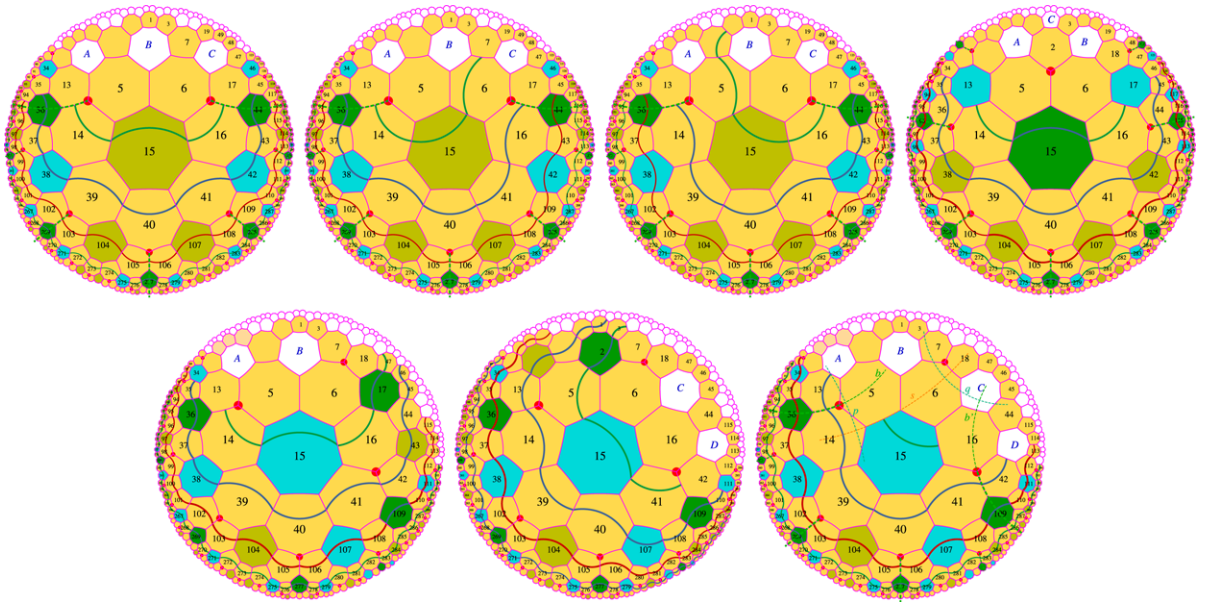

Fig. 20. The black tile property and the levels: In the first row: the three cases for an F-sector and the single case of an **8**-one. In the second row, the three possible cases for a G-centre.

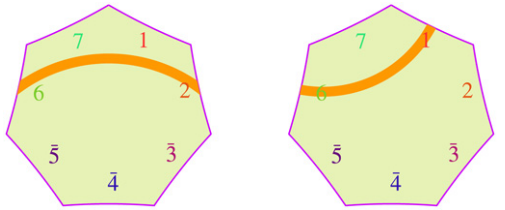

Fig. 21. The black tile property and the levels: On the left-hand side, a black F-centre. On the right-hand side, a white F-centre, here, the case $Fw61$.

Table 8
Table of the relations between the centre of a sector and its sons, taking into account the incidence of the isoclines

Centre	Sons:			
Fb	$G_r w$	Fb	Fb	$G_\ell w$
$Fw61$	$G_r w$	Fb	Fb	$G_\ell b$
$Fw72$	$G_r b$	Fb	Fb	$G_\ell w$
$G_\ell w$	$G_r b$	Fb	$G_\ell b$	
$G_\ell b$	$G_r b$	Fb	$G_\ell w$	
$G_r w$	$G_r b$	Fb	$G_\ell b$	
$G_r b$	$G_r w$	Fb	$G_\ell b$	
8	$Fw61$	Fb	Fb	$Fw72$

configurations are reproduced by the recursive definition of the sectors: in fact, we have nine kinds of sectors: one kind for **8**-centres, three kinds for the F-centres, one black and two white ones, and four kinds for the G-centres: two kinds of G_ℓ-centres, a black and a white one, and the same for G_r-centres. This defines eight different situation of sectors. Now, as in each sector the above properties are satisfied for the sons of the centre of the sector, they are also satisfied inside the sectors by the recursive structure of the sectors and by the property which we established on the borders of sectors.

Note that Fig. 20 represents seven pictures only as, in fact, $G_\ell w$ and $G_r w$ are identical sectors: their difference lies in the father of the sector. It does not stand in the same place with respect to the centre. Remember that, in a G-sector, the G-centre has two centres in contact with its parental tiles, see the places B and C for the tiles to be fixed in Fig. 14. For a G_ℓ-centre the father is in B, while the father is in C for a G_r-centre. ■

It is not difficult to note the following. Number the sides of a heptagon from 1 up to 7, starting from the side which is shared by the father and counter-clockwise turning around the tile. This defines the **local numbering**. In this numbering, the arc joins the mid-point of sides 2 and 7 in a white node and the mid-points of sides 3 and 7 in a black node.

At the level of a centre, looking at the different pictures of Fig. 20, we can see that the sons of a centre, in the sense of the Fibonacci tree, share a common side with another son and that this side is side 7 in the local numbering, in the white son(s). This also can be checked for the second level of the Fibonacci tree, starting from the centre. Then, the property can be

Table 9
Table of the centres and petals equipped with the isoclines

Tile	st	Edges	Relative	Tile	st	Edges	Relative
F	B	6-2	6-2	11∘2	B	((−•)-(2-1))	7-3
	W	6-1	6-1	11∘2	W	((−•)-2)	7-2
	W	7-2	7-2	37∘7	B	(7-(3-7))	2-5
8	B	$\overline{6}$-$\overline{2}$	$\overline{6}$-$\overline{2}$	37∘7	W	((7-3)-(3-7))	3-5
G_ℓ	B	2-$\overline{6}$	2-6	1∘14	W	((1-4)-(4-1))	3-5
G_ℓ	W	1-$\overline{6}$	1-$\overline{6}$	$\overline{5}$∘77	B	((7-$\overline{5}$)-(•−))	5-1
G_r	B	$\overline{2}$-6	$\overline{2}$-6	$\overline{66}$7∘	W	($\overline{6}$-$\overline{6}$)	2-4
G_r	W	$\overline{2}$-7	$\overline{2}$-7	1$\overline{22}$∘	W	($\overline{2}$-$\overline{2}$)	4-6
2∘77	B	((7-2)-(•−))	5-1	11∘$\overline{3}$	B	((−•)-($\overline{3}$-1))	7-3
2∘77	W	(2-(•−))	6-1	47∘7	W	((7-4)-(4-7))	3-5
1∘1$\overline{3}$	B	((1-$\overline{3}$)-1)	3-6	1∘15	B	((1-5)-1)	3-6
1∘1$\overline{3}$	W	((1-$\overline{3}$)-($\overline{3}$-1))	3-5	1∘15	W	((1-5)-(5-1)	3-5
1∘$\overline{4}$7	W	((1-$\overline{4}$)-($\overline{4}$-7))	3-5	6∘77	B	((7-6)-(•−))	5-1
$\overline{5}$7∘7	B	(7-($\overline{5}$-7))	2-5	6∘77	W	(6-(•−))	6-1
$\overline{5}$7∘7	W	(7-$\overline{5}$)-($\overline{5}$-7)	3-5	137∘	B	((1-3)-7)	3-6
11∘6	B	((−•)-(6-1))	7-3	157∘	B	(1-(5-7))	2-5
11∘6	W	((−•)-6)	7-2				

continued by induction, thanks to the recursive structure of the sectors. Now, we already noticed that the structure of the sectors is similar to the structure of Fibonacci carpets which are described in [24,14]. And so, we can continue the argument upwards. Accordingly, the arcs which we have described can be joined by the common edge of tiles which are on the same level of a Fibonacci tree. Now, as can be seen from the picture, which is a result of our above analysis of the status of the tiles along the border of a sector, the arcs also cross the sectors. The isoclines from the different sectors match, even when they are disjoint. Accordingly, the arcs constitute infinite paths which split their complement in the hyperbolic plane into two connected infinite parts. We shall call these infinite paths **isoclines** and we shall say that the isoclines cross the hyperbolic plane from one end to another.

In the following, it will be important to mark the path of an isocline on each tile of the mantilla. As can be seen by a careful study of the sectors based on Fig. 20 and on Tables 1 and 2, the 21 tiles which define the mantilla now become 33 tiles. They are displayed in Table 9. In the table, we have indicated the position of the arcs in terms of the marks of the tile and also in a **relative numbering**. This numbering is obtained by starting from the red vertex of the tile when it is a petal and then, numbering the sides from 1 to 7 by turning counter-clockwise around the tile. For the centres, we keep the numbering of the mantilla.

From now on, **number the isoclines periodically, from 0 to 19**, the number of an isocline crossing a centre C being smaller than the number of the next isocline which crosses the sons of C. This numbering allows to define the directions **up** and **down** in the hyperbolic plane. The isoclines allow to define the directions **to the left** and **to the right**.

From the pictures of Lemma 2.13 we easily derive the following important property:

Lemma 2.14. *Let the root of a tree of the mantilla T be on isocline* 0*. Then, there is a seed in the area of T on isocline* 5*. If an* **8***-centre A is on isocline* 0*, starting from isocline* 4*, there are seeds on all the levels.*

We have a very important density property:

Lemma 2.15. *For any tile τ in a realization of the mantilla, fitted with the isoclines, there is a seed on an isocline* 0 *within a ball around τ of radius* 21*.*

Proof. From Figs. 13 to 15, there is an **8**-centre H at a distance at most 3 from τ. Let i be the number of the isocline on which H stands. Consider the ray issued from H which goes down along the axis of reflection of H which crosses its red vertex. If $i \in \{3..16\}$, then, going down along this ray, we find another **8**-centre H_1 on isoclines 14, 15 or 16, depending on the remainder of i modulo 3 at a distance at most 12 from H. The different situations are examined by Table 10 which, for each case, indicates a path from H_1 to a seed σ on an isocline 0.

These indications immediately follow from Figs. 13 to 15 which display the structure of the sectors and from Lemma 2.14. Indeed, in an **8**-sector, there are two F-flowers at distance 2 from the **8**-centre and which are white tiles: we indicate this by denoting them by Fw. There are also black F-flowers, denoted by Fb, also at distance 2. Now, the Fw-tiles are on the isocline $+1$ and the Fb-tiles are on the isocline $+2$. In the tree cases, the F-centre which appears on an isocline 0 is a seed. It can be checked that the distance from H_1 to the seed is 9, 6 and 6 when H_1 is on isocline 14, 15 or 16 respectively. Accordingly, the distance from H to σ is at most 18, so that the distance from τ to σ is at most 21.

We remain with the case when $i \in \{0..2\} \cup \{17, 18, 19\}$.

First, consider the case when $i \in \{17, 18, 19\}$.

In this case, we look at the centre A which is at distance 3 from H, above H, on the continuation of the ray of **8**-centres issued from H. We know that A is on the isocline $i-3$.

If A is an **8**-centre, we are done, as A lies on an isocline 14, 15 or 16. The distance of a seed σ on isocline 0 from A is at most 9, from Table 10. Hence, the distance of the seed from τ is at most 15. These cases are indicated in Table 11.

Table 10
Checking the density of the seeds: on a ray of **8**-centres

Node	Iso.	Dist.	Node	Iso.	Dist.	Node	Iso.	Dist.
8	14	9	**8**	15	12	**8**	16	12
8	16	+3	*Fw*	16	+2	*Fw*	17	+2
Fw	17	+2	*Gb*	18	+2	*Gw*	18	+2
G_r	18	+2	*Fb*	0	+2	*Fb*	0	+2
Fb	0	+2						

NOTE: The indication of the distance, in tiles, is relative to the node of the previous row, in the table. Also note that the distance indicated in the first line corresponds to *H* on an isocline 5, 3 and 4 respectively. For another position, we subtract a multiple of 3, according to the remainder of *i* mod 3.

Table 11
Table of the paths to σ when *H* is on an isocline 19, 18 or 19

			0	19	18	17	16	15	14
				8					
12	9	+6	σ				**8**		
10	7	+4	σ		*G*		*Fw*/*G*		
							Fb		
17	14	+11	σ						**8**
14	11	+8	σ		*G*		*G*		*Fw*/*G*
16	13	+10	σ		*G*		*Gb*	*Gw*	*Fb*
					8				
12	9	+6	σ					**8**	
14	11	+8	σ				**8**	*F*/*Gb*	
								Gw	
14	11	+8	σ					**8**	
						8			
14	11	+8	σ						**8**
12	9	+6	σ		*G*		*G*		*Fw*/*G*
14	11	+8	σ		*G*		*Gb*	*Gw*	*Fb*

The first column indicates the distance from τ to σ. The second indicates the distance from *H* to σ and the third one indicates the distance between *A* and σ. The columns entitled 0, 19, 18, 17, 16, 15 and 14 indicate the element of the path on the isocline with the number of the columns. When the path goes to the next row, there is no number on the first three columns.
NOTE: The difference between the numbers in the first three columns is 3, the distance from τ to *H*.

If *A* is not an **8**-centre, then it is an *F*- or a *G*-centre. The possibilities are given by Table 11. Now, depending on which isocline *A* is, we split the cases into two ones.

If *A* is on an isocline 16, there is a *G*-son of *A* on an isocline 18 when *A* is a *G*-centre or when it is an *Fw*-centre, see Fig. 20. Indeed, when *A* is an *Fb*-centre, as its *G*-son will be on an isocline 17, we have to proceed in another way. This is indicated in the table by another row below the one corresponding to the case denoted by *Fw*/*G*. In the new row, we have *Fb* in column 16, indicating the position of the centre. As there is nothing else in the row, this means that we go up to the father of *A*. Again we have two cases, depending on which father, on the same criterion as before as we are simply higher by two isoclines. Of course, the situation with *Fw*/*G* receives a similar solution: there is simply one more *G*-son on the path. Now, we can solve the case *Fb*, as it is on an isocline 14: it has a *Gw*-son on an isocline 15 and the black *G*-sons of this *Gw*-centre are on an isocline 16. Hence, we know how to find σ on isocline 0. It is easy to check that the distances are what the table indicates.

Next, we have the case when *A* is on an isocline 15. Now, as we assume that *A* is an *F*- or *G*-centre, we split the situation into two cases, depending on whether *A* is a *Gw*-centre or not. If it is not, we find an **8**-centre at a distance 2 from *A* on isocline 16. This is easy to check in Fig. 20. And then, we use the path indicated in Table 10. If *A* is a *Gw*-centre, then we can see from the same figure that its parental **8**-centre is on the same isocline as itself. And so, we get a **8**-centre on an isocline 15, at a distance 2 from *A*.

We arrive at the last case when *A* is on an isocline 14. Now, we split the cases as for isocline 16, as long as we are now higher by two isoclines. We need just to introduce another *G*-son to the path: it is always possible to have a *G*-son of a *G*-centre by two isoclines below, at a distance 2 from the father, as usual.

Second, consider the case when $i \in \{0..2\}$.

Whatever *A* be, we are on an isocline $i-3$, *i.e.*, an isocline 19, 18 or 17. If *A* is an **8**-centre, then we can apply the results of the previous table: the maximal distances from *A* to the seed are now 13 for isoclines 19 and 11, for isoclines 18 and 17 too. For the maximal distances from τ to σ, this gives us 19 and 17 respectively.

Now, we have to look at what happens when *A* is an *F*- or a *G*-centre.

First, we start when *A* is on isocline 19. If *A* is not a *Gw*-centre, then at a distance 2 from *A*, we find an **8**-centre on an isocline 18 and so, from there, by Table 11, we arrive at a seed σ on an isocline 0 by a path of length at most 11. Accordingly, this gives a distance from τ to σ which is at most 19.

If *A* is a *Gw*-centre, we can go from there at a distance 2 to an **8**-centre on the same isocline 19. We would get a maximal distance of 21. But we can get a better result. Take the father *B* of this *Gw*-centre which is necessarily at a distance 2 and on isocline 17, see Fig. 20. Then, we take again the father *C* of *B*. Now, *C* is at a distance 2 from *B*, either on isocline 16 or

Table 12
Table of the paths from H to σ when H is on an isocline 2, 1 or 0

		2	1	0	19	18	17	16	15
		8							
19	13				**8**				
					F/Gb				
19	$2+11$					**8**			
					Gw				
							F/G		
14	$2+2+4$							Fw/G	
18	$2+2+8$							Fb	
18	$2+2+8$								F/Gb
18	$2+2+8$								Gw
			8						
17	11					**8**			
						F/G			
18	$2+10$							F/G	
18	$2+10$						F/G		
				8					
17	11						**8**		
16	10						F/G		

on isocline 15. If C is on an isocline 16, we split this case into two situations which we already analyzed in Table 11: the case Fw/G and the case Fb. In the first case, C is at a distance 4 from σ and so A is at a distance $2+2+4=8$ from σ. In the second case, C is at a distance 8 from σ and so A is at a distance 12 from σ.

We remain with the case when C is on an isocline 15. This time, we split the situation into the case F/Gb and the case Gw. In both cases, Table 11 shows us that C is at a distance at most 8 from a seed σ on isocline 0. Accordingly, this tells us that σ is at a distance at most 18 from τ.

Now, we arrive at the case when A is on an isocline 18. Now, as A is assumed to be not an **8**-centre, its father B is an F- or a G-centre at a distance 2 from A and on isocline 17 or on isocline 16. Now, we have encountered the former situation in Table 11 and the latter in the discussion when A is on an isocline 19. And so, we find the indications of the table: if B is on an isocline 17, its distance to a seed σ of the isocline 0 is at most 10. If B is on an isocline 16, its distance to a seed σ is also at most 10.

At last, we arrive at the case when A is on an isocline 17. We already computed the distance of an F- or a G-centre on an isocline 17 to a seed σ of isocline 0, and we have found that it is at most 10. Accordingly, in this case, τ is at most at a distance 16 from σ. This completes the indications of Table 12.

Accordingly, the longest distance between τ and σ which we have found in this discussion is 21. This proves the lemma. ■

3. A parenthesis on brackets

Now, we turn to the basic process of the construction. This process is also used by Berger and by Robinson in their respective proofs. However, the process, although different, is more explicit in Berger's presentation where it is one dimensional, while Robinson directly deals with the two-dimensional extension of the same process. To better understand the process, we look at it from an abstract point of view. In the first sub-section, we shall consider the case when the process evolves on the whole line. In the second sub-section, we shall look at what happens if we restrict it to a ray.

3.1. The infinite models

Consider the following process:

We have a bi-infinite word of the form ${}^{\infty}(RMBM)^{\infty}$. We call this **row** 0. We define the next **rows** k as follows. Assume that the row k is of the form

$$ {}^{\infty}(R\_^{2^k-1}M\_^{2^k-1}B\_^{2^k-1}M\_^{2^k-1})^{\infty}, $$

where _ is called the blank. The word $R\_^{2^k-1}M\_^{2^k-1}B$ is called the **basic pattern** of the generation k or the **k-basic pattern**. Assigning positions to the letters by indexing them in $\mathbb{Z}$, we say that we superpose the rows one above the other by successively looking at the letters of the same position in the successive rows. We fix a way to superpose them by requiring that the letter R or B of the row $k+1$ is put over the M of a k-basic pattern. This fixes the position of the row $k+1$ with respect to the row k up to a shift by the length of the basic pattern. To better visualize the process, we consider the **even rows** as written **in blue** and the **odd rows** as written **in red**.

These rows can also be obtained from one another by a cancellation process: on the row k, we rewrite with blanks the letters R and B and the M letters are rewritten R or B according to the following rule. At random, we fix a basic pattern and

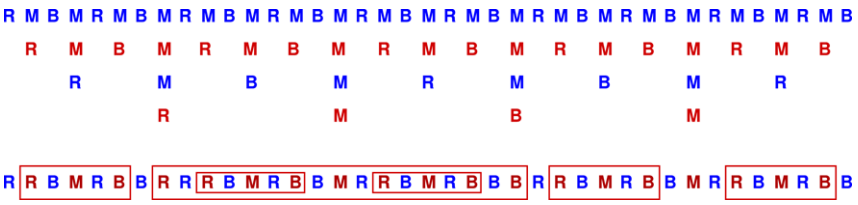

Fig. 22. The abstract rows and the transparent letters: inside the long red frame the transparent letters which are not in the smaller red frames. (For interpretation of the references to colour in this figure legend, the reader is referred to the web version of this article.)

then, we replace its M by R. The next M to the right is left unchanged and the second one is replaced by B and the third one is again left unchanged. Starting from the following M we repeat this process periodically. We also repeat the reverse sequence of actions to the left of the initially chosen M.

We shall call **active intervals** the set of positions delimited by the R and the B of a basic pattern. We shall specify blue or red interval according to the colour of the delimiting R and B. We shall also consider the set of positions defined by a B followed by the next R. We shall call this a **silent interval**, also specifying red or blue, depending on the colour of the delimiting B and R. At this point, we notice that active and silent intervals of the same generation have the same length and the same structure of proper sub-intervals, whether active or silent.

Now, assume that we superpose the rows of the generations from 0 to $2n+1$. In this superposition, we assume that the blanks and the blue letters are transparent. We are interested in counting the number f_n of letters inside a red active interval of the generation $2n+1$ which are not contained in a red active interval of a previous generation. This is illustrated in Fig. 22. Such letters will be called **free**. Note that, from this definition, the letters which are the ends of a red interval cannot be free.

We have the following property which can easily be derived from Figs. 22 and 23 by induction.

Lemma 3.1. *The number of free letters inside a red interval of the generation* $2n-1$ *is* 2^n+1, *with* $n \geq 1$.

Proof. Denote by f_n the number of free letters in a red interval of the generation $2n+1$. By the definition of the construction, we can see that active and silent intervals of the same generation can be transformed into each other by a simple shift of the length of these intervals. As this length is a multiple of the lengths of the intervals of smaller generations, such a shift changes nothing for the sub-intervals. In particular, the structure of the sub-intervals of an active and a silent interval of the generation n is the same, as already mentioned.

From Figs. 22 and 23, we can see that in a red active interval I of the generation $2n+1$, with $n \geq 1$, there are two red active intervals of the generation $2n-1$. The complement in I of these two red active intervals consists in an open silent interval J of the generation $2n-1$, and two intervals J_1 and J_2 of equal lengths which are a half of J. Clearly, what is free in J, J_1 and J_2 remains free in I. This counting gives us: $f_n = f_{n-1} + 2.\left(\frac{f_{n-1}-1}{2}\right) = 2.f_{n-1} - 1$, as f_n is odd, which is easy to see: the mid-point of a red active interval is free. As $f_1 = 3$, we get the expression of the lemma for f_n. ■

Now, we can also ask the same questions for the blue intervals, considering that now, blank and red letters are transparent. We easily get the following result, again by induction:

Lemma 3.2. *There is exactly one free letter inside of a blue interval of the generation* $2n$, *for* $n > 0$.

Proof. The same argument leads us to the same recursion relation with g_n the number of free letters in a blue interval and the induction starts from $n = 1$. Now, $g_1 = 1$ and so, we find $g_n = 1$ for all n. ■

The result of Lemmas 3.1 and 3.2 explains why we shall consider the red intervals in our construction.

The free letters also have another interesting property in the red intervals.

Lemma 3.3. *Let* $a_1, \ldots, a_{2^n+1}$ *be the positions of the free letters in a red interval of the generation* $2n+1$, *the first position in such an interval being* 1, *the ends not being taken into account. Then* $a_{i+1} - a_i \geq 2$ *except for* $i = 2^n$ *and* $i = 2^n + 1$ *for which* $a_{i+1} - a_i = 1$.

The proof is done by induction on n, the property being already true for generation 1. Note that in the proof of Lemma 3.1, we had to look at halves of intervals of the form $]BMR[$. In such intervals, the central M is never counted as well as the ends. Accordingly, by induction, the contribution of a half consists of isolated free letters.

We can describe the structure of the red active intervals contained in a bigger red active interval and of the free letters with better precision. First, it is not difficult to see that the free letters come from letters which are already present in generation 0:

Lemma 3.4. *Let* I *be a red active interval of the generation* $2n+1$, *with* $n > 0$. *Let* x *be a letter* R, M *or* B *belonging to a blue active interval of the generation* $2m$, *with* $0 < m \leq n$. *Then* x *cannot be a free letter.*

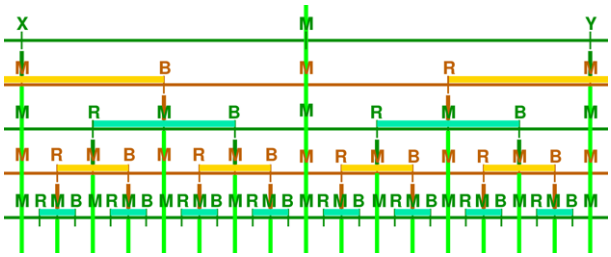

Fig. 23. The silent and active intervals with respect to mid-point lines. The light green vertical signals send the mid-point of the concerned interval to the next generation. The colours of the rows are *orange* and *green* with {orange, green} = {red, blue}. Similarly, $\{X, Y\} = \{R, B\}$. These conventions allow us to use the figure to study both active and silent intervals, whatever their colour. (For interpretation of the references to colour in this figure legend, the reader is referred to the web version of this article.)

The proof comes from the simple observation that, by construction, the R and the B of a blue interval of a positive generation $2n$, with $n > 0$, are generated by a red active interval of the generation $2n-1$. And so, they cannot be seen in a red interval of a generation m, when $m > 2n$.

Now, we can describe the positions of the red active intervals and of the free letters contained in a given active interval. They are given by the following lemma, giving a much more precise information:

Lemma 3.5. *Let I be a red active interval of the generation $2n+1$. Then, I can be split into its ends, its free letters and a finite set of intervals which exactly contains 2^k intervals of the generation $2(n-k)+1$. Similarly, if J is a blue active interval of the generation $2n$, then J can be split into its ends, its unique free letter and a finite set of intervals which exactly contain 2^k intervals of the generation $2(n-k)$.*

Proof. Consider H_n an interval of the generation n. Using the argument which we used for the proof of Lemmas 3.1 and 3.2, we obtain that

$$(*) \qquad |H_{n+2}| = 2.|H_n| + |H_n| - 2 + 2.\frac{|H_n| - 3}{2} + 2,$$

where $|H_n|$ is the number of letters contained in H_n.

This gives us $|H_{n+2}| = 4|H_n| - 3$, leading to $|H_{n+2}| - 1 = 4(|H_n| - 1)$. As $|H_1| = 5$ and $|H_0| = 3$, we get $H_{2n+1} = 4^{n+1} + 1$ and $H_{2n} = 2.4^n + 1$.

Rewriting (*) as $|H_{n+2}| - 3 = 2|H_n| + 2(|H_n| - 3)$, and replacing H_n by the just computed value in the first term of the second member of the latter equation, we get, by elimination, for odd generations:

$$\boxed{|H_{2n+1}| - 3 = 2^{n+1} + \sum_{k=0}^{n-1} 2^{n-k}(4^{k+1} + 1)}$$

and, for the even ones:

$$\boxed{|H_{2n}| - 3 = \sum_{k=0}^{n-1} 2^{n-k}(4^k + 1)}$$

From this decomposition in numbers, we get the splitting indicated in the lemma: in the left-hand side part of the equality, the subtraction represents the ends of the interval together with its mid-point. ■

We conclude this sub-section with additional important information on the silent interval, whose structure is very different from that of the active ones.

Say that a finite sequence $\{I_k\}_{k\in[0..n]}$ of silent intervals is a **tower** if and only if for each $k \in [0..n]$, I_k belongs to the generation n and if the mid-point of these intervals is the same position in I_n which thus, contains all of the members of the sequence. Note that if $\{I_k\}_{k\in[0..n]}$ is a tower, we have $I_k \subset I_{k+1}$ for all k with $0 \leq k < n$. The common mid-point of the silent intervals of a tower is called the **mid-point** of the tower. The last interval in the tower which contains all of them is called the **area** of the tower. We also say that this last interval **closes** the tower.

We have the following lemma:

Lemma 3.6. *Let I be a silent interval of the generation n. The silent intervals which it contains or intersects can be partitioned into finitely many towers. The set of the mid-points of these towers contains the mid-point of I. For the generations $n \geq 2$, it also contains both ends of I. Finally, for the towers which are contained in I and whose mid-point is not that of I, their areas belong at most to the generation $n-2$ and their mid-points are ends of proper intervals of I.*

The proof of this lemma is simply by induction on the generation to which I belongs. It can be illustrated by Fig. 23.

This gives a simple algorithm to construct the active and silent intervals generation after generation, considering that each generation is put on another line which we call **layer**.

Initial step:

$n := 0$;

the current layer is the layer n; the active and silent intervals of this generation are determined.

Induction step:

(i) The mid-point of the active intervals of the generation n which are determined on the layer n sends a red signal to the layer $n + 1$: it is the current **end signal** which consists of two kinds of signals. Each second signal is called R and the others are called B, the initial R being taken at random.

(ii) The mid-point of the silent intervals of the generation n sends a light green signal to the further layers: it is the current **mid-point signal**.

(iii) The layer $n + 1$ stops the end signals. The R-signals define the beginning of an active interval of the generation $n + 1$ and the next B-signal received on the layer defines the terminal end of the considered active interval. The end signals are absorbed by the layer $n + 1$. The complement intervals are the silent intervals of the generation $n+1$. The current mid-point signals which meet the mid-point of a silent interval go on to the next layer. The current mid-point signals which reach the mid-point of an active interval will emit the end signal of the next generation.

(iv) $n := n + 1$;

Algorithm 1. The algorithm to construct the active and silent intervals, generation after generation.

We shall go back to this algorithm in the next sub-section.

We conclude this sub-section with a look at the possible realizations of the abstract brackets. From now on, such a realization will be called an **infinite model** of the abstract brackets, **infinite model** for short. At each generation, we have two choices for defining the position of the active intervals of the next generation. Accordingly, this yields uncountably many infinite models, even if we take into account that if we fix a position which we call 0, there are countable models which can be obtained from each other by a simple shift with respect to 0. However, the different models do not behave in the same way if, for instance, we look at the towers of silent intervals. In this regard, we have two extremal models. In one of them, 0 is the mid-point of an infinite tower of silent intervals. As this model is symmetric with respect to 0, we call it the **butterfly model**. In another model, 0 is always contained in an active interval of each generation. We call it the **sunset model**.

As we shall later have to deal with the butterfly model, let us briefly indicate the following. Let a_n, b_n and c_n denote the addresses of the R, the B and the M of an active interval I of the generation n. Denote by d_n the address of the M which follows the B defined by b_n. If I_{n_1} is the active interval of the generation n for which a_n is the smallest positive number, we have $a_{n_1} = 2^n$, $b_{n_1} = 3.2^n$, $c_{n_1} = 2^{n+1}$ and $d_{n_1} = 2^{n+2}$.

We have the following 0-1 property for the infinite models:

Lemma 3.7. *Consider an infinite model of the abstract brackets. We have the following alternative: either for any position x, x belongs to finitely many active intervals or, for any x, x belongs to infinitely many active intervals.*

The proof relies on the fact that if x belongs to finitely many active intervals, there is a layer n such that if x belongs to an interval of the generation m with $m \geq n$, then the interval is silent. Let I be the silent interval of the generation n which contains x. Then, it is plain that the tower to which I belongs is infinite. Otherwise, there would be an active interval containing x and belonging to a generation k with $k > n$, a contradiction. Now, as an infinite tower is unique when it exists, the property holds for any position.

3.2. The semi-infinite models

Now, we consider what happens if we cut the result of the previous process, as illustrated by Fig. 23, at some position.

To simplify things, we take the M of a silent interval of generation 0. We imagine a vertical line δ starting from M, the layers being horizontal, and we say that δ cuts all the layers. By definition, we forget what happens on the left-hand side of δ and we look only at what remains on the right-hand side. Moreover, all active intervals which are cut by δ are removed. What remains will be called a **semi-infinite model**.

There are a lot of realizations of the semi-infinite model. A shift of the length of an active interval of the generation n in the infinite model leaves the smaller generation globally invariant but it affects the bigger generations. And so two different cuts do not affect the infinite model in the same way. Indeed, consider two cuts: one at δ_1 and the other at $\delta_1 + 2L_n$, where L_n is the length of an active interval of the generation n. In between δ_1 and $\delta_1 + 2L_n$ there is an interval of the generation $n+1$ which is contained in the semi-infinite model defined by $\delta_1 + 2L_n$ and not in the one defined by δ_1. And so, the interval of the generation $n + 1$ of the semi-infinite model closest to the cut is active in one semi-infinite model and silent in the other.

Say that when a position is contained by an active interval, it is covered by this interval.

Consider an infinite model of the abstract brackets, fix a position x and focus on the semi-infinite model defined by the cut at x. Then we have:

Lemma 3.8. *Consider an infinite model of the abstract brackets and the position x of a cut. In the semi-infinite model defined by the cut at x, for any position y after x, y is covered by finitely many active intervals.*

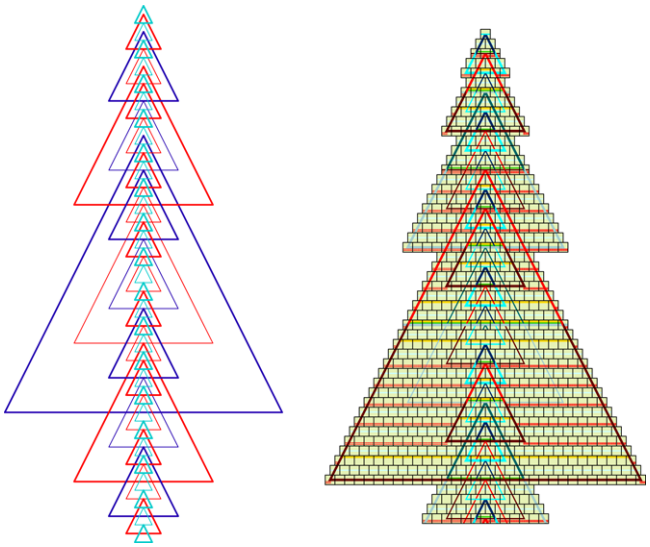

Fig. 24. Left-hand side: an illustration for the interwoven triangles; right-hand side: realization of the same triangles in the Euclidean plane by appropriate tiles. Note the towers of phantoms.

The proof is straightforward from the following property:

Lemma 3.9. *Consider an infinite model of the abstract brackets and the position x of a cut. Let y be a position with $x > y$ and assume that in the model, any position is covered infinitely many often. Then, there is an active interval I which contains both x and y.*

From Lemma 3.9, the proof of Lemma 3.8 is easy: as active intervals of the same colour are either disjoint or embedded, if an active interval J contains both x and y, this is also the case for any active interval I which contains J. This rules out all the active intervals of the same colour and of bigger generations which contain y. For the other colour, either all active interval containing y do not contain x or at least one of them contains x and so, we have the same conclusion for intervals of the other colour. Note that it is not difficult to construct infinite models where 0 is covered by infinitely many blue active intervals and by no red active interval.

Now, the proof of Lemma 3.9 is not difficult. From one generation to the next one, the length of an interval gets twice bigger. This means that if $y \in I_n$, where I_n is an active interval of the generation n, then $]y - \frac{|I_n|}{2}, y + \frac{|I_n|}{2}[$ is contained in K_{n+1}, the interval of the generation $n + 1$ which contains y. As infinitely many active intervals contain y, we may assume that $|I_n| > 2|y-x|$. Accordingly, $x \in K_{n+}$. If K_{n+1} is active, we are done. If not, K_{n+1} is contained in a tower of silent intervals which cannot be infinite, by the assumption of the lemma. Now, by construction of the model, the area of a tower is contained in an active interval of the next generation. And so, K_{n+1} is contained in an active interval which, thus, contains both x and y. And so, both lemmas are proved.

From Lemma 3.8, from the uniqueness of the infinite tower in the butterfly model and from Lemma 3.9, we can draw the following conclusion:

Lemma 3.10. *Let x be the position of a cut in a semi-infinite model. Let y be another position with $x < y$. Then, except if y is the position* 0 *in the butterfly model, y is always covered by an active interval.*

Deep results on the space of all these realizations are given by an accurate analysis to be found in [10]. The interested reader should have a look at this paper.

In the next two sub-sections, we deal with the implementation of these models first, in the Euclidean plane and then, in the hyperbolic plane. The study of the semi-infinite models is especially needed by the implementation in the hyperbolic plane.

4. The interwoven triangles

In this sub-section, we make the first step to lift up the infinite models of abstract brackets to the hyperbolic plane. This consists in a detour via the Euclidean plane.

We lift up the intervals as **triangles** in the Euclidean plane. The triangles are isosceles and their heights are supported by the same line, called the **axis**, see the left-hand side picture of Fig. 24. The legs of the same side of the triangles are parallel.

From now on, we restrict the word **triangle** to the objects which represent an active interval of the infinite model. For the silent intervals, also represented in our lifting, we use the word **phantom**. For properties shared by both triangles and phantoms, we shall speak of **trilaterals**. For the set of all trilaterals, we shall speak of the **interwoven triangles**.

The interwoven triangles have a lot of properties which they inherit from the infinite models. The first one corresponds to the non-intersection property of the active intervals.

Lemma 4.1. *The triangles of the generation $n+2$ do not meet the triangles of the generation n. Accordingly, the area of a triangle of the generation n is contained in the area of some triangle of the generation $n+2$.*

The proof comes from the same property for the active intervals. If the triangles would meet, their intersection would produce an intersection in the projections.

Note that the property does not hold for the phantoms. For the phantoms, we can collect them into towers, exactly as this was done for the silent intervals. We have:

Lemma 4.2. *Phantoms can be split into* **towers** *of embedded phantoms. The phantoms of a tower have the same mid-point. This mid-point may be the vertex of a triangle or the mid-point of a basis of a triangle. In a tower, the colours of the phantoms it contains alternate and each phantom of a tower contains phantoms of all smaller generations.*

This is a direct consequence of Lemma 3.6. As for towers of intervals, we shall say that the biggest phantom of a tower **closes** the tower.

The problem of intersections between trilaterals can be made a bit more exact. We have the following general properties.

Lemma 4.3. *Between trilaterals, the crossings occur between legs of one figure and the basis for the other figure.*

Lemma 4.4. *A leg of a trilateral is never cut inside the open interval delimited by the mid-distance line and the basis of the trilateral.*

The easy proofs of Lemmas 4.3 and 4.4 rely on the proof of Lemma 3.5 and on the following property. To formulate it, consider two intervals $I = [x, u]$ and $J = [y, v]$ on the axis, x, y, u and v being positions of letters. Let T_I be the isosceles triangle, with its vertex at x, its legs parallel to the legs of the interwoven triangles, and its basis cutting the axis at u. Similarly, define T_J from J. Denote by $ar(T_I)$ and $ar(T_J)$ the areas of T_I, T_J respectively. Then, obviously, we have:

Lemma 4.5. *Let $I = [x, u]$ and $J = [y, v]$ be two intervals on the axis. Assume that $x < y$. If $u < y$, then, $ar(T_I) \cap ar(T_J) = \emptyset$. If $y < u < v$, then the basis of T_I cuts the legs of T_J. If $v < u$, then $ar(T_J) \subset ar(T_I)$.*

Now, from the analysis of towers of phantoms and from the construction of the generation $n + 1$ from the generation n, we have:

Lemma 4.6. *A trilateral T of a generation $n+1$ exactly meets two triangles P_1 and P_2 of the generation n: the legs of T meet the basis of P_1 while the legs of P_2 meet the basis of T. If T is a triangle, it also meets a trilateral F of the generation $n+2$: the legs of F meet the basis of T.*

Lemma 4.7. *A trilateral T of the generation $n+1$ meets all the phantoms contained in the triangles P_1 and P_2 of the generation n which generate T. The intersections occur by the bases of the phantoms inside P_1 meeting the legs of T and by the basis of T meeting the legs of the phantoms inside P_2, at their mid-point.*

From the construction of the abstract brackets, we get a simple algorithm to construct the interwoven triangles.

Algorithm 2. The construction of the interwoven triangles, generation after generation.

(i) Generation 0 is fixed by alternating triangles and phantoms. It is marked by the colour **blue-0**. The mid-point of the phantoms emits a horizontal green signal in both directions.
(ii) When the generation n is completed:

- At random, we choose the mid-point of a **triangle** of the generation n. We put there the vertex of a trilateral, choosing between a triangle or a phantom at random.
- This vertex grows legs of a colour which is opposite to that of the generation n: here too, blue and red are opposite to each other. Blue is the colour of the trilaterals of positive even generations. Red is the colour of trilaterals of the odd generation. Red is also considered as the opposite of blue-0.
- The legs grow until they meet a green signal. If the trilateral is a triangle, the legs stop the green signal. If the trilateral is a phantom, the green signal crosses the legs. In both cases, the legs go on until they meet a basis of their colour. They stop it and constitute a trilateral of the generation $n + 1$. Now, the intersection of the basis of the trilateral with the axis requires a vertex: of a triangle if the basis belongs to a phantom, of a phantom if the basis belongs to a triangle.
- The process is repeated endlessly: downwards and upwards.

(iii) $n := n + 1$;

To detect what corresponds to the free letters and which we call the **free rows** of a red triangle, we append the following mechanism to point (ii) of Algorithm 2: the legs of red triangles emit red horizontal signals outside the triangle. Moreover, these signals have a laterality: a right-hand side leg emits a right-hand side signal and a left-hand side leg emits a left-hand side signal except at the vertex and when crossing the basis of a red phantom. Such signals are forbidden to meet inside a triangle and they cross legs of outer trilaterals, only of their laterality for red triangles: accordingly, they cannot run on a free row inside a red triangle. This mechanism does not alter the detection of the green signal and of the correct basis.

We shall go back to this algorithm in the next sub-section.

In [18], we proved:

Lemma 4.8. *The interwoven triangles can be obtained by a tiling of the Euclidean plane which can be forced by a set of* 190 *tiles.*

In Sections 6.2.1 and 6.2.2, we describe the tiles, taking into account the properties of the above lemmas. In [18], the corresponding tiles are displayed in a square format, as required for *à la* Wang tiles. Note that the set of prototiles referred to by the lemma also provides the detection of the free rows of red triangles which are marked by an appropriate signal, called the **yellow** signal.

5. Implementing the interwoven triangles in the hyperbolic plane

The idea of the implementation in the hyperbolic plane is based on the fact that the isoclines which we introduced in Section 2.5 provide us with the horizontals which are needed to construct a space–time diagram. Recall that the isoclines are periodically numbered from 0 to 19.

From Lemma 2.14, we define isoclines 0, 5, 10 and 15 to play the role of the rows in the Euclidean implementation. The trilaterals will be constructed on trees of the mantilla. The vertex is realized by a seed, and the legs are supported by the borders of the tree rooted at the seed. The basis is defined by an isocline which cuts both borders of the tree.

As there are 6 seeds on isocline 5 inside the tree defined by a seed on isocline 0, there are 6 trilaterals of generation 1 raised by a triangle of generation 0. And so, contrary to what happens in the Euclidean construction where a triangle generates a single trilateral of the next generation, here we have several trilaterals of the same generation for the same set of isoclines crossed by the legs of these trilaterals.

Call **latitude** of a trilateral the set of isoclines which are crossed by its legs, vertex and basis being included.

We shall look at a thread as a frame for the implementation of a semi-infinite model of the abstract brackets through the interwoven triangles. In case of ultra-threads, we can even implement an infinite model. But, even when there are ultra-threads, there are also threads, so that semi-infinite models cannot be avoided. Moreover, each latitude is crossed by infinitely many threads so that there will be infinitely many trilaterals within a given latitude. This property will be proved a bit later. Now, due to the working of the Euclidean implementation, the realizations associated to the threads cannot be independent: the same latitude cannot be used both for a triangle and for a phantom of the same generation. Consequently, the implementation of the semi-infinite models must be **synchronized**. The semi-infinite models must be considered as different cuts of the same infinite model, implemented in such a way that the latitudes of the triangles match. Consequently, the possibility of the realization of the infinite model in the case of ultra-threads brings in no harm: it can be viewed as a cut at infinity.

The goal of the synchronization is to guarantee that Algorithm 2 will be in action here too, up to a few tunings needed by the synchronization. These changes will concern the definition of the axis of the implementation and the synchronization of the horizontal signals: the vertices, the bases of trilaterals, the mid-points of their legs and the horizontal signals emitted by the legs of a triangle. The colours defined in Section 4 are also used here. Generation 0 is blue-0, even generations are blue or simple blue, and odd generations are red. Legs and bases of triangles are drawn with thick strokes, those of phantoms are drawn with thin ones. In order to facilitate the detection of the various horizontal signals, the first half of blue-0 and blue trilaterals is dark while the second half is light. We use the opposite convention for red trilaterals: the first half is light and the second half is dark. The tile of the mid-point of a leg is both dark and light coloured: the first colour for a first half in the upper part of the tile, the second colour for a second half in the lower part.

5.1. The scent

By definition, we decide that all seeds which are on an isocline 0 are **active**. This means that they actually grow legs of a triangle of generation 0. We can reformulate Lemma 2.15 by saying that **the set of active seeds is uniformly distributed in the hyperbolic plane**. By *abus de langage*, we shall say that it is **dense** in $\mathbb{H}^2$.

Next, an active seed diffuses a **scent** everywhere inside its trilateral until the fifth isocline, starting from this seed, is reached. Seeds which receive the scent on isoclines 5, 10 and 15, and only those, become active. The other seeds of these isoclines become **silent**: they do not give rise to a trilateral.

The green signal is triggered by the mid-point of the legs of the phantoms of generation 0: they namely lie on an isocline 15. Note that, by construction, the triangles of generation 0 are not determined by the meeting of a green signal: the change from the first half of the leg to its second half is performed when the first isocline 5 is encountered. But, for the phantoms of generation 0 and for the trilaterals of the other generations, the construction is determined by the meeting of a green signal, always on an isocline 15.

We can see that the scent process constructs a tree. Each branch of the tree materializes a thread which implements the considered semi-infinite model. Note that the above synchronization mechanism fixes things for spaces between triangles but also inside them. Indeed, these spaces become larger and larger and so, starting from a certain latitude, isoclines 0 produce active seeds which are inside these spaces, creating new implementations of semi-infinite models.

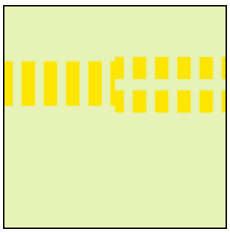

Fig. 25. The pattern of a join-tile. (For interpretation of the references to colour in this figure legend, the reader is referred to the web version of this article.)

5.2. Synchronization: The mechanisms

Due to the occurrence of several trilaterals within a given latitude, we have now to require that all triangles, red, blue and blue-0, emit a signal along each isocline which meets their legs the signal going outside the triangle. The signal has the colour of the triangle and it has the laterality of the leg which emits it. The signal will be called **upper** as, in the tiles, it will be placed over the path of the isocline. The signal will be emitted by the legs of triangles, except the vertex which never emits this signal and at the meeting of a basis of a phantom of the same colour. This is a simplification with respect to the implementation described in [16,18]: it also reduces the number of tiles. Now, as in [16,18], we require that the corners of a phantom also emit an upper signal of its colour, outside the phantom, and of the laterality of the corner.

Various problems

Now, in between two contiguous triangles of the same latitude, horizontal signals of the same colour but with a different laterality will meet. We have to allow such a meeting. It will be performed by an appropriate tile which we call the **join-tile**. There is a join-tile for red signals and another for blue signals. The join-tile, see the pattern illustrated by Fig. 25, illustrates such a junction. Note that, on the left-hand side, we have the right-hand side signal and that, on the right-hand side, we have the left-hand side signal. Now, the opposite junction does not exist. This is conformal with the working of Algorithm 2, see Section 4. Moreover, the opposite junction cannot be obtained from this tile, as completely turning tiles is impossible in our setting. This is guaranteed by the existence of the isoclines and by their numbering.

We also require that an upper horizontal signal of a given laterality may cross a leg of a trilateral of the same colour only if it has the same laterality as the leg. When the colours are different, the crossing is always permitted, whatever the lateralities of the leg and of the signal.

From the impossibility to get the opposite junction to the junction realized by a join-tile, we obtain the following principle:

Lemma 5.1. *An upper horizontal signal with a constant laterality cannot join two legs of the same trilateral.*

Proof. This is an easy corollary of the rule about the meeting of the legs with an upper horizontal signal. ■

The second mechanism which we introduce to force the synchronization of different constructions is that all bases on a given isocline merge. This changes the tiles of the corner, but this does not affect Algorithm 2. This also does not change the fact that corners emit an upper horizontal signal of their colour and of their laterality outside the trilateral to which they belong, see Fig. 26.

Now, the upper signals allow to differentiate the various parts of a basis. If a basis has an upper horizontal signal of its colour, we are outside a trilateral of the generation of the basis. If not, we are inside. We say that the basis is **covered** if it is accompanied by an upper horizontal signal of its colour. Otherwise, we say that the basis is **open**.

This distinction is important. When a leg meets a basis: if it is the first half of a leg, *i.e.* between the vertex and the mid-point of the leg, it meets the basis without changing it. When the second half of a leg meets a basis, it crosses it if the colour is different. If the colour is the same, it crosses it only if the basis is covered. Indeed, from Lemma 5.1, an upper horizontal signal cannot go from one leg of a trilateral to the other: there must be a triangle of the same colour in between. And so, an open basis does not cross the second half of a leg of a trilateral of the same colour. Accordingly, for the second half of the leg, when the leg meets such a signal, this means that the expected basis is found.

Now, there is a problem if we consider the situation of a missing trilateral. In the same latitude, other trilaterals are realized. This comes from the following result.

Lemma 5.2. *Within a given latitude corresponding to an interval of the model realized by the tiling, there are infinitely many trilaterals.*

Proof. Consider the lowest row β of the latitude. As we know the interval I corresponding to the considered latitude, we also know the highest row κ of the latitude. Now, fix a tile τ on β. There is at least one **8**-centre H over κ such that the ray ρ crossing the **8**-centres below H, look at Figs. 13–15, meets the isocline of β on the left-hand side of τ. We may assume that there is an isocline 0 between H and κ. Considering a seed σ on this isocline which is on the left-hand side of H, it is now plain that the tree rooted at σ is on the left-hand side of ρ and that, as all the triangles of the generation 0 starting

Fig. 26. In between two consecutive triangles of the same generation, within the same latitude. In the red circle, a zoom on the configuration. Note that this figure makes use of the half-plane model of hyperbolic geometry, using the lines which are parallel to the x-axis to support the isoclines, as they follow horocycles. (For interpretation of the references to colour in this figure legend, the reader is referred to the web version of this article.)

from σ are present, there is a trilateral associated to β and κ inside the tree rooted at σ. By taking the reflection in ρ of this construction, we can prove the same property for the right-hand side of the tile τ. Now, taking two tiles τ_1 and τ_2, with τ_1 on the left-hand side of τ_2, we have a trilateral on the left-hand side of τ_1 and another one on the right-hand side of τ_2. Repeating this argument, we get infinitely many trilaterals. ■

Now, consider two such trilaterals T_1 and T_2, with T_1 on the left-hand side of T_2 and such that there is no other trilateral of this latitude in between T_1 and T_2. Each T_i, $i \in \{1, 2\}$, contains a triangle P_i such that P_i contributes to the generation of the basis β of T_1 and T_2. We may assume that there is no triangle of the latitude of P_1 between P_1 and the right-hand side leg of T_1 and, we may assume the same for P_2 and the left-hand side leg of T_2. Consider the upper horizontal signal σ which accompanies β and which is produced by the right-hand side corner of T_1. It is of the colour of β which is opposite to the colour of P_1. The signal σ crosses the legs of the copies of P_1 which are in between T_1 and T_2. Consider such a copy P. Inside P, whose mid-distance line is on the isocline of β, σ meets towers of phantoms of the generations smaller than that of P. Now, if β crosses the phantoms of a tower and if there are at least two phantoms in the tower, as the colours of the phantoms alternate in a tower of phantoms, we get a contradiction with Lemma 5.1.

We postpone the solution to this problem after the presentation of another problem of this kind.

Indeed, if we assume that the bases of triangles of the same generation and the same latitude match, the mid-distance lines of trilaterals of the same latitude also match. Let ι be the isocline 15 of the mid-distance lines. Now, we have towers of phantoms inside these trilaterals whose mid-distance line is also supported by ι. We already know that, within a given latitude, there are infinitely many trilaterals, see Lemma 5.2. Consequently, all of them have the same colour and all of them are triangles or all them are phantoms. Now, in between two consecutive **triangles**, there are phantoms of smaller generation which have the same mid-distance line as these triangles. Such phantoms do occur inside a triangle, this is clear from the study of the abstract brackets and the tower structure of the phantoms. But this also occurs in between consecutive triangles. This comes from the fact that the seeds of the isoclines 0 are all active. Accordingly, they trigger the generation of new semi-infinite models of the same infinite model.

The conclusion is that, in between two triangles of a positive generation, of the same latitude and on the isocline of their mid-distance line, there is a green signal inside the triangles, and there are also others outside them. Now, for the correctness of the algorithm, it is important that triangles stop the green signal and that phantoms do not stop it. Accordingly, these different green signals must not meet when they travel on the same isocline.

We have a common solution for these problems, but their exact implementations present a few differences. Also, it will be useful to have a closer look at what happens in between consecutive triangles. Lemma 5.2 only gives a qualitative information which is not enough to clearly understand the reason of the situation. Now, we turn to this point and later, we shall present the solutions to the problems which we raised in this sub-section.

The remotest ancestor

Consider a trilateral T_0 of generation $n+1$. In the infinite model, there is a **triangle** T_1 of generation n such that the vertex of T_0 is on the mid-distance line of T_1. If T_1 is realized, we say that T_0 **has a father**: T_1. Note that if a trilateral has a father, it is unique, but several trilaterals have the same father. We say that T has a **remotest ancestor** if there is a sequence $\{T_k\}$, $k \in \{0..n\}$, such that T_{i+1} is the father of T_i, $i \in \{0..n-1\}$ and that $T_0 = T$. It is plain that T_n belongs to generation 0. In many cases we shall also call **remotest ancestor** the vertex of T_0. The context will be clear whether we speak of the seed or of the tree. Note that a trilateral may be without a father and, consequently, it may have no remotest ancestor.

We can formulate the following property.

Lemma 5.3. *For any trilateral T, there are infinitely many copies of T within the same latitude which have a remotest ancestor A. If n is the generation of T, then the distance, in number of isoclines* 0, 5, 10 *or* 15 *from the vertex of T to the vertex of A, is $2^n - 1$. Now, let T_1 and T_2 be two trilaterals of the same generation within the same latitude. Assume that both of them have a remotest ancestor. Then, there is a trilateral of the generation of T_1 in this latitude in between T_1 and T_2 which also possesses a remotest ancestor, if and only if there is an active seed between the remotest ancestor of T_1 and that of T_2.*

Proof. We know that, in the infinite model, the father of T exists and there, this can be recursively repeated. This means that the remotest ancestor A exists in the infinite model. Now, as n is the generation of T, the distance, in number of isoclines 0, 5, 10 and 15, from the vertex of T to the vertex of A is

$$\sum_{k=0}^{n-1} 2^k = 2^n - 1.$$

Note that, measured in the same way, the height of T is $2^{n+1} + 1$. In the infinite model, the mid-distance line of T generates the basis of a trilateral Q. From the just performed computation, we conclude that each term of the sequence $\{T_k\}$, $k \in \{0..n\}$ is contained in Q. In particular, A is contained in Q. Now, from the proof of Lemma 5.2, we know that in any latitude, there are infinitely many realizations of the trilateral corresponding to this latitude. Also, we know that when a trilateral is realized, all trilaterals of previous generations which it contains are also realized. Accordingly, there are infinitely many copies of T, within the same latitude, which possess a remotest ancestor.

The last assertion of the lemma immediately follows from the definitions. ■

From the proof of the lemma, we can derive an important piece of information on the trilaterals inside a given latitude.

Lemma 5.4. *Let T_1 and T_2 be two trilaterals of the same positive generation $n+1$ and within the same latitude. Let ι be the isocline of their mid-distance lines. Assume that there is no trilateral of the generation $n+1$ in between T_1 and T_2. Then, there is a phantom of the generation n in between T_1 and T_2 whose mid-distance line is also on ι.*

Proof. Consider the seeds S_1 and S_2 which are on the closest isocline 0 above the vertex of T_1 and from which the scent comes to the vertices of T_1 and T_2 respectively. The closest distance between two consecutive active seeds on the same isocline, measured in the number of tiles crossed by the isocline between these seeds is 26. It is realized by the F-sons of the G_ℓ- and G_r-sons of a black F-flower. The biggest distance is 416, which is reached at the twelfth isocline from an **8**-flower. This is proved by the recursive structure of the tiling by its splitting into the sectors defined in Section 2.2 and by a checking of the first twenty one isoclines from the centre of a sector by a computer program. Now, two consecutive white nodes give rise to two non-intersecting Fibonacci trees which have both 144 tiles on their fifth level. Accordingly, as the distance in isoclines from S_1 and S_2 to the vertices of T_1 and T_2 is at least 5 and as there are at least 10 white nodes between S_1 and S_2 the distance between the vertices of T_1 and T_2 is big enough to give room to a lot of active seeds. In each of them, by synchronization and by what happens inside T_1, there is a phantom of the generation n: its latitude is placed between the latitude of the triangles of the generation n which contains the basis of T_1 and the latitude of the triangle which contains the head of T_1. ■

Now, we are ready to turn to the solutions of the problems which were raised at the beginning of this sub-section. The idea is to create signals which will go from a triangle to the next one in such a way that signals 'overpass' the biggest concerned phantom of a tower within the considered latitude. The signals will satisfy two constraints: they must not disturb the working of Algorithm 2 inside each phantom of the tower; they will convey their characteristics unchanged, as if the tower of phantoms was not present.

We shall see that both constraints, apparently a bit contradictory, can be satisfied within a satisfactory compromise.

We start with the green signal: its solution is simpler.

A solution for the green signal

To solve the problem, we introduce another upper horizontal signal, the **orange signal** which shares isoclines 15 with the green signal. Now, contrary to the green signal which has no laterality, the orange signal exists in two versions only: a left-hand side and a right-hand side ones. They both occupy the indicated isoclines with the green signal, but alternately, never on the same segment of the isocline, even inside a tile.

Clearly, when a leg of a triangle meets the green signal which is inside it, the leg turns to its second half, it stops the green signal and, at the same time, it emits an orange signal of the laterality of the leg, outside the triangle. We can see this signal as an **antenna** of the triangle which looks forward to handle the other antenna which is emitted, from the other side, by the closest triangle of the same latitude, see Fig. 27. Now, during this search, the signal meets phantoms on its way, as can be seen from Lemma 5.4.

When the orange signal meets the first phantom standing in front of it, it climbs up along the leg of the phantom until it reaches the vertex. There, it goes down along the other leg, until it meets the isocline which contains the green signal which is inside the phantom, on the other side of the leg, in the tile which realizes the junction of the leg with the green signal and, also, the turn to the second half of the leg. This tile also sends an orange signal on the right isocline, so it goes on its way to the orange signal of the opposite laterality which is running to it, at some point, in front of it.

Note two points: during this climbing up and down, the signal keeps its laterality. Inside the phantom which supports the orange signal on the upper parts of its legs, there may be other phantoms for which the same green line is used to make

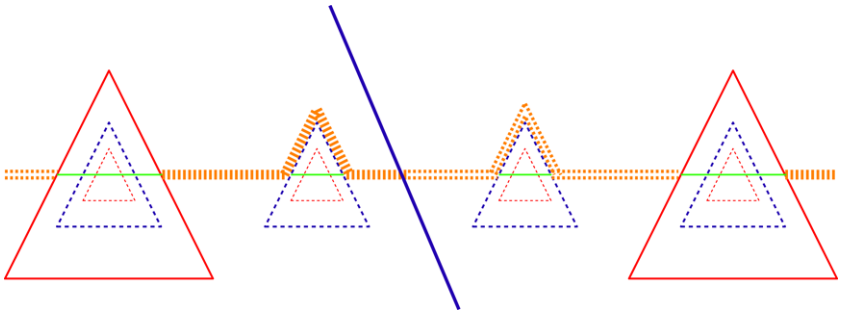

Fig. 27. In between two consecutive triangles of the same generation, within the same latitude. The phantoms in between them which have the same mid-distance line as the triangles.

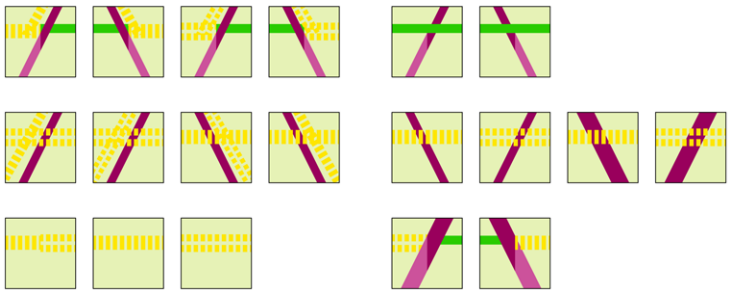

Fig. 28. The tiles for the antennas of triangles. A solution which also works for horizontal signals. (For interpretation of the references to colour in this figure legend, the reader is referred to the web version of this article.)

the separation between the first and second halves of their legs. Note that the just described climbing of the orange signal can be repeated for other phantoms of the same generation standing in between our triangles, within the same latitude. This is repeated until the signal, coming from the next triangle, meets the one we consider. Both signals can be joined by a tile similar to that of Fig. 25.

Now, legs of trilaterals can be crossed by an orange signal: this is possible if the signal travels on an isocline which is not the mid-distance line λ of the trilateral. Such a situation occurs: from the study of the abstract brackets, we know that a phantom contains inside itself the same trilaterals as a triangle of its generation. For these inner triangles, their mid-distance lines do not travel on the isocline of λ. Accordingly, the orange signals emitted by inner triangles cross the legs of the trilaterals whose mid-distance line is on λ, either in their first half or in their second one. We provide tiles for such a crossing, see Fig. 28, noticing that here too, we apply the rule that the orange signal of a given laterality must cross legs of the same laterality. As proved in [21], in between two consecutive triangles, there is a finite interval $[a, b]$ on the isocline of their mid-distance line such that, on the left-hand side of a, legs which cross the topmost isoclines of the latitude belong to a bigger generation and all of them are right-hand side legs. On the right-hand side of b, legs which cross the topmost isocline of the latitude belong to a bigger generation and all of them are left-hand side legs. Consequently, the join-tile can be placed at any tile of the interval $[a, b]$ which is not inside a phantom. In fact, as a corollary of Lemmas 5.3 and 5.4, we can prove the following:

Lemma 5.5. *Consider two consecutive triangles of the same generation and within the same latitude. Then, there is at most one leg of a trilateral of a bigger generation which crosses the topmost isocline of the latitude between the two triangles.*

Proof. Indeed, denote by T_1 and T_2 the two triangles. Let n be their generation. Consider a leg in between them, of a bigger generation. Let T be the trilateral to which this leg belongs. As the generation of T is bigger than n, we may assume that the vertex of T_1 or that of T_2 belongs to T. Otherwise, both legs of T would be in between T_1 and T_2 and, by synchronization, there would be inside T the vertex of a trilateral T_3 of the generation n. Accordingly, T_1 and T_2 would not be consecutive. Assume that the vertex of T_1 is inside T. From the proof of Lemma 5.3, T_1 has a remotest ancestor A: the vertex of T has a distance at least 2^n-1 from the isocline of the vertex of T_1 if T is of the generation $n+1$ or $n+2$, and it is much higher if the generation is bigger. Let B be the closest active seed to A on its right-hand side. By synchronization, B generates a copy T_3 of T_1 which is of the generation n and within the same latitude as T_1. Clearly, T_2 is in between T_1 and T_3. Now, as the leg of T is in between T_1 and T_2, it is also in between T_1 and T_3, which means that the leg is also in between A and B. Now, from the proof of Lemma 5.4, we know that the distance between A and B is much smaller than the distance between two legs of a generation bigger than n issued from vertices which are higher than A by at least five isoclines. And so, there cannot be another leg of a bigger generation in between T_1 and T_2. ■

From this study, we also conclude that Lemma 5.1 applies to the horizontal orange signals. In particular, if an orange signal crosses a leg of a trilateral, this means that there is a triangle of a smaller generation inside this trilateral. This is

indeed the case, as a trilateral of a given generation n, with $n \geq 2$, always contains trilaterals of a smaller generation than the generation $n-1$.

A solution for the horizontal signals

The solution for the horizontal signals is inspired from the previous one.

Let us go back to the situation of two triangles T_1 and T_2 of the same generation, within the same latitude, with no triangle of the same generation and the same latitude in between. Let P_1 and P_2 be the triangles which generate the basis of T_1 and T_2 and which are the closest to the appropriate legs of T_1 and T_2, as in the initial description of the problems. The right-hand side leg of T_1 emits right-hand side upper horizontal signals and the left-hand side leg of T_2 emits left-hand side upper horizontal signals, all of them of the colour of T_1. Let n be the generation of T_1 and assume that $n \geq 2$. If there was neither a triangle nor a phantom between T_1 and T_2, which is the case for the generations 0 and 1, the join-tile of the appropriate colour would be the solution.

Now, inside the latitude of T_1, we find two triangles of the generation $n-2$, S_1 and S_2 and three phantoms F_1, F_2 and F_3 with the following conditions: S_1 is above S_2, F_1 is above S_1, F_2 is between S_1 and S_2, and F_3 is below S_2. In fact, within the latitude of any of these five trilaterals, we may find several copies of the same trilateral. Now, if an upper horizontal signal comes from T_1 on an isocline which meets a leg of S_1 or S_2, as the left-hand side legs of S_1 and S_2 emit left-hand side upper signals, they meet the signals sent by T_1 with the join-tile. On the right-hand side of S_1 and S_2, the right-hand side legs emit a left-hand side signal and so, we have the same situation with the next copies of S_1 and S_2, until the last right-hand side signals again meet the left-hand side signals emitted on the same isoclines by the left-hand side leg of T_2. Again, the join-tile solves this situation.

Now, for the upper signals travelling on an isocline which meets F_i, the situation is different, as a phantom does not emit signals, except at its corners. However, there is also a simple solution. If the phantom contains a triangle of its colour, this triangle will emit the upper signals which are not stopped by the legs of the phantom as we may assume that their laterality is that of the legs of the phantom. But the phantom has free rows, exactly as a triangle of the same generation. We have already come across this property: the structure of the inner trilaterals of a phantom is the same as that of a triangle of its generation. Now, for a free row, Lemma 5.1 forbids the signal to cross the phantom. Now, we can do the same as what we did for the green signal. We simply allow the upper horizontal signals to climb up the leg of the phantom when they meet a free row of the phantom. In the case of a blue phantom, we have exactly the same situation as for the green signal as a blue trilateral exactly has one free row, namely on its mid-distance line.

In a red phantom, the situation is a bit more complex, as there are a lot of free rows. In fact, starting from the deepest upper signal within this latitude, the signal climbs up along the left-hand side leg and stops all the upper signals travelling on the isocline of a free row, inside F. When the climbing signal arrives at the vertex, it goes down, keeping its laterality. Now, going down along the right-hand side leg of F, each time it meets the isocline of a free row of F, it emits an upper signal of the same laterality outside the phantom and it still goes down. When the going down signal or the climbing up one meets the isocline of a non-free row inside F, the upper signal travelling on the isocline crosses the leg of F, as it will meet a leg of a red triangle. To simplify the managing of this case, the climbing up signal starts from the basis of F and the going down one stops at the basis of F. Again, the laterality of the signal is unchanged while passing over the vertex, as this is the case for the orange signals. Now, the conclusion is clear: the climbing up and going down signals realize two combs on each side of the phantom and they gather up upper signals of the same laterality arriving on the free rows of the phantom. On one side of F, this laterality is different from that of the upper signals which cross the legs of F.

Now, we can see that the above two conditions are satisfied: inside the red phantom, nothing is disturbed and outside the phantom, the signals behave as if the phantom and its inner phantoms were not present. Also, Lemma 5.1 applies to the signals which travel on the isoclines of the free rows.

It is easy to check that the join-tile must be used for the red signals which travel on the isoclines of the free rows of trilaterals they meet. Due to the conservation of the laterality during the passing of the phantoms, the join-tile must be used but it can be used only once. As Lemma 5.1 is still in force, the signal cannot be used inside the phantom on the isocline of a free row: using the join-tile, we would get wrong lateralities on both sides.

For the upper horizontal signals, we remember the rule: when they meet the leg of the first phantom of their colour at a free row of the phantom, the signal goes up along the leg, possibly joining a similar signal of the same colour and the same laterality, already climbing up along the phantom. In this situation, a red signal also sends a similar red signal along the leg of the phantom, but downwards. When the upper horizontal signal meets the leg of the first phantom of its colour at a non-free row, possibly using the join-tile, it crosses the leg of the phantom and a possible climbing signal.

Note a difference with the orange signal which climbs up along the first phantom which it meets on the mid-distance line.

Let us give a last precision which will be useful for the description of the tiles.

When we consider two consecutive triangles T_1 and T_2 of the same generation n and within the same latitude, the biggest phantom P which we find on the mid-distance line of T_1 between T_1 and T_2 is of the generation $n-1$. And so, the colour of P is opposite to that of T_1. However, in between T_1 and T_2, there are other towers, of lower size, as follows from another application of Lemma 5.4. For some of these towers, it is possible that their biggest phantom has a generation number of the same parity as n. In this case, the orange signal and the horizontal one of the colour of T_1 will climb up along the leg of the same phantom. Now, we must not forget that inside a phantom which deviates a horizontal signal, as the free rows remain free, the inner phantoms do not receive a horizontal signal and so, the tiles must also foresee this possibility.

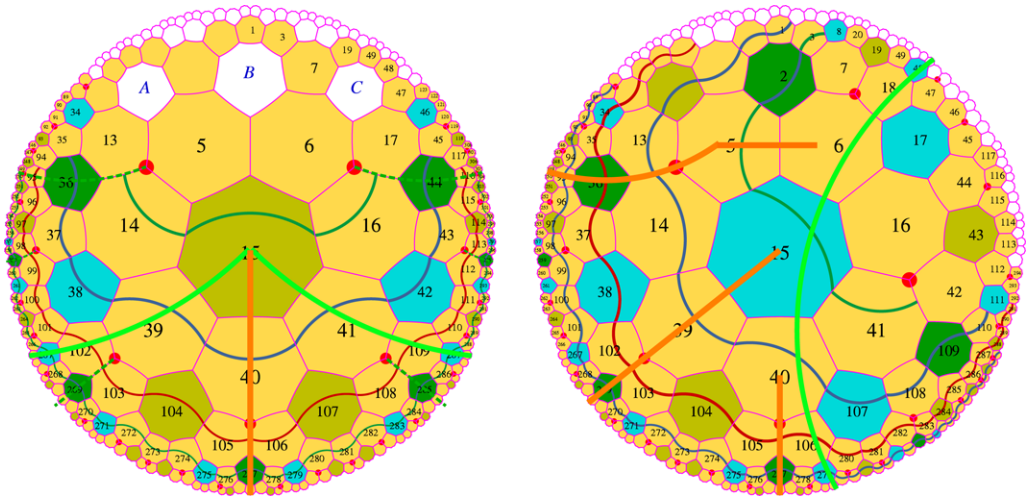

Fig. 29. The vertical starting from a point of the border of a triangle which represents a square of the Turing tape. On the left-hand side: the case of the vertex. On the right-hand side, the three other cases for the right-hand side border are displayed on the same figure. (For interpretation of the references to colour in this figure legend, the reader is referred to the web version of this article.)

At last, it is interesting to note that, in the butterfly model, see Section 3.1, the mechanism of the orange signal forces the green signal to run over the whole isocline which is the mid-point of the latitude which contains no triangle. Indeed, the laterality constraints of the tiles for the crossing of legs of trilaterals prevent an orange signal from running at infinity.

Now, we can conclude that the tiling forces the construction of trilaterals, generation after generation, as indicated by Algorithm 2.

Later on, we shall refer to the solutions which we have just presented as the **circumvention technique**.

6. Completing the proof

6.1. The computing areas

The active seeds were defined in Section 5. They allow to define the trilaterals in the hyperbolic plane. Now, to define the **computing areas**, we ignore the blue and blue-0 triangles and their associated blue signals, the phantoms of any colour with the corresponding green and orange signals, as well as the covered parts of the bases of red triangles. Accordingly, we only focus on what occurs inside the red triangles: red and yellow signals.

We have already mentioned that Lemma 5.1, applied to horizontal red signals, allows to detect the free rows inside the red triangles. We have also mentioned that the yellow signal, without laterality, marks the free rows of the red triangles.

The free rows of the red triangles constitute the horizontals of the grid which we construct in order to simulate the space–time diagram of a Turing machine.

Now, we have to define the verticals to complete the implementation of the grid in which we perform the simulation. Then, we shall describe the implementation of the simulation itself.

The verticals consist of rays which cross **8**-centres. We have already encountered such rays when we defined the border of a sector in Section 2.2. Now, such rays have to be connected with a tile of the border of a tree of the mantilla attached to a red triangle. We know that there are no **8**-centres on the borders of a tree of the mantilla, but as can be seen in Fig. 29, we can find them not far from the border: always at a distance 3 from the border, three or two isoclines below. Fig. 29 illustrates how this connection is realized in the different cases of the tile of the border of a red triangle which receives a yellow signal. As indicated in Section 2.2, the border of a tree is periodic after the tile which follows the root of the tree. The periodic pattern consists of the three tiles: $11 \circ 2$, G_r and $1 \circ 15$ for the right-hand side border and $6 \circ 77$, G_ℓ and $37 \circ 7$ for the left-hand side one, in both cases, for the tiles which belong to the area of the tree. In each case, the vertical goes to the closest **8**-centre which is in the area of the tree.

Note that, in Fig. 29, the vertical signal is represented by a ray. This is not exactly the case. Looking at the left-hand side picture of the figure, the signal goes from tile 15 to tile 40, then from tile 40 to tile 105 and from there to the **8**-centre, tile 277. In terms of petals and of the denotations of Tables 2, 1 and 8, the route is as follows:

$$Fb,\ 1\bar{4}7 \circ w,\ 2 \circ 77w,\ \mathbf{8},$$

and then, periodically: $1\bar{4}7 \circ w$, $2 \circ 77w$, **8**.

In the right-hand side picture of Fig. 29, the three cases of signals starting from a tile of the right-hand side border are represented. In terms of petals and centres, the aperiodic part of the routes, up to the first **8**-centre, is given as follows:

Table 13
Correspondence between the square and heptagonal tiles

Square	Heptagon	
	Black	White
n	1, 2	1
w	3	2
s	4, 5, 6	3, 4, 5, 6
e	7	7

For the latter ones, the correspondence also depends on the status of the tile: black or white.

- from a tile $11 \circ 2$: $11 \circ 2b$, $1\overline{22} \circ w$, $2 \circ 77w$, **8**;
- from a tile G_r: $G_r b$, $47 \circ 7w$, $6 \circ 77w$, **8**;
- from a tile $1 \circ 15b$: $1 \circ 15b$, $2 \circ 77w$, **8**.

Similar initial parts of verticals can be defined for the left-hand side border of a tree. This is left as an exercise to the reader.

The verticals represent the history of a square of the Turing tape. Each tile of the vertical which is on the border represents an empty square, *i.e.* a square containing the blank. The computing signal starts from the seed. It travels on the free rows. Each time it meets a vertical, this means that the head of the Turing machine scans a square of the tape: the square whose content is conveyed by this vertical. As the current state of the machine is conveyed by the computing signal, the corresponding instruction can be performed. If the direction of the motion of the head is not changed and if the corresponding border is not reached, the computing signal goes on on the same row, and now, the vertical conveys the new content of the same square of the tape. Otherwise, the computing signal goes down along the vertical signal with the new state of the Turing machine, the new content of the tape and the direction of the move of the head. When the next free row is encountered, the new content goes on on the vertical and the computing signal goes on its way on the new row, in the direction indicated for the move and with the new current state.

Concrete details for the implementation are dealt with in the next sub-section, devoted to the precise description of the tiles. They are rather close to the classical proofs.

6.2. Description of the tiles

In this sub-section, we shall describe as precisely as possible the tiles needed for the constructions defined in the previous sub-sections. The description is split into two parts. First, we describe the set of **prototiles** which allow to construct the interwoven triangles according to the instructions of Algorithm 2. To this description we also attach the detection of the free rows in the red triangles, although the free rows are needed for the simulation of a Turing machine. The tiles which convey the signal are described in the second sub-section devoted to what we call the **meta-tiles**. Indeed, such tiles are variables. As they convey the information connected with the computation of the Turing machine, in particular the content of the tape, the symbol scanned by the head and the state of the head, the tiles contain information dependent on the machine. As we represent this dependency on the above mentioned variable elements in general terms, what we describe are not actual tiles but variables for concrete tiles, whence the term of meta-tiles.

6.2.1. The prototiles

The set of tiles we turn to now is called the set of **prototiles**. A prototile is not a true tile. Indeed, a tile is a copy of a prototile. Better, a tile is the indication of two elements of data: the location of a tile in the heptagrid and the indication of a copy of the prototile which is placed at this location.

The set of prototiles forces the construction of the mantilla with the isoclines. It also forces the activation of the seeds and the consecutive construction of the interwoven triangles including the detection of the free rows in the red triangles.

In the definition of the tiles, Lemma 3.10 plays an important role. As the tiles have a very **local** character, it is important to look at all possibilities. In many respects, Lemma 3.10 tells us that, putting aside the exceptional case of the position 0 in a realization of the butterfly model, any tile is always eventually in some triangle T. The fact that T itself is or is not inside a bigger triangle depends on the cut of the model which is implemented by the thread T belongs to. On the other hand, the accompanying signal of the same colour of a basis allows us to know by its presence or absence whether the considered tile of the basis is inside or outside a trilateral of the generation of the basis.

All the prototiles are constituted by tiles of the format given by Fig. 8 in which we append several signals.

However, we shall use squares to represent the tiles as, for example, in Figs. 31 and 28. This is suitable for the Euclidean implementation. Now, it is not difficult to see that it is also convenient for the hyperbolic plane. The correspondence between the sides of a square and those of a regular heptagon is easy. Denote the sides of the square by the self-evident notations n, w, s and e, and denote the sides of a heptagon by its local numbering. The correspondence is given by Table 13. It is also illustrated by Fig. 30.

All signals which appear on a prototile may be described as a **superposition** of **elementary** signals. In their turn, elementary signals are defined in terms of a few **basic** signals combined by the applications of **masks**.

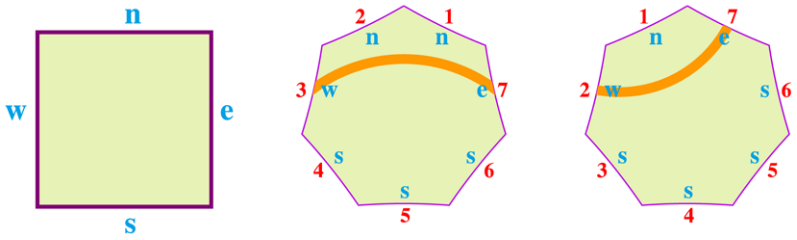

Fig. 30. The translation from a square tile onto heptagonal ones. From the left to the right: the square, a black heptagon and a white one.

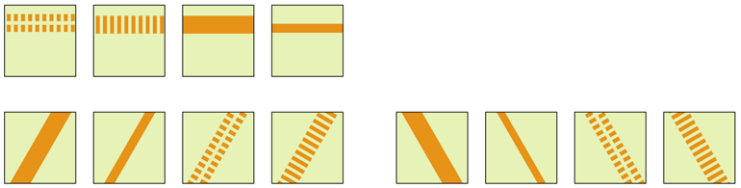

Fig. 31. The basic signals for the prototiles. First row: horizontal signals. Second row: vertical signals. On the left-hand side: the left-hand side verticals; on the right-hand side: the right-hand side verticals.

We have four kinds of basic signals: vertical, horizontal, uniform and lateral signals. There are also colours associated to the signal as well as a thickness, as already mentioned in Section 5.

Fig. 31 illustrates these signals without any colour. They can easily be imagined in the appropriate colours defined in Section 5.

Note that from the study of Section 5 we know that the vertical signals connected with a trilateral go along black tiles only. A left-hand side signal goes from side 1 to side 4, and a right-hand side signal goes from side 2 to side 6. Note that this route for the leg of a trilateral T remains within the area of the tree defined by the vertex of T. It is inside with respect to the border defined by the mid-point line. As the local numbering is known by the tile by the position of the isocline signal, the tile also knows the laterality of a vertical signal.

For the colours, we distinguish between the **skeleton** signals and the **control** ones. The skeleton signals materialize the trilaterals. The control signals implement the horizontal signals emitted by the trilaterals, the scent and the signals which they emit as well as the auxiliary synchronization signals which we introduced in Section 5.2.

For the skeleton, remember that we have three colours: **blue-0**, **blue** and **red**. The blue-0 colour is given to generation 0 only. The blue colour is given to the positive even generations and the red colour is given to the odd ones. This is dictated by the construction of Section 5. As already mentioned, the distinction between triangles and phantoms is implemented by the thickness of the signal. Triangles are represented by thick signals. Phantoms are represented by thin ones. The first and the second halves of legs are distinguished by **hues** in the colours. In red trilaterals, the first half is light while the second half is dark. In blue-0 and blue trilaterals, the first half is dark and the second half is light. The basis always has the same hue as the second half of the legs: this is conformable to the matching at corners. Note that the blue-0 colour is needed to force generation 0. Blue-0 and blue triangles determine the red trilaterals. By the distinction between blue-0 and blue, the red triangles determine blue trilaterals only.

Now, the elementary signals involve **masks** which allow to cut out a part of the basic signal. There are four kinds of masks: μ_ℓ, the left-hand side mask, which hides the right-hand side half of the tile; μ_r, the right-hand side mask, which hides the left-hand side half; μ_u, the upper mask, which hides the lower half of the tile and μ_d, the lower mask, which hides its upper half. Also, elementary signals have a colour and, for horizontal signals, they have a **position**.

To define this latter notion, we define five **channels**, from top to bottom, numbered from 1 to 5:

- **channel 1**, the signals emitted by the legs: blue or red, left-hand side or right-hand side; note that the dotted structure representing the lateralities allows us to have both red and blue horizontal signals on the same channel;

- **channel 2**, the special signal travelling on the mid-distance lines of a trilateral: green or orange; remember that the green signal is uniform while the orange one has a laterality;

- **channel 3**, the signal of the isocline crossing the tile; it joins the mid-point of side 2 or 3 to the mid-point of side 7;

- **channel 4**, the signal of a free row, if any;
- **channel 5**, the skeleton signal of a basis.

For vertical signals, we have two channels: one for the skeleton signal, necessarily that of a leg, possibly with a mask, and one more for a possible orange signal or a coloured one or even both, always with a laterality which is independent of the laterality of the leg.

Fig. 28 gives an illustration of the application of this method for the tiles needed for the implementation of the circumvention technique used by the orange signal as well as the red and blue horizontal signals.

We can notice that the possible values for the channels are not completely independent. As an example, if the tile is on an isocline 0, the skeleton is necessarily that of a phantom of generation 0. We know that there is a possible yellow signal on channel 4. On the other hand, if the tile is on an isocline 5, there is no yellow signal and the skeleton is necessarily that of a red phantom or of a red triangle, in fact of generation 1.

We may define the tiles as follows. First, we define the general compatibility conditions. For this purpose, we define three parts of a leg, excluding vertices and corners which we consider as characteristics of the bases. The three parts are: the first half of the leg, the mid-point tile and the second half of the leg. Similarly, we can define three attributes to the bases: vertex, plain and corner. By definition, a plain basis is a part of the basis where there is no vertex and no corner. Now, we can define a table, see Table 14, which indicates the possible meetings of legs with bases. We append a fourth row for an empty leg: this means that we have a basis which meets no leg for the considered tile. Note that, on the other hand, a leg always meets a basis. Indeed, in the case of a butterfly model, we shall consider that the green signal which crosses the hyperbolic plane from the left to the right is accompanied by the basis of an infinite trilateral. But, as bases travel on isoclines 0, 5, 10 and 15 only, we have a fourth column for no basis, which corresponds to the meeting of the legs with the other isoclines.

And so, we have nine basic cases, denote them by $C_{1,1}$, $C_{1,2}$, $C_{1,4}$, $C_{2,2}$, $C_{3,2}$, $C_{3,3}$, $C_{3,4}$, $C_{4,2}$ and $C_{4,4}$, in obvious notations. Now, in each case, there are conditions which restrict the choice of the parameters entering the definition of the leg and/or the basis.

From the lemmas of Sections 4 and 5, we have the following constraints. Note that in these conditions, when not specified, the word 'leg' alone means 'leg of a trilateral'.

- c_1: the leg of a triangle may meet an open basis of a triangle only if the colours are different;
- c_2: a horizontal lateral signal crosses a leg of its colour only if its laterality is that of the leg;
- c_3: the first half of a leg meets covered or uncovered bases, leaving them unchanged in this regard;
- c_4: the second half of a leg meets covered bases only;
- c_5: when there is a yellow signal, always inside a red triangle, there is neither a horizontal red signal inside the triangle nor a red basis on this row;
- c_6: the yellow signal never travels on isoclines 5; it may travel on the others;
- c_7: the green and orange signals occur on isoclines 15 only;
- c_8: an orange signal cannot cross the mid-point tile of a trilateral;
- c_9: an orange signal crosses first and second halves of legs, only of its laterality.

Some constraints concern all the situations, namely c_5, c_6 and c_7. Others concern several cases or sometimes a single one.

Let us briefly indicate that these constraints guarantee the execution of Algorithm 2.

Indeed, the condition c_3 and the extension of the tiles of Fig. 28 to horizontal signals with legs of phantoms allow to distinguish all situations. Number the elements of Fig. 28 by a-b, where a is the number of the row and b the number of the column, $a \in \{1..3\}$ and $b \in \{1..8\}$. A basis crossing a leg looks like the tiles 1-5 and 1-6 of the figure. A covered basis is the superposition of such a tile with one of the tiles 3-2 or 3-3. The condition c_3 says that we have either the case 1-5 or 1-6 and the case with the superposition of the tiles 3-2, 3-3 together with the modification of the tiles 1-1 and 1-2 by removing the green signal and by appending a basis. Indeed, let T be the trilateral which the leg belongs to and assume that it is the first half of a leg and that it meets a basis. Then, if there is an inner triangle of the colour of the basis, an appropriate tile 3-2 or 3-3 must be superposed. If the row of the basis is open, then we have either the tiles 1-5 and 1-6 or the modified versions of 1-1 and 1-2. Indeed, Lemma 5.1 rules out the superposition of the tiles 3-2 or 3-3. Now, the case 1-1 and 1-2 is possible only for the biggest phantom of the concerned colour γ in between two triangles of the colour γ: a position of the modified tile 1-1 or 1-2 on an inner phantom is also ruled out by Lemma 5.1. There would be a contradiction with the legs of an outer phantom.

And so, the implementation of the conditions guarantees the correct implementation of Algorithm 2 by the set of tiles.

If there were no constraints, it would be enough to multiply the number of possible signals for each channel, horizontal and vertical, and to multiply all of them in order to count the tiles. As this is not the case, we have to exactly number the cases which satisfy the required constraints: they only will be taken into the counting.

First, we look at the case $C_{4,2}$, for which the number of constraints is the smallest. Then, we shall look at the situation of legs which do not meet a basis, the cases $C_{1,4}$ and $C_{3,4}$, first and second halves respectively.

Table 14
Compatibility conditions of a leg with a basis

	Vertex	Plain	Corner	Empty
First half	YES	YES	NO	YES
Mid-point	NO	YES	NO	NO
Second half	NO	YES	YES	YES
None	NO	YES	NO	YES

The last row indicates the case when the basis is present but not the leg. The last column indicates the case when the leg is present but not the basis.

Table 15
Denotation of the possible values on the horizontal channels of a tile

hc_1	hc_2	hc_3	hc_4	hc_5
ϵ, $b\xi$, $r\xi$, bj, rj, $b\xi_1 r\xi_2$, $bjr\xi$, $b\xi rj$	ϵ, g, $o\xi$, oj	0, 5, 10, 15	ϵ, y	$\gamma\xi$, $\gamma \in \{b_0, b, r\}$, $\sigma \in \{\tau, \varphi\}$
15	5	4	2	6

NOTE: In this table and the following ones, ξ is a variable for the laterality of a signal. Accordingly, in hc_1, ξ, ξ_1, $\xi_2 \in \{L, R\}$.

Case $C_{4,2}$

The possible values for the different horizontal channels are given by Table 15. The table indicates 3600 possible patterns. However, as will soon be seen, this is a very high estimate. As an example, we can see that the choice of certain values is more restricted on certain isoclines than on the others. And so, the actual number is much lower: more than ten times lower.

Let us briefly explain the indicated values of the horizontal channels which we denote by hc_i, with $i \in \{1..5\}$, in the table.

For hc_3 and hc_4, the values immediately follow from the definition of the channel. For hc_1, we have two possible colours, blue b and red r, two possible lateralities, L and R, and for each one, but not together, there is the possibility of a join pattern j. Also, there are cases when the basis is accompanied by a single signal. This is the case for a blue one inside the triangles of generation 1. This may be the case for a red signal on an isocline 15. There may be both signals on most isoclines 15 and there may be no horizontal signal at all in channel 1 on an isocline 15, for instance inside a phantom of generation 0.

For hc_2, the five values which are indicated correspond to the possibilities dictated by the definition. Note that a signal is present on this channel only on an isocline 15. For hc_5, as there is a basis on each isocline 0, 5, 10 or 15, we have three possible colours and the choice of a triangle or a phantom. The value of this latter parameter is called the **status** of the basis. Later, we shall also speak of the **status** of other parts of a trilateral with the same meaning.

In the counting of the prototiles corresponding to the case $C_{4,2}$, we separate the cases according to the number of the isoclines so that hc_3 has a single value in each case. The cases are indicated in Table 16 by an encircled number in the first column of the table. Each case is analyzed in the corresponding row. Just below, an additional row with small numbers indicates the number of possible values for each channel. We call it the counting row. In the last column of this row, the product of the previous values is indicated: it gives the number of patterns for this case.

Now, we discuss the indications of the table, case by case:

Case 1

This case is associated to generation 0 when the signal is accompanied by a yellow signal. And so, the isocline is 0 or 10. On an isocline 0, the basis is that of a phantom of generation 0: we have a thin blue-0 basis. On an isocline 10, the basis is that of a triangle of generation 0: we have a thick blue-0 basis. This fixes the value of hc_5 when that of hc_3 is fixed.

As there is a yellow signal in channel 4, we are inside a red triangle. This rules out a red signal on channel 1. There may be a blue signal if we are in between two blue-0 trilaterals which stand on the basis which runs on channel 5. There is no blue signal if we are inside a trilateral of generation 0. And so, we exactly have the indicated numbers of the counting row.

Case 2

This is still about generation 0 but there is no yellow signal in channel 4 and we again assume that we are on an isocline 0 or 10. Then, the tile may be almost anywhere. Clearly, the occurrence of both red and blue horizontal signals can easily be realized on an isocline 0 or 10. Let us see that the case when there is no signal on channel 1 and the case when there is only one coloured signal in this channel are also possible. The case when there is no signal occurs inside a red phantom P of generation 1: the rows inside P are free but they are not marked as yellow, as we are inside a phantom. Now, inside P there are triangles of generation 0. There is a basis of such a triangle T inside P. Inside T, the basis is open, and so it has no blue signal. This is for isocline 0. Now, P also contains a phantom P_0 of generation 0. The same argument as for T applied to the basis of P_0 gives us a situation where there is no signal in channel 1 on an isocline 0. Now, outside P_0 or T, we have parts of the considered bases which are covered. Accordingly, we have the occurrence of a blue signal without red signal. There remains to see that the situation with a red signal without a blue one is also possible. This is the case, for instance, in between two triangles of generation 1, on the basis of a trilateral T of the generation 0, inside T. From Lemma 5.1 and from the configuration of the join-tiles, there cannot be a horizontal blue signal inside a blue 0 trilateral.

Table 16
Table of the values for the horizontal channels of a tile in the case $c_{4,2}$

	hc_1	hc_2	hc_3	hc_4	hc_5	#
1	$\epsilon, b\xi, bj$	ϵ	0 | 10	y	$b_0\varphi \mid b_0\tau$	
	4	1	2	1	1	8
2	*all*	ϵ	0 | 10	ϵ	$b_0\varphi \mid b_0\tau$	
	15	1	2	1	1	30
3	*all*	ϵ	5	ϵ	$r\sigma$	
	15	1	1	1	2	30
4	$\epsilon, b\xi, bj$	g	15	y	$b\sigma$	
	4	1	1	1	2	8
5	$\epsilon, r\xi, rj$	g	15	ϵ	$r\sigma$	
	4	1	1	1	2	8
6	$\epsilon, \gamma\xi, \gamma j$	g	15	ϵ	$\overline{\gamma}\sigma$	
	7	1	1	1	4	28
7	$\gamma\xi, \gamma j, \gamma j\overline{\gamma}\xi,$ $\gamma\xi_1\overline{\gamma}\xi_2, \gamma\xi\overline{\gamma}j$	$o\xi, oj$	15	ϵ	$\overline{\gamma}\sigma$	
	11	3	1	1	4	132
Total:						244

NOTE: *all* indicates all the 15 values of Table 15 for channel 1. Here, γ in $\{b, r\}$.

Case 3

This case deals with isocline 5. We always have a red basis, either of a triangle or of a phantom. Of course, there is no yellow signal and we again have ϵ on channel 2. We have just to check that all cases are possible for channel 1. Again, the occurrence of both blue and red signals is not difficult to realize. Let us see that the case with no signal is possible: from the discussion of case 2 , this is the case inside a blue-0 triangle T_0 which generates the basis of a triangle T of generation 1. The basis of T is open inside T, hence it has no red signal and it has no blue signal inside T_0. The same situation on the basis of T and outside the triangles of generation 0 gives us a situation where we have a blue signal only. The situation of a red signal only occurs around the vertex of T which is also on an isocline 5, but inside another triangle T_1 of generation 0. Accordingly, there is no blue signal. But the vertex of T may be in a part of an isocline 5 which is not covered by a red phantom. And so, in this case, the red signal is present alone.

Now, we arrive at the situations of an isocline 15 which are dealt with by cases 4 , 5 , 6 and 7. First, we consider the case when we have both a yellow and a green signal, then the situation when we have the green signal only and, finally, the situation when we have the orange signals which clearly rule out a yellow signal.

Case 4

We assume that the green signal is present and that it is accompanied by a yellow signal. This means that the tile is on the mid-distance line of a red triangle. By Algorithm 2 and by the synchronization principles, see Section 5.2, the basis occurring in channel 5 is blue. It cannot be a blue-0 basis, as red triangles do not generate generation 0. Of course, the status of the basis is not fixed. We know that there is no red signal on channel 1, as there is a yellow signal. There may be no blue one: this is the case if the trilateral corresponding to this basis exists at this point of the considered latitude. If it does not exist, the basis is covered and so, we then have a blue signal on channel 1. Hence there is also the possibility of a blue join-tile.

Assume that we have no yellow signal, but that the green signal is still present. As the green signal is present, we are inside a trilateral on its mid-distance line. We have two cases: either inside a triangle or inside a phantom.

Case 5

We assume that we are inside a triangle. It must be blue, as a red one would require the occurrence of a yellow signal. And so, the basis on channel 5 is red and the status may be a triangle or a phantom. The red basis may be open or covered, depending on the realization or not of the red trilateral possibly generated by the blue triangle. As we are on the mid-distance line of a blue triangle, there is no blue signal.

Case 6

We have the last case inside a trilateral with a green signal and no yellow one: inside a phantom P on its mid-distance line. By synchronization, a basis accompanies the green signal. This basis may be red or blue. Note that it cannot be blue-0. The basis may be of any status. Now, it cannot be accompanied by a signal of the same colour, even if the corresponding trilateral does not exist. Indeed, if the trilateral does not exist, horizontal signals of the corresponding colour cannot cross the phantom as they circumvent it, due to Lemma 5.1. However, it may be crossed by a horizontal signal of the opposite colour. This is the case when the phantom is in between two consecutive triangles of the next generation, within the same latitude. It may also happen that the basis is not accompanied by any horizontal signal of the opposite colour: in a phantom of a generation at least $2n + 3$, we have a tower of three phantoms, a blue one, the larger, then a red one and then a blue-0 one. Inside this blue-0 phantom B, there is neither a blue signal nor a red one, as a red phantom contains B. The colour of the horizontal signal is denoted by γ in the table, with γ in $\{b, r\}$, and $\overline{\gamma}$ is the opposite colour.

Table 17
Table of the effect of the scent on a basis

	0	5	10	15
Seed	**e**/**t**	**i**/**t**	**i**/**t**	**i**/**t**
Others	**i**/**h**	**i**/**h**	**i**/**h**	**i**/**h**

For each entry, the left-hand side indicates what happens if the tile does not receive the scent and the right-hand side indicates what happens when the scent is received.
NOTE: **e**, **i**, **t**, and **h** mean **emit**, **idle**, **transmit** and **halt** respectively.

Case 7

The last case, still on an isocline 15 deals with the situation when we have an orange signal. In this case, we are necessarily on the common mid-distance line λ of two consecutive triangles T_1 and T_2 of colour γ, between T_1 and T_2. And so, we have a signal γ on channel 1. Note that, as we are on an isocline 15, the colour cannot be blue-0: the mid-distance line of a blue-0 triangle is an isocline 5. Depending on whether the trilateral associated to this basis is realized or not on the considered part of λ where our tile is, the basis is opened or not and so, we may have a signal $\overline{\gamma}$ on channel 1. Accordingly, we have all the situations indicated by the table.

Now, Table 16 only looks at the horizontal channels of the tile. Now, the tile must be superposed on a tile of the mantilla. We have 33 patterns for these tiles. This gives us 8052 prototiles. However, we have to take into account that the tiles may receive or not the scent. Table 17 indicates the structure of the tiles with respect to the scent, depending on the pattern of the mantilla and of the number of the isocline.

Indeed, from the table we check that when the tile receives the scent, it stops it if it is not a seed. If it is a seed, it transmits it. If the tile does not receive the scent, it does nothing, except if it is a seed on an isocline 0 which then emits the scent.

Accordingly, for each tile, we have exactly two different possibilities with respect to the scent. And so, this defines 16,104 prototiles. In fact, we can significantly reduce this number by introducing the following constraints:

- c_{10}: a tile can receive at most one join-pattern for horizontal signals of the same colour with lateralities;
- c_{11}: a join-tile for horizontal signal with lateralities of the same colour must be placed on the border of a sector.

Now, Table 16 indicates only the number of patterns we can have for the different channels, regardless of the tile of the mantilla which will support the signals. To take into account the constraint c_{10}, already implemented in the table, and c_{11}, we have to count the occurrences of j which may occur at most once separately. If $\#hc_i$ is the number of possibilities for hc_i in a row of the table, the rough estimate we have indicated is obtained by the sum of the rows of the products $\pi = \#hc_1.\#hc_2.\#hc_3.\#hc_4.\#hc_5.33$. Now, for hc_1 and hc_2, we split the counts as follows: $\#hc_i = \#hc_i^0 + \#hc_i^j$, where hc_i^j is the set of all the patterns containing j. Now, π must be replaced by:

$$\pi' = \#hc_1^0.\#hc_2^0.\#hc_3.\#hc_4.\#hc_5.33 + (\#hc_1^0.\#hc_2^j + \#hc_1^j.\#hc_2^0).\#hc_3.\#hc_4.\#hc_5.3$$

Applied to the rows of Table 16, the computation gives us 4332 patterns. Taking into account these constraints together with the effect of the scent, we obtain that Table 16 defines 8664 prototiles. However, we can perform a better reduction. The scent does not affect all the patterns of the mantilla. Indeed, it is emitted by a seed and then, it is stopped at the fifth isocline. Now, an analysis performed by a computer program shows us that on the fifth isocline, the number of the mantilla patterns is 22, the case of a seed being also taken into account, see Table 25. And so, this time we have to recompute the data, considering that 21 patterns only may be concerned by the scent. The computer program also shows that the patterns used for the join-tiles may also receive the scent, the join-tile with an orange signal being excepted. Indeed, no orange signal occurs inside a trilateral within the first five isoclines. An accurate account gives us 7080 prototiles.

Case $C_{1,4}$

Now, we turn to the situation when the tile is on the first half of a leg and when it does not meet a basis.

As a general remark, note that for a triangle we have two lateralities and three possible colours, which makes 6 cases. For a phantom, we have still two lateralities and three possible colours. But a leg of a phantom may receive an orange signal or a coloured lateral signal or both. For each colour and for each laterality of the leg, these possibilities represent 9 cases for a phantom. We discuss them according to the isoclines and the possible patterns of the mantilla.

For the blue-0 trilaterals, the first half concerns isoclines 1..4 for a triangle and isoclines 11..14 for a phantom. It is not difficult to see that the tiles of the mantilla which are on these places are fixed by their position on the border and by their distance from the root. This justifies the corresponding row of the table.

Now, the situation is different for the blue and red trilaterals. What remains is that the first tile following the root is always the same. It occurs on isoclines 16 for the blue trilaterals and on isoclines 6 or 16 for the red triangles. For the other isoclines, any tile belonging to a period of a border is possible. There is three possibilities for each laterality. Also note that the isoclines which are concerned by the case $C_{1,4}$ are isoclines 1..4, 6..9, 11..14 and 16..19 which means 16 isoclines.

Now, we have to consider the possible contribution of the scent. The first half of a blue-0 trilateral always contains the scent, by definition of the scent. The scent is also present on the legs for the first five isoclines following the root. But these isoclines may also not bear the scent when the length of the leg becomes important. And so, we have to append the tiles for the scent: they concern the four isoclines which follow the root and so on each isocline, the tile of the mantilla is fixed by its

Table 18
The case $C_{1,4}$: counting the first half of the legs

	Triangle	Phantom	Isocline	Mantilla	Partial
Blue-0	2	18	4	1	80
Blue	2	18	1	1	20
Blue	2	18	16	3	$960 + 80$
Red	2	18	2	1	40
Red	2	18	16	3	$960 + 80$
Total					2220

NOTE: In each row, we sum up the first two columns and then we multiply the result by the product of the next two columns. This new result is put in the last column. The added numbers in the last column indicate the contribution of additional tiles for the scent which is counted in the other rows.

Table 19
The case C_{34}: counting the second half of the legs

	Triangle	Phantom	Isocline	Mantilla	Partial
Blue-0	2	2	4	1	16
Blue	2	2	16	3	192
Red	2	6	16	3	384
Total					592

NOTE: In each row, we sum up the first two columns and then, we multiply the result by the product of the next two columns. This new result is put in the last column.

position on the border. Accordingly, this makes $20 \times 4 = 80$ new prototiles for each colour. They appear on the appropriate row of the table. Accordingly, we obtain 2220 prototiles for the case $C_{1,4}$, as indicated by Table 18.

Case $C_{3,4}$

This time, we consider the case of the second half. We have the same analysis as previously with several simplifications. For the phantoms, there is no orange signal, no blue climbing signal. However, there may be a red climbing signal for a red phantom. Moreover, on the second half, we are always in the periodic part of the border, the tiles being still fixed by the position in the case of the blue-0 trilaterals. At last, there is no scent to be taken into account.

The information is gathered in Table 19.

Case $C_{1,1}$

Now, we deal with the vertices of the trilaterals. First, we notice that their pattern can be described in terms of basic signals, combining them with appropriate masks. Denote the basic signal of a leg by $L_\pi\gamma\sigma\xi$, where the status σ is in $\{\tau, \varphi\}$, the colour γ is in $\{b_0, b, r\}$, the laterality ξ is in $\{L, R\}$, and π indicates which half of the leg we consider, with π in $\{1, 2\}$. Remember that μ_α is the operator consisting in applying a mask, with α in $\{u, d, \ell, r\}$. Then, the vertex of a phantom has the general form $\mu_d(L_1\gamma\varphi L) + \mu_d(L_1\gamma\varphi R)$, and that of a triangle has the general form $\mu_d(L_1\gamma\tau L) + \mu_d(L_1\gamma\tau R)$, see Fig. 34. Fitted with appropriate colours, we call these signals **elementary**. Clearly, we have just defined 3 patterns for triangles. For phantoms, we have this number of patterns multiplied by the number of cases connected with the possible presence of circumventing signals. As there are two lateralities for each signal and as two of them at most can be present, the orange one included, when there are two signals, we get 27 patterns. And so, there are 30 elementary signals representing a vertex.

However, a vertex stands on an isocline 0, 5, 10 or 15 and so, it is accompanied by a basis. We take advantage of Table 16 to extract the bases and their accompanying signal which can be met by a vertex. From the constraint c_{11}, we know that we can rule out any basis which has the join-pattern of a horizontal signal. We discuss the different cases according to the isoclines. For each one, Table 20 indicates the vertices and the bases which are met.

On an isocline 0, we can only have the vertex of a blue-0 triangle: a single pattern. Now, on an isocline 10, we only have the vertex of a blue-0 phantom, and we know that there are 9 patterns. On an isocline 5, we have a red trilateral: either a red triangle, 1 pattern, or a red phantom, again 9 possible patterns. On an isocline 15, we have the vertices of blue or red trilaterals. For each colour, the counting of isocline 5 shows that we have 10 patterns, and so we get 20 patterns, as indicated in the table.

Let us look at the possible meetings with a basis.

On an isocline 0, we may meet only a basis of a blue-0 phantom. All cases of Table 16 are possible.

Now, consider the case of an isocline 5. The vertex is raised inside a blue-0 triangle. Accordingly, there is no horizontal blue signal. There may be a red signal on channel 1. And so, only three cases are possible: those indicated by the table.

In the case of an isocline 10, by construction of the scent, we are inside a red trilateral of generation 1 whose vertex is on an isocline 5: there cannot be a red signal. And so, the father of this red trilateral exists, which is a blue-0 triangle. This means that the basis where the vertex on isocline 10 occurs is open: there cannot be a blue signal. Now, there can be a yellow signal, hence the two signals indicated by the table.

Table 20
The case $C_{1,1}$: the counting of the prototiles for the vertices

Isocline	0	5	10	15	Total
Vertex	$b\tau$	$r\sigma + K$	$b\varphi + K$	$\gamma\sigma + K$	
	1	10	9	$10 + 10$	
Basis	$y, b\xi y, \epsilon, b\xi, r\xi, b\xi_1 r\xi_2$	$\epsilon, r\xi$	ϵ, y	Determined	
	12	3	2	1	
Scent	2	1	1	1	
#tiles	24	30	18	20	92

NOTE: K represents the repetition of the same pattern entailed by the different possible lateral signals accompanying the leg of a phantom, also at the vertex.

Table 21
The case $C_{1,2}$: the counting of the prototiles for the crossing of bases with the first half of a leg of a trilateral

Cases	1	2	3	7	Total
Isocline	0, 10	0, 10	5	15	Total
$b\tau$, 2	$y, yb\xi + yb\xi$	$b\xi, b\xi r\xi_2 + b\xi, b\xi r\xi_2$	$b\xi, b\xi r\xi_2$	$b\xi, b\xi r\xi_2 \mid b\xi r\xi_2 + r\xi_2, b\xi r\xi_2$	
	$2 + 1$	$3 + 3$	6	$3 \times 2 + (2 + 2 \times 2)$	54
$b\varphi$, 18	$y, yb\xi + yb\xi$	$b\xi, b\xi r\xi_2 + b\xi, b\xi r\xi_2$	$b\xi, b\xi r\xi_2$	$b\xi, b\xi r\xi_2 \mid r\xi_2, b\xi r\xi_2$	
	$2 + 1$	$3 + 3$	6	$(3 + 4) \times 2$	522
$r\tau$, 2	$y, yb\xi_2 + y, yb\xi_2$	$b\xi_2 r\xi + b\xi_2 r\xi$	$b\xi_2 r\xi + b\xi_2, b\xi_2 r\xi$	$b\xi_2 r\xi + b\xi_2, b\xi_2 r\xi \mid r\xi, b\xi_2 r\xi$	
	$3 + 3$	$2 + 2$	6	$6 + 2 \times 3$	56
$r\varphi$, 18		$\epsilon, b\xi_2, b\xi_2 r\xi + \epsilon, b\xi_2, b\xi_2 r\xi$	$b\xi r\xi_2 + b\xi_2, b\xi_2 r\xi$	$b\xi_2, b\xi_2 r\xi \mid r\xi, b\xi_2 r\xi$	
	0	$5 + 5$	6	$(4 + 3) \times 2$	540
Total:					1172

Remember that ξ is fixed.

NOTE: In columns 1 and 2 , the sign + separates the case of an isocline 0, on the left-hand side, from that of an isocline 10, on the right-hand side. Similarly, in column 5 , when needed, the sign + distinguishes between the case of the basis of a triangle and that of a phantom respectively. In column 7 , the symbol | distinguishes between the case when γ is blue and when it is red. Inside a fixed colour of γ, if present, the sign + distinguishes between triangles and phantoms as performed for the case of column 5 . Remember that ξ is fixed in this table: it represents the laterality of the leg. The coefficient of the first column takes into account both possible lateralities.

At last, we arrive at the situation of an isocline 15. By definition of the construction of the trilaterals, there is a green signal as the vertex is on an isocline 15: it is generated on the mid-distance line of a triangle. By the scent constraint, the vertex is inside a blue-0 phantom. And so, there cannot be a blue signal. Now, if the vertex is red, as we are on an isocline 15, the triangle is at least of generation 3. Accordingly, as the blue triangle generating this vertex exists, it is at least of generation 2 and so, it contains a phantom of generation 1 which contains the vertex. From our study of the circumventing signals, if the trilateral associated to the red basis does not exist, there cannot be a horizontal red signal at this vertex. And so, for what the horizontal signals accompanying the basis are, they are completely determined, as well as the basis itself which contains the vertex. And so, there is only one case.

We have the cases indicated in the table. As we separately multiply the indications of the basis and the vertices for isocline 15, depending on the colour of the vertex, we obtain the 20 patterns indicated in the last row of the table.

Accordingly, we find 92 prototiles.

Case $C_{1,2}$

This time, we arrive at an important sub-case, also from the point of view of the number of prototiles: this case corresponds to the crossing of the first half of a leg with a basis.

We present the counting of the tiles in Table 21 and we describe the tiles in the justification of the counting. Note that the table contains four columns which correspond to four items among the seven rows of Table 16. For a convenient correspondence between the tables, the columns of Table 21 have the same number as the corresponding rows of Table 16. The first column of Table 21 indicates the case of the leg, together with a multiplicative coefficient used in the counting: 2 for a triangle, as the leg has two possible lateralities, 18 for a phantom as, besides the laterality of the leg, the phantom may be accompanied by an orange signal, a coloured one, either blue or red, or the orange signal together with a coloured one. In the second row of the table, we remind the reader of which isocline the different cases refer to. Then, each row indicates the case of the leg. The last column indicates the number of the patterns.

Now, in the table, we assume that the laterality of the leg is fixed. It is called ξ. As the meeting of a leg may change the horizontal signals of several channels, we consider that the meeting concerns the part of the tile which is opposite to the laterality of the leg: a left- or right-hand side leg is concerned with the right- or left-hand side part of the channels of the tile respectively.

Moreover, the legs are either blue or red. The colour blue-0 is ruled out: the leg of a trilateral of generation 0 meets either an isocline 5 or an isocline 15, but it is always at the mid-point tile of the leg. And so, we have four cases for the leg which

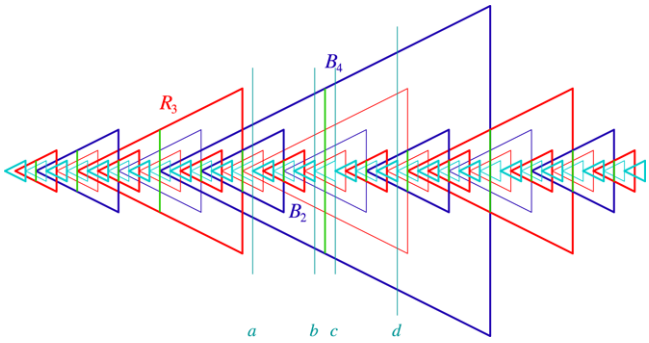

Fig. 32. An illustration for case 2 . This figure is used for Tables 21 and 23. The vertical thin blue lines *a*, *b*, *c* and *d* represent horizontal signals which travel on isocline 0, 10, 0 and 10 respectively. For Table 21, we imagine that B_4 generates the basis of a phantom P of generation 5: in this case the basis of P runs on the mid-distance line of B_4, in green in the figure. For Table 23, we imagine that B_4 is a phantom in the case when the blue leg belongs to a phantom. (For interpretation of the references to colour in this figure legend, the reader is referred to the web version of this article.)

we denote by $b\tau$, $b\varphi$, $r\tau$ and $r\varphi$, see the first column of Table 21. From Lemma 2.8, the condition c_{11} rules out the presence of a join-tile on the leg of a trilateral. This significantly reduces the number of tiles.

The first remark deals with the selection of the columns. Indeed, cases 4 , 5 , and 6 of Table 16 concern the case when a basis is accompanied by a green signal. By the principles of algorithm 2, the green signal triggers the change from the first half to the second one of a leg which is materialized by its mid-point tile. This is dealt with in the case $C_{2,2}$. Accordingly, here, these rows do not appear.

Consider the first half of a leg of a blue trilateral T. We shall discuss it column by column, dealing with the case of a triangle and of a phantom at the same time.

Case 1

On isocline 0, taking into account Table 16 and the condition c_{11}, we have at most two cases: an open or a covered basis. Both cases occur. Indeed, an open basis of a blue-0 phantom is crossed by any leg which is triggered on isocline 15 which crosses this phantom. Such a situation occurs with any blue trilateral of a generation at least 2. The situation with a covered basis is obtained if T belongs to generation 2: the first half of its leg cuts the basis of a phantom P of generation 0 contained in T, outside P but inside the triangle of generation 1 which generates T. On isocline 10, the basis is that of a triangle. By the condition c_1, the basis must be covered. And so, we have only one case here, remembering that ξ is fixed.

Case 2

We still meet an isocline 0 or 10 but, this time, the basis is not accompanied by a yellow signal. If we meet isocline 0, we again have the basis of a blue-0 phantom.

Note that T belongs to a positive even generation. It is easy to realize a situation when the basis is accompanied by both a red and a blue signal on channel 1. Let us see that we can have a basis which is accompanied by a blue signal only. Indeed, consider a red phantom P of a large enough generation, say $2n + 5$. It contains two red triangles of the generation $2n + 3$: in fact, we should say that there are exactly two latitudes of red triangles of the generation $2n + 3$ in the latitude of P. As we shall always pick up one of these triangles, we shall use this way of speaking for trilaterals of a latitude through one of them. Let R_3 be the lower one. It generates a triangle B_4 of the generation $2n + 4$ which generates the basis of P. The basis β of R_3 is on an isocline 15. Now, from the decomposition given by Lemma 3.5, it is not difficult to see that the next row below β is an isocline 0 which is free in P: see the line *a* of Fig. 32. Now, the basis of P is the mid-distance line of B_4, and B_4 contains two blue triangles of the generation $2n + 2$. The upper one B_2 generates the basis of R_3. Now, the blue-0 phantom whose basis is on isocline 0 which is just below β generates a blue signal which cuts the leg of B_2 and that of B_4. As the row is free in P, there is no red signal on it, which realizes the announced situation. This solves the case when T is a triangle. Now, if T is a phantom, we can take the same situation where R_3 is the upper red triangle of the generation $2n + 3$. Now, we may assume that R_3 generates a blue phantom Q_4 of the generation $2n + 4$. We also have an isocline 0 which is just below the basis of $R3$. This isocline is a free row in P and so the corresponding basis cuts Q_4 with no accompanying red signal. Fig. 32 illustrates the situation. Note that P is not present in the figure.

Now, the absence of a blue signal means that the leg is raised inside a phantom. Now, as a blue leg is raised by a red triangle, there must be a yellow signal also on the basis of the blue-0 phantom. And so, this case cannot happen. Also note that we cannot have a red signal only. If a red signal is present, it is generated by a red triangle. Now, it is not difficult to see that the leg of a red triangle of generation 1 is crossed by horizontal blue signals. Now, by induction, as free rows in a red triangle come from inner blue-0 trilaterals, the legs of a red triangle are always crossed by a horizontal blue signal. And so, a red signal alone is impossible here.

If the leg meets isocline 10 and if T is a triangle, we have the basis of a blue-0 triangle T_0. The basis must be covered, by the condition c_1. As previously, the basis can be accompanied by a red signal. Also, it can be accompanied by a blue signal only. Indeed, take the same example as with isocline 0. But this time, consider the basis of P. It is on an isocline 15. The next row above this isocline is an isocline 10, see line *b* of Fig. 32, and it is also a free row in P. As P is a red phantom, there is no

red signal on this isocline, and the basis of a blue-0 triangle which travels on this isocline 10 cuts the legs of B_4 in their first halves. And so, we have the cases indicated by the table: the signals $b\xi$ and $b\xi r\xi_2$, giving rise to 3 cases. This solves the case when T is a triangle. When T is a phantom, the case Q_4 also gives an example of the required situation, taking isocline 10 which is just above the mid-distance line of P: it is also a free row in the phantom P and so, there is no red signal. Again, Fig. 32 illustrates the situation.

Here also, a red signal is necessarily accompanied by a blue signal, for the same reason as in the case of a leg of a blue triangle.

Case 3

This time, the leg meets an isocline 5. Hence, we have a red basis. It cannot be generated by T, as T belongs to a bigger generation. The basis may be covered or not, depending on whether the corresponding trilateral exists or not. Now, the red basis belongs to triangles of generation 1 and it is generated by blue-0 triangles. As T belongs to a positive generation, it cannot be inside a triangle of generation 0. And so, there is always a horizontal blue signal on the basis. Note that our argument depends neither on the status of the red basis nor on the status of the leg.

Case 7

Here, we can have a discussion in general terms. From Table 16, we know that the orange signal is present so that the tile is outside the trilateral associated to the basis present in its channel 5. Remember, that the isoclines of the trilaterals of a given generation characterize the generation. From Table 16 too, we know that the signal $\gamma\xi$ is present, ξ being fixed and γ being possibly either blue or red. We also know that the colour of the basis is $\overline{\gamma}$.

Consider two consecutive triangles T_1 and T_2 of the colour γ within the same latitude. On the isocline λ of their mid-distance line, which is an isocline 15, they generate a basis of the colour $\overline{\gamma}$. In between T_1 and T_2, the basis is covered by a signal oR and oL. From Lemma 5.5, see the Section 5.2, we know that there is at most one leg of a generation higher than that of T_1. Accordingly, the situation which we are considering in the table is namely the one we have just described. If the trilateral corresponding to the basis $\overline{\gamma}$ does not exist on this part of λ, then there is a signal $\overline{\gamma}\xi$ or $\overline{\gamma}\xi_2$, depending on the colour of the leg and on the colour $\overline{\gamma}$. If the trilateral exists, denote it by K, then the basis $\overline{\gamma}$ is open and so the signal $\gamma\xi$ or $\gamma\xi_2$ is alone. We know that if n is the generation of T_1, that of K is $n+1$. If K is a triangle, the mid-distance line of K generates a trilateral M of the generation $n+2$ of the colour γ which may freely cut the basis $\overline{\gamma}$: it is the leg which we consider. If K is a phantom, its mid-distance line generates a trilateral M of the generation $n+2+k$ which may have a colour independent of γ. Now, as K is a phantom, the leg of M may freely cut the basis of K, whatever its colour. Moreover, whether K is a triangle or a phantom, from Lemma 4.4, the meeting between the leg and the basis $\overline{\gamma}$ occurs within the first half of the leg. The situation is illustrated by Fig. 33. Applying this argument to our situation, we can see that all the combinations permitted by Table 16 are possible, provided that the compatibility conditions on the colours of legs and basis are observed. Later on, we shall refer to this by saying that case 7 is only limited by combinatoric constraints.

For the present situation of the first half of a leg, we have the following possibilities.

In any case, we have the signal of the colour γ. We have this signal alone if K exists. If K does not exist, we also have to append the signal of the colour $\overline{\gamma}$.

If γ is the colour of the leg, we have the following possibilities: $\gamma\xi$ and $\gamma\xi\overline{\gamma}\xi_2$, which means 3 cases. Moreover, in each case, the status of the basis β of the colour $\overline{\gamma}$ is free. And so, we have 6 patterns.

If the colour of the leg is $\overline{\gamma}$, the signals are $\gamma\xi_2$ and $\gamma\xi_2\overline{\gamma}\xi$. Now, in case the signal $\overline{\gamma}\xi$ is present, the status of β is free. Now, $\overline{\gamma}$ is the colour on channel 5 and so, as the colour of the leg is the same, the signal $\overline{\gamma}\xi$ must also be present. And so, as the leg belongs to a triangle, we have 6 cases when γ is blue, as the status of β is free. When γ is red, we have 2 cases when β belongs to a triangle and 4 of them when it belongs to a phantom.

Accordingly, in this case, we have 12 patterns for case 7 when the leg belongs to a blue triangle and 14 patterns when it belongs to a blue phantom.

Now, consider the case of the first half of a leg of a red trilateral T. Again, we shall discuss it column by column, dealing with the cases of a triangle and of a phantom at the same time.

Case 1

The situation is a bit different with respect to the case with a blue leg.

The presence of a yellow signal is possible with a red leg of a triangle only. As we have a free row, we are either on an isocline 0, an isocline 10 or an isocline 15, but this latter case is ruled out. On isocline 0, we have a blue-0 basis of a phantom. Now, this basis is accompanied by a blue signal, unless we are inside the phantom. This is possible for a red triangle of any generation: the tower of phantoms around its vertex starts with a blue-0 phantom. On isocline 10, this is also possible: the vertex of a red triangle of generation 1 is inside a blue-0 triangle. Apart from these cases, the basis is always accompanied by a blue signal.

This gives us 6 patterns for case 1 , for each laterality of the leg. Note that the leg of the triangle emits a horizontal red signal of the laterality of the leg, outside the triangle.

Case 2

This time, the basis is not accompanied by a yellow signal. And so, if the leg of T belongs to a triangle, necessarily, we have a red signal $r\xi$. This rules out the possibility of a leg inside a trilateral of generation 0: we know that the first free row

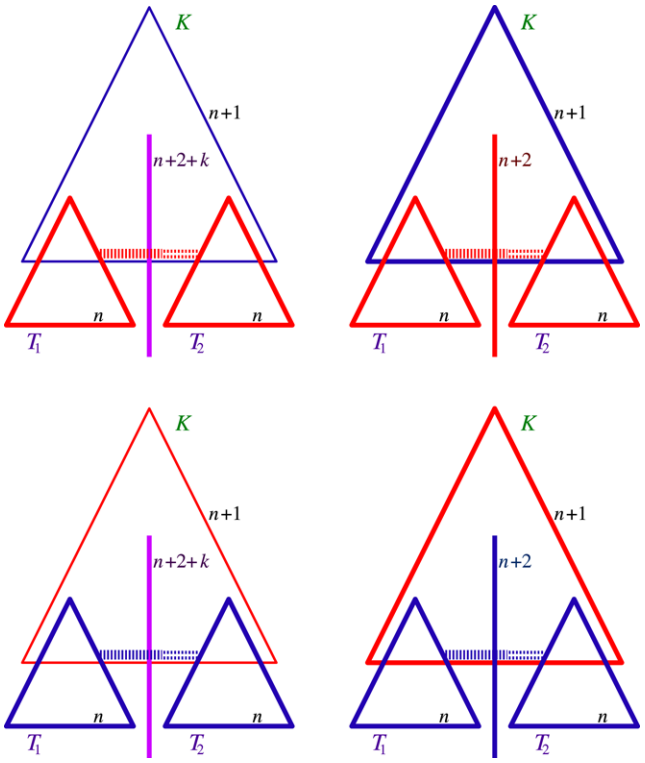

Fig. 33. The situation in between consecutive triangles of the same generation and latitude. The triangles, the small ones in the figure, belong to the generation n. Note the signals of their colour $\gamma\xi$ in between them. When it exists, K is represented by the big triangle. On the left-hand side, the case when K is a phantom, the leg may be red or blue, purple on the picture. On the right-hand side, the case when K is a triangle: the leg is of the colour γ, necessarily. (For interpretation of the references to colour in this figure legend, the reader is referred to the web version of this article.)

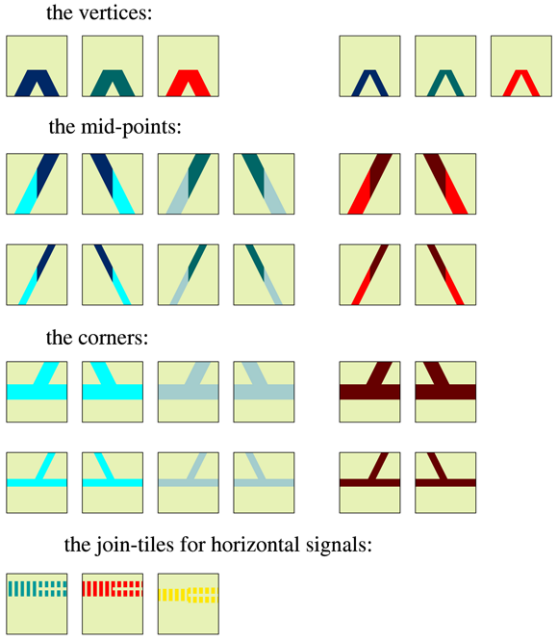

Fig. 34. The elementary patterns for the skeleton of the construction.

of a triangle occurs on the first row below the vertex. Accordingly, the red signal is accompanied by a blue signal: there are blue-0 trilaterals outside and inside the red triangle which generates the considered leg.

When the leg belongs to a red phantom, we know that the free rows exist, exactly as for a red triangle, but they are not marked by a yellow signal. So, in this case, the blue basis may be accompanied by no signal at all. This may happen for a

phantom of generation 1 which is raised in a blue-0 triangle and so, this is a meeting with isocline 10. But this also happens for any red phantom on the row below its vertex: this row is the basis of a blue-0 phantom and the red leg meets the basis inside the phantom. This is also a free row inside the considered red phantom.

We may also have a blue signal alone: this is the case of a free row of the red phantom, neither close to its vertex nor to its basis.

This gives us 10 patterns for each laterality of the leg.

Case 3

In this case, the red leg meets an isocline 5. If we have the leg of a red triangle T and a red basis of a triangle R, the basis is covered, as required. Now, the vertex and the basis of R are generated by a blue-0 triangle. As the leg of T cannot be inside T which belongs to a bigger generation than that of R, there is also a horizontal blue signal. Accordingly, we have a signal $b\xi_2 r\xi$.

If the leg of T meets the basis of a red phantom P, the vertex and the basis of P are also generated by a blue-0 triangle. And so, we have a blue signal on channel 1. Now, the vertex of T generates a tower of phantoms and so, if the generation of T is at least 3, the legs of T meet a red phantom of generation 1 inside this phantom and so, we have only the blue signal in channel 1. This happens whatever the status of T is.

Consider the case when T is a phantom. If the red basis belongs to a phantom, the just previous paragraph applies: we may have a blue signal alone or a blue one with a red one. If the red basis belongs to a triangle R and if there is no red signal, this would require that T is raised inside R, which is impossible as R belongs to generation 1. And so, we have the conclusions of the table: only a signal $b\xi_2 r\xi$ for the basis of a triangle and both $b\xi_2$ and $b\xi_2 r\xi$ for the basis of a phantom.

Case 7

In this case, the leg of our red trilateral T meets an isocline 15. The discussion which we had in the case of a blue leg also applies here exactly the same way, see Fig. 33 too. And so, we have $6 + 6$ patterns when T is a triangle and $8 + 6$ of them when T is a phantom, as indicated by the representation of the possible cases in the table. In both cases, the laterality of the leg is fixed.

For the counting of the prototiles, we obtain $1172 \times 3 = 3516$ prototiles. Indeed, the legs meet three possible tiles of the mantilla only, these tiles being fixed by the laterality of the leg which is taken into account in the final counting of the table.

Case $C_{2,2}$

This case concerns the meeting of a leg of a trilateral with a basis at its mid-point. As for the vertices, we can define an elementary signal to represent this part of the leg when the first half changes to the second one. We take the same representation of the legs as for the vertices. But now, we use a left- and a right-hand side masks. The signal is $\mu_\ell(L_2\gamma\sigma\xi) + \mu_r(L_1\gamma\sigma\xi)$. Fig. 34 illustrates the application of these operators. However, as previously, the information from the horizontal channels is taken from the part of the tile which is on the opposite side with respect to the laterality of the leg.

According to Algorithm 2, the basis must have the green signal, excepted for triangles of generation 0 which have their mid-distance line on an isocline 5.

Now, we are always in a trilateral. As we are on the mid-distance line of the trilateral, we are on a free row, whatever the colour and the status of the trilateral. Accordingly, this means that in a triangle we have no signal of the colour of the leg on channel 1. Now, from the study of the circumvention technique, we know that this is also the case for a phantom as the mid-distance line is a free row. However, channel 5 always contains the signal of a basis whose colour is opposite to that of the leg in a triangle but free in a phantom.

We display the description and the counting in Table 22 which is organized as Table 21.

We start our study with a blue-0 triangle.

In this case, the mid-point occurs on the first isocline 5 which is met by the leg from its root. This corresponds to the situation described in case 3 . The basis is red and it may be open or covered. Indeed, the basis is open if the corresponding trilateral of generation 1 exists. If it does not exist at this place, it exists somewhere else in the same latitude from Lemma 5.2. And so, the basis is covered. Note that both lateralities of the red signal may occur, of course not on the same tile. This gives the number of tiles indicated by the table.

Next, we look at the case of a blue-0 phantom. This case is different from the previous one as now, the mid-point of the leg occur on an isocline 15 in the meeting with a green signal. The difference of behaviour of the green signal which may or may not cross the leg is taken into account by the multiplicative coefficient which represents the different situations of the phantom: alone, with an orange signal, or a lateral blue signal or both signals.

Consider that the leg is in case 4 , which corresponds to the meeting of a blue basis accompanied by a green signal and a yellow one. This means that the phantom is contained in a red triangle. In this case, the basis is open as the triangle exists, due to the yellow signal. And so, we have a single case for each kind of basis.

Now, consider that the leg is in case 5 , which corresponds to the meeting of a red basis accompanied by a green signal. If the trilateral exists, the basis is open, otherwise, it is covered. And so, we have three cases for each kind of basis.

Eventually, we are in case 6 , where the colour of channel 5 is opposite to that of channel 1, if present. As channel 1 must be red if it is present, then, channel 5 is blue. This situation is possible: the phantom is in between two red triangles of a smaller generation with respect to that of the generation of the blue basis.

Table 22
The case $c_{2,2}$; the counting of the prototiles for the crossing of bases at the mid-point of a leg

Cases	3	4	5	6	Total
Isocline	5	15	15	15	Total
$b_0\tau$, 2	$\epsilon, r\xi_2+\epsilon, r\xi_2$				
	$3+3$	0	0	0	12
$b_0\varphi$, 18		$\epsilon+\epsilon$	$\epsilon, r\xi_2+\epsilon, r\xi_2$	$\overline{\gamma}\sigma, r\xi_2+\overline{\gamma}\sigma, r\xi_2$	
	0	$1+1$	$3+3$	$6+6$	360
$b\tau$, 2			$\epsilon, r\xi_2+\epsilon, r\xi_2$	$\epsilon+\epsilon$	
	0	0	$3+3$	$1+1$	16
$b\varphi$, 18		$\epsilon+\epsilon$	$\epsilon, r\xi_2+\epsilon, r\xi_2$	$\overline{\gamma}\sigma \mid r\xi_2+b\sigma$	
	0	$1+1$	$3+3$	$4+4$	288
$r\tau$, 2		$\epsilon, b\xi_2+\epsilon, b\xi_2$			
	0	$3+3$	0	0	12
$r\varphi$, 18		$\epsilon, b\xi_2+\epsilon, b\xi_2$	$\epsilon+\epsilon$	$\overline{\gamma}\sigma \mid b\xi_2+r\sigma$	
	0	$4+4$	$1+1$	$4+4$	324
Total:					1012

The situation with no signal in channel 1 is possible: consider the basis of a trilateral of a generation at least 2. Then, there are a lot of blue-0 phantoms whose mid-distance line is this basis. We may assume that the corresponding trilateral exists and so, the basis is open. As it is inside a blue-0 phantom, there is no blue signal on channel 1.

This time, we turn to the case of a blue trilateral T.

In this case, the meeting happens on an isocline 15.

If T is a triangle, we necessarily have a red signal along the mid-distance line, together with a green signal and no yellow signal as the triangle is blue. So, we are in case 5 or in case 6.

In case 5 , the basis is open if the corresponding trilateral exists, otherwise it is covered.

In case 6 , we are in the case of no accompanying signal or when the colours of the signals in channels 1 and 5 are opposite. In the first case, we have the mid-distance line of a blue triangle which generates the basis of an existing red trilateral: the basis is open. If the basis is blue and if there is no accompanying signal besides the green one, then we are on line 0 of the infinite tower of the butterfly model. But in this case, we know that this line is never crossed by a triangle. And so, this case is ruled out. In the second case, when there is a signal in channel 1, the signal cannot be blue: it is red. This forces the basis to be blue: impossible for a blue triangle. And so, we have two patterns: no accompanying signal and a red basis of a triangle, or a phantom.

If T is a phantom, cases 4 , 5 and 6 are all possible.

Consider case 4 . The basis is blue and accompanied by both a green and a yellow signal. The basis must be open as it is blue, from the circumvention technique, and so there is a single case for each possible status of the basis.

In case 5 , channel 5 is red and channel 1 is empty or red: this depends on whether the basis is open or not.

Case 6 is possible. If channel 1 contains a signal, it is red and so the basis is blue. The phantom which the legs belong to is in between two consecutive red triangles of a bigger generation, within a common isocline. If there is no signal, the basis may be red or blue and it is open, which is also possible: the mid-distance line of a tower of phantoms is always the basis of a trilateral. This gives us 4 cases if channel 1 is empty: $\overline{\gamma}\sigma$ is free. If channel 1 is red, the basis is blue, but the laterality of the channel is free as the status of the basis. And so, this gives 4 cases again.

Now, we discuss the situation for the leg of a red trilateral T.

Consider the case when T is a red triangle.

This time, case 5 is ruled out for a red triangle.

In case 4 , typically, we are in a red triangle which exists, thanks to the yellow signal. Moreover, the blue basis may be open or covered, depending on the existence or not of the corresponding trilateral. And so, we have 6 cases.

Case 6 with no accompanying signal is ruled out: a red basis is impossible and a blue one requires a yellow signal which is case 4 . Now, case 6 with opposite colours in channels 1 and 5 requires a blue signal in channel 1, and so a red basis: but this is impossible with a triangle. Accordingly, this case is impossible.

Consider the case when T is a red phantom.

This time, all cases are possible with an isocline 15 and a green signal.

In case 4 , the basis is blue and it is open or covered. All these cases are possible: inside a tower of phantoms whose mid-distance line is a basis of an existing blue trilateral, there is no signal on channel 1. Now, if T is a red phantom of the generation $2n+1$ whose mid-distance line is the basis of two consecutive blue triangles of the generation $2n+2$, then the legs of T are crossed by a horizontal blue signal which is stopped by a blue phantom of the generation $2n$ which is necessarily present inside T.

In case 5 , the basis is red and it is necessarily open: a red signal cannot cross the legs of T due to Lemma 5.1.

In case 6 , the case with no accompanying signal also gives rise to the possibilities defined by $\overline{\gamma}\sigma$: the same argument with a tower of phantoms works, as in the case of a blue phantom. If there is a signal in channel 1, it is blue and so, the basis is red. The tile is on the basis of an existing red trilateral, in between two consecutive blue triangles of the same latitude which generate this red basis; hence the indications of the table.

Table 23
The case $C_{3,2}$: the counting of the prototiles for the crossing of bases with the second half of a leg of a trilateral

Cases	1	2	3	7	Total
Isocline	0, 10	0, 10	5	15	Total
$b\tau$, 2	$yb\xi + yb\xi$	$b\xi, b\xi r\xi_2 + b\xi, b\xi r\xi_2$	$b\xi r\xi_2$	$b\xi r\xi_2 \mid b\xi r\xi_2$	
	$1+1$	$3+3$	2	$(2+2)\times 2$	36
$b\varphi$, 2	$yb\xi + yb\xi$	$b\xi, b\xi r\xi_2 + b\xi, b\xi r\xi_2$	$b\xi r\xi_2$	$b\xi r\xi_2 \mid b\xi r\xi_2$	
	$1+1$	$3+3$	2	$(2+2)\times 2$	36
$r\tau$, 2	$yb\xi_2 + yb\xi_2$	$b\xi_2 r\xi + b\xi_2 r\xi$	$b\xi_2 r\xi + b\xi_2 r\xi$	$b\xi_2 r\xi \mid b\xi_2 r\xi$	
	$2+2$	$2+2$	4	$(2+2)\times 2$	40
$r\varphi$, 6		$b\xi_2, b\xi_2 r\xi + b\xi_2, b\xi_2 r\xi$	$b\xi_2 r\xi + b\xi_2 r\xi$	$b\xi_2 r\xi \mid b\xi_2 r\xi$	
	0	$4+4$	4	$(2+2)\times 2$	120
Total:					232

NOTE: The factor 2 in the counting of case 7 refers to the two possible statuses of the basis of the colour $\overline{\gamma}$.

The computations performed by the table give us 1012 patterns. Again, as we are on a leg of a trilateral, three tiles of the mantilla are used for each laterality. As the laterality is already counted, we have $1012 \times 3 = 3036$ prototiles.

Case $C_{3,2}$

This case concerns the crossing of the second half of a leg with bases.

We have a discussion which is very similar to the case $C_{1,2}$. However, the case is simpler as we have an important new constraint, namely the constraint c_4: the second half of a leg meets covered bases only.

Here also, we organize the discussion according to the cases of Table 16. Now, as in the case of Table 21, cases 4 , 5 and 6 are ruled out as they all contain a green signal: the meeting with this signal is impossible in the second half of a leg as well as it was impossible in the first half. Also, as in the case of the first half, blue-0 trilaterals are ruled out from this discussion, for the same reason.

With respect to the case $C_{1,2}$ we have another simplification: the orange signal does not occur along the second half of a leg of a phantom. For the same reason, there cannot be a lateral blue signal climbing along the second half of a leg: this may happen with the first half only. We remain with the possibility of a lateral red signal climbing along the second half of a leg of a red phantom: this gives 3 possibilities for each laterality of the leg. This situation is taken into account by the multiplicative coefficient in the first column of Table 23, as we did for Table 21, with the same conventions on the representation of the content of channel 1.

Table 23 displays the different cases and their counting.

First, we look at the case of a leg of a blue trilateral T.

In case 1, the case with no signal on channel 1 is ruled out by the constraint c_4, whatever the status of T. And so, we remain with a single possibility for each kind of basis, knowing that the laterality is fixed.

In case 2, the blue signal in channel 1, with the laterality of the leg, is again mandatory. This signal can be the single one in the channel. Consider a red phantom of the generation $2n+7$. It contains two red triangles of the generation $2n+5$. Call the upper one R_5. It contains two red triangles of the generation $2n+3$, call the lower one R_3. Now, R_3 generates a blue triangle B_4 of the generation $2n+4$ which generates the basis of R_5. Below R_5, there is a triangle of generation 1 which is in between two free rows of P, see the lines c and d of Fig. 32. One of them is an isocline 0: it is above the vertex of the red triangle of generation 1. The other is an isocline 10: it is below its basis. Both isoclines cut the legs of B_4 in their second half as the mid-distance line of B_4 is the basis of R_5. This is an example when the leg belongs to a triangle.

If the leg belongs to a blue phantom, consider again the case of a red phantom P of the generation $2n+5$. Now, we consider its mid-distance line. There is a tower of phantom with the same mid-distance line. One of them belongs to the generation $2n+4$, call it B_4. Now, the free row of P which is just below the mid-distance line cuts the legs of B_4 in the second half and it is an isocline 0, the line c of Fig. 32. A bit further, below the first triangle of generation 1, there is another free row of P, this time an isocline 10, the line d of Fig. 32, which also cuts B_4. And so, we have examples of this situation when the leg belongs to a phantom.

Of course, it is not difficult to imagine situations where the blue signal is also accompanied by a red one: take a blue-0 triangle around a vertex of a red triangle of generation 1, its isocline 10 is accompanied by a red signal outside the triangle. Symmetrically, a blue-O triangle generating the basis of a red triangle of generation 1 provides us with an isocline 0 where the blue signal is also accompanied by a red signal.

In case 3 , we have the case of the meeting of an isocline 5. There is a red basis which is always covered when it meets the leg of T, from the condition c_4. Now, this red signal is also accompanied by a blue one. If there were no blue signal, this would mean that we are inside a trilateral of generation 1. This is possible for the first half of T, not for the second half.

At last, we arrive at case 7 , on an isocline 15.

The colour of the basis is $\overline{\gamma}$ by definition and, from the condition c_4, the basis is covered. Now, from the discussion of the case 7 when we established Table 16, the signal γ is always present in channel 1. Accordingly, we only have the signals $\gamma\xi\overline{\gamma}\xi_2$ when γ is the colour of the leg and $\gamma\xi_2\overline{\gamma}\xi$ when the colour of the leg is $\overline{\gamma}$. In both cases, the status of the basis of the colour $\overline{\gamma}$ is free as the basis is covered. Accordingly, we get 8 possible cases in any case of the leg.

Now, consider the case of a leg of a red trilateral T.

In case 1 , the leg meets a free row of a red triangle. We have the signal $yb\xi_2$, as in the case of the first half of a leg. This crossing is impossible with the leg of a phantom, as in the case of the first half of a leg.

In case 2 , first consider the case when T is a triangle. As the basis is covered, we have the signal $b\xi_2$. Now, as we are not on a free row, otherwise the yellow signal would be there, we also have a red signal. And so, the signal is $b\xi_2 r\xi$, whatever the status of the basis. This gives us 4 patterns only.

When T is a phantom, the basis is also covered and so we have the signal $b\xi_2$. Now, we may be on a free row of the phantom, in which case, $b\xi_2$ is alone, or not, in which case, we also have $r\xi$. This gives us 8 patterns.

In case 3 , the leg meets an isocline 5 on which there is a red signal as the basis is covered. Now, this basis is generated by a triangle of generation 0 which always exists. As we are not inside a trilateral of generation 1 which does not contain any red trilateral, there is also a blue signal. Hence the signal $b\xi_2 r\xi$ whatever the status of T. This gives us 2 patterns in each case.

At last, we arrive at case 7 for which we have the same situation as for a blue trilateral and, consequently, the same number of patterns.

From the table, we can see that this gives us 232 patterns. As only the three tiles of the period on the border of a tree are involved, being in the second half of a leg, we get 696 prototiles.

Case $C_{3,3}$

Now, we arrive at the case of the corners. This is the point where the second halves of the legs meet the basis of their trilateral.

As for the tile for the mid-point of a leg, we can describe the skeleton structure of a corner by an appropriate assembling of basic signals. The elementary pattern is represented in Fig. 34 and it consists in the skeleton signal of the basis, on channel 5 of the tiles, with a colour γ and a status σ. Then, we superpose the skeleton signal of the second half of a leg $L_2\gamma\sigma\xi$, for a corner of the side ξ. However, the superposition is not complete: it goes from the top of the tile until channel 5. The part of the leg going from channel 5 to the bottom of the tile is erased. This can be obtained by an appropriate new mask. There is also a lateral signal $\gamma\xi$ on channel 1 but the signal does not cross the leg: it goes from side 3 of the leg when $\xi = L$, along channel 1, until it meets the leg. When $\xi = R$, it goes from side 7, along channel 1, until it meets the leg.

In the case of a red phantom, then we have $\sigma = \varphi$. The corner, associated to a red phantom, may also bear a lateral red signal which climbs along the leg. When this is the case, the signal travels on a second vertical channel going through the same sides as the signal of the leg. This red lateral signal goes from the top of the tile until the channel 4. Its laterality is independent of that of the corner. With respect to the vertical channel on which the signal of the leg travels, the second vertical channel is in the part of the tile which is outside the phantom.

Now, this elementary pattern can be combined with the signals which travel on the other channels. As known from Section 5, the basis must be open inside the trilateral. This explains why the signal on channel 1 coming from outside the trilateral is stopped by the leg. Remember that when we wait for the meeting of the leg with a basis to form a corner, we look at the side of the basis which is inside the trilateral.

When the basis travels on an isocline 15, which is the general case, it cannot contain a green signal, which rules out cases 4 , 5 and 6 . Accordingly, it meets an orange signal which crosses the leg. The signal has the laterality of the corner.

The discussion is organized in Table 24. It has the same cases as those in the crossing of a second half of a leg with a basis. However, here we have one more colour, as there are also blue-0 corners for blue-0 triangles and blue-0 phantoms.

Consider the case of a blue-0 trilateral.

As the corner of such a trilateral necessarily occurs on an isocline 0 or on an isocline 10, cases 3 and 7 are ruled out.

In case 1 , if we are in a blue-0 triangle, necessarily, it gives rise to a red phantom of generation 1, otherwise, it would raise a red triangle of generation 1, in which case there would be a red signal in place of the yellow one. And there is no other possibility.

If we are in a blue-0 phantom P, we also have the yellow signal only. Indeed, we cannot have the red signal because of the presence of the yellow one. Now, a blue signal cannot be raised inside P, even if there is a vertex of a blue triangle of a positive generation on the mid-distance line of P: the condition c_3 prevents the first half of the leg of the blue triangle from changing channel 1: as the basis was open, it must remain open.

In case 2 , we have no yellow signal.

We may have no signal at all: this happens when the corner of the trilateral is on a free row of a red phantom. In the previous examples, in cases $C_{1,2}$ and $C_{3,2}$, we encountered such situations, see Fig. 32.

In the case of a blue-0 triangle B, we have no blue signal inside B. But we may have a red one on the basis of the corner: this is the case when B generates a red triangle of generation 1. There is no other situation. We also note that, in this case, the laterality of the red signal at the corner of B is that of B. But the red signal can be present for another reason: the case of a latitude of a red triangle at a place where one of them is missing. If B generates a red phantom of generation 1, and if it is on a free row of a red phantom, then there is no red signal at the corners of B.

In the case of a blue-0 phantom P, we may have no signal at all: take the examples when isocline 0 is a free row of a red phantom, as shown in Fig. 32 for instance. There cannot be a blue signal as already seen in case 1 , from the condition c_3. But a red signal is possible when isocline 0 is not a free row in a red phantom.

And so, we have 3 patterns, whatever the status of the blue-0 trilateral.

Table 24
The case $C_{3,3}$: the counting of the prototiles for the corners

Cases	1	2	3	7	Total
Isocline	0, 10	0, 10	5	15	Total
$b_0\tau, 2$	y	$\epsilon, r\xi_2$			
	1	3	0	0	8
$b_0\varphi, 2$	y	$\epsilon, r\xi_2$			
	1	3	0	0	8
$b\tau, 2$				$r\xi_2$	
	0	0	0	2	4
$b\varphi, 2$				$r\xi_2$	
	0	0	0	2	4
$r\tau, 2$			$b\xi_2$	$b\xi_2$	
	0	0	2	2	8
$r\varphi, 6$			$b\xi_2$	$b\xi_2$	
	0	0	2	2	24
Total:					56

NOTE: The factor 2 in the counting of case 7 refers to the two possible statuses of the basis of the colour $\overline{\gamma}$.

Table 25
The counting of the tiles of the mantilla which are inside a tree of the mantilla in the first five isoclines, starting from a seed

Isocline	1	2	3	4		5
Mantilla patterns	3	5	10	18	36	22

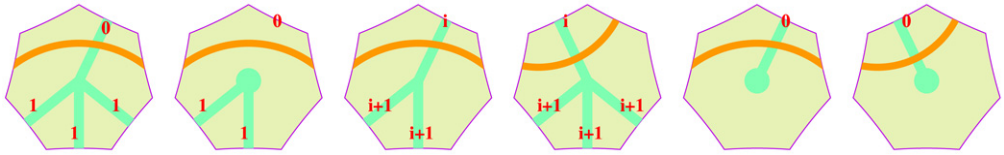

Fig. 35. The elementary patterns for the scent in the passive rows.

Now, consider the case of a blue trilateral. Its basis is necessarily on an isocline 15, and so we have to consider case 7 only. Now, in this case, as the basis must be open, we have the single case $\gamma\sigma$, where γ is the colour which is opposite to the colour of the basis which is $\overline{\gamma}$, here blue.

Accordingly, this represents two patterns per laterality and per kind of trilateral.

Now, we consider the case of a red trilateral.

Only cases 3 and 7 are considered.

In case 3 , there is no red signal as the basis must be open. Now, the red basis is generated by a blue-0 triangle which cannot contain the corner which we consider. And so a blue signal must be present in channel 1, whatever the status of the corner.

In case 7 , the signal of the basis must be red and the basis is open. Accordingly, as the signal γ, here blue, is mandatory, there is a signal $b\xi_2$.

This gives us 56 patterns. Now, the corner is on the border of a tree after the second half of a leg. When the isocline of the basis is an isocline 15, we may have the three possible cases for a tile of a border of a tree in the period of the border. But for isoclines 0, 5 and 10, we always have the same tile. And so, we have to multiply the number of patterns on an isocline 15 by 3. Accordingly, we find 80 prototiles.

Case $C_{4,4}$

At last, we have the case when there is no basis and no leg. Of course, this situation exists. It is the case of isoclines 1..4, 6..9, 11..14 and 16..19. All possible tiles of the mantilla can be met in this case, except the tile of an active seed. Accordingly, the number of prototiles would be $33 \times 16 = 528$.

However, we also have to take into account that the scent may also be dispatched to tiles within these latitudes. And so, the tiles may be crossed by the scent. The needed patterns are illustrated by Fig. 35. However, the number of tiles is not 528×2. Indeed, as already mentioned in the counting of the patterns for a basis, the checking performed with the help of a computer program shows us that not all tiles of the mantilla occur within the first five isoclines below the root. An exact counting of the number of tiles on each isocline is given by Table 25.

From Table 25, we can see that 36 tiles of the mantilla are used for isoclines 1..4. Note that this number takes into account the patterns, the number of the isoclines and the status of the tile. Now, the scent may also be activated on isoclines 5, 10 and 15, so that the same tiles occur on isoclines 6..9, 11..14 and 16..19 when the scent occurs. Accordingly, the number of these prototiles is $36 \times 4 = 144$. Appended to the 528 prototiles which are used when there is no scent, we get 672 prototiles.

Table 26
Counting of the prototiles by summing the partial totals of the previous tables

	Vertex	Plain	Corner	Empty
First half	92	3516	0	2220
Mid-point	0	3036	0	0
Second half	0	696	80	592
None	0	7080	0	672
Final account:				17,984

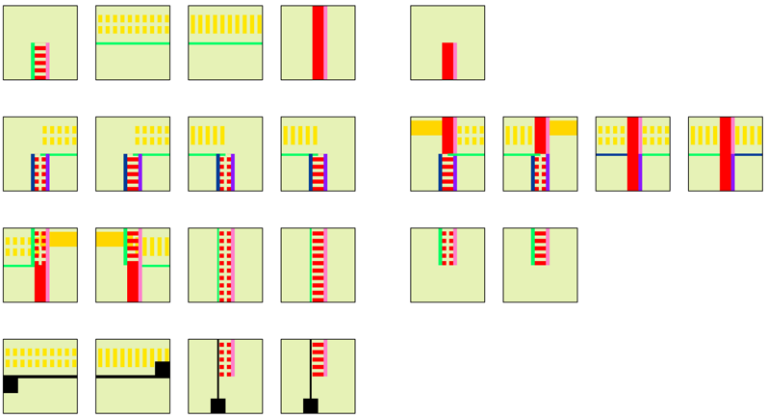

Fig. 36. The computing tiles.

Now, we are in a position to count the total number of prototiles which are needed for the construction. For this purpose, we again use Table 14, in which we replace the YES/NO indications by numbers. Of course, NO is replaced by 0. We replace YES by the number of prototiles which we found for the corresponding case.

Accordingly, looking at Table 26, we find that we need 17,984 prototiles for the construction.

6.2.2. The meta-tiles

Now, we turn to the description of the meta-tiles which are the tiles needed for the simulation of the computation of a Turing machine. This part of the description corresponds to the sub-section devoted to the computing areas.

Fig. 36 illustrates these tiles which we call meta-tiles as they are **variables**, which is not the case for prototiles which are constant. Indeed, the actual prototiles depend on the particular Turing machine whose execution is simulated by the tiling. For convenience, in the following explanations, we denote the tiles by two numbers as follows: *a*-*b*, where *a* and *b* are the numbers of the row and the column respectively, where the tile stands in the figure.

The set of meta-tiles can be split into four groups of tiles, corresponding to the rows of Fig. 36. In the first row, we have the tiles used to convey the information. In the second row, we can see the tiles used to perform an instruction. In the third row, we have the tiles which transmit the new information after performing an instruction. In the fourth row, we have the tiles for the halting of the machine.

We remind the reader of the fact that the tape of the simulated Turing machine is placed on the border of the tree on the tiles where the border meets a free row of the concerned red triangles. The history of each square of the tape is represented by the verticals which run along a ray of **8**-centres which is the closest to the initial tile representing this square. The execution itself is materialized by what we call the **computing signal**. It is a signal which first conveys the current state of the Turing machine. The signal travels on the horizontals of the grid, materialized by the yellow rows of the red triangle where the simulation occurs. It also travels on the verticals which we have just mentioned. An instruction is performed when the computing signal, travelling on a horizontal, meets a vertical. The tile which is placed at this intersection, one of the tiles 2-1..2-8, represents all the data of the instruction: the current content of the tape which arrives from the top of the tile, and the current state of the Turing machine which is conveyed by the computing signal and which arrives on a side of the tile crossed by the isocline on which the tile stands. The exact side is determined by the motion of the head which is represented on the horizontal by a lateral yellow signal which replaces the standard unilateral yellow signal for this part of the row. A right-hand side yellow signal indicates a motion to the right and a left-hand side yellow signal indicates a motion to the left. A lateral yellow signal enters the tile from the side of the opposite laterality.

The other part of a tile representing the execution of an instruction contains all the information of the output of the instruction: the new state of the machine which is now conveyed by the computing signal, the new content of the square which is transmitted by the same vertical, and the new move of the head.

If the move is the same as the previous one and if the computing signal has not reached the border of the tree yet, the computing signal goes on on the same isocline. This situation is represented by the tiles 2-7 and 2-8. If the move is the same, but the instruction tile is on the border of the tree, we use the tiles 2-1 and 2-4.

If the move is the opposite, and, without loss of generality, we may assume that we only have a move to the left or a move to the right, then the computing signal goes down along the vertical, using the tiles 2-5 and 2-6, or the tiles 2-2 and 2-3 if the execution of the instruction happens on the border of the tree. Note that when the move is the same but the instruction is executed on the border, the computing signal also goes down along the vertical, which is clear from the tiles 2-1 and 2-4 used in this case.

The computing signal goes down until the next free row is met. During this travel, it conveys two pieces of information: the state of the Turing machine and the move of the head to perform the next instruction. Remember that the new content of the square is conveyed by the vertical only. The move to be performed is represented by a vertical lateral signal on the vertical portions of the path followed by the computing signal and by the horizontal lateral yellow signal on the horizontal parts. The laterality of the signal is that of the move dictated by the instruction last performed.

When the next free row is met, the new content goes on along the vertical which again becomes unilateral, see the tiles 3-1 and 3-2. The vertical signal goes on conveying the new content of the square, using the tile 1-4. But the new state now travels on the new free row. On the new row, a lateral yellow signal replaces the unilateral yellow signal. The laterality of the new yellow signal is that of the move, which is indicated by the laterality of the upper part of the vertical signal of the tiles 3-1 or 3-2. The side through which the computing signal exits has the laterality of the yellow signal, again see the tiles 3-1 and 3-2. On the new free row, the computing signal goes on its way, using the tile 1-2 or 1-3, depending on the direction of its move.

There are two ways to stop this simulation. The first way is that the machine calls its final state, which triggers the abutting of one of the tiles 4-1..4-4 on the instruction tile. As the tiles cannot be completely rotated, any tile from the tiles 4-1..4-4 blocks the construction of the tiling. The second way is that the halting state is not reached by the execution of the Turing machine program but the basis of the triangle is met by the computing signal travelling on a vertical. This situation is represented by the tiles 3-5 and 3-6. We shall say that the computation is interrupted.

Before turning to the precise description of the tiles and their counting, let us formulate two remarks. First, the tiles which we consider now are superposed with tiles of the mantilla, exactly as for what we saw with the prototiles. Secondly, they are also superposed with the prototiles which we have seen but, in some cases, they replace the prototiles. There is a simple rule to define this situation: the vertical signals are superposed on the signals of the prototiles. For the horizontal signals, the signal of the current state is superposed but the motion signal, a lateral yellow signal, replaces the yellow signal of the concerned prototiles.

Note that not all prototiles are concerned with the computing signal. Basically, the basis signals containing the yellow signal are concerned together with the three tiles used for the border of a sector, following a ray of **8**-centres. Of course, the beginning part of a vertical belongs to an aperiodic part of the vertical. But very few tiles are involved with this process and they mainly concern the tiles 1-5 and 2-1..2-4.

The counting of the tiles is displayed by Table 27. We consider the main groups which are attached to the rows of Fig. 36.

Let us start with the first row of Fig. 36.

The first tile is 1-1, which deals with the vertex of a red triangle. Looking at Table 20, there are 3 cases of red vertices on an isocline 5 and also 3 of them on an isocline 15, which makes 6 meta-tiles. Note that this tile can be considered as a prototile: we may assume that the Turing machine always starts its computation in state 1 with a move to the right and, by assumption, it is on an empty square of the tape. We also may assume that the Turing machine always puts the symbol 1 in this square but this is already not relevant to our purpose.

Next, we have the meta-tiles 1-2 and 1-3 which convey the current state on a horizontal. This time, we have to know how many patterns are concerned with a yellow signal. For the plain bases, which is our case, Table 16 indicates that there are 16 possible patterns. Now, any tile of the mantilla can be considered. Moreover, on the fifth isocline after a seed, 22 tiles may receive the scent or not. This gives us 1760 meta-tiles. Note that we find the same counting for the tiles 4-1 and 4-2 for the same reason: they stand on a yellow row.

At this point, we can divide the number of these meta-tiles by 2 by noticing that for a half of the 16 patterns accompanying the yellow signal, these patterns involve an isocline 15. Now, from Lemma 3.4, in a red triangle, there is a single yellow row on an isocline 15, which is negligible in comparison with the 2^n others in a red triangle of the generation $2n+1$. And so, we decide that the computing signal will not travel on a yellow row when this row is accompanied by the green signal. Accordingly, this gives us 880 meta-tiles of the types 1-2 and 1-3; so does it for the types 4-1 and 4-2.

Then we have the tile 1-4.

The copies of the tile travel on a vertical. And so, basically, they use 3 tiles of the mantilla, but they can meet any isocline, which we count in the patterns. This makes 60 meta-tiles. Note that this tile is not affected by the scent. This could happen from the vertex of a red triangle. However, the vertex makes use of the tile 1-1 which calls the tile 3-4 until the next yellow row is found. This exceeds the number of isoclines crossed by the scent along a vertical, as a vertical does not meet the border of an inner tree. However, the tile may be affected by the irregular part of a vertical. This happens with the tile 1-5 but, depending on the isocline which crosses the tile 1-5, the following tile 1-4 may fall in the aperiodic part again. In fact, 4 tiles are concerned with this aperiodic part: the tile $1\overline{2}\overline{2}\circ b$ when the vertical starts from a tile $11\circ 2b$, the tiles $47\circ 7w$ and $6\circ 77w$ when it starts from a tile G_r. The period is immediately reached after the first tile when the vertical starts from a

Table 27
Organization of the counting of the meta-tiles

Tiles	Coef	Patterns	Mantilla	Scent	Total
1-1	1	V, 6	1	1	6
1-2, 1-3	2	Y, 8	33	2	880
1-4	1	p, 16	3	1	$48 + 18$
1-4	1	B, 244	3	1	732
1-5	1	Y, 8	6	1	48
2-1..2-4	4	Y, 8	3	1	96
2-5..2-8	4	Y, 8	3	1	96
3-1, 3-2	2	Y, 8	3	1	48
3-3, 3-4	2	p, 16	3	1	$96 + 52$
3-3, 3-4	2	B, 244	3	1	732
3-5, 3-6	2	B, 11	3	1	66
4-1, 4-2	2	Y, 8	33	2	880
4-3, 4-4	2	iso, 2	3	1	12
Total:					3810

tile $1 \circ 15b$. This comes from the study of Section 6.1 and it concerns the right-hand side border of a tree. Note that we have a symmetric situation on the left-hand side border. Accordingly, we have 6 patterns but the concerned isoclines may be any of the usual isoclines 0, 10 and 15 as there is no yellow row on an isocline 5. And so, we have 18 more meta-tiles, which makes 78 meta-tiles.

Now, when the tile 1-4 crosses an isocline 0,5, 10 or 15, it crosses a plain basis and, inside a big enough red triangle, it may be any basis among the patterns which are defined by Table 16. And so, taking into account that these different patterns contain the different cases of isoclines met by the tile, we get 732 new meta-tiles. Note that this counting again contains 12 tiles of the 60 ones which we have already counted with all the isoclines: those which are on an isocline 0, 5, 10 or 15.

Next, we arrive at the tile 1-5.

The copies of this tile occurs on the border of the tree at an intersection with a yellow row. This tile is the starting point of a vertical which does not receive the visit of the computing signal. Accordingly, we have the 8 patterns associated with a yellow row but, at the same time, as we are on the border of a tree of the mantilla, only 3 tiles are concerned for each border. Moreover, the scent does not reach such a tile. Accordingly, this gives us $8 \times 6 = 48$ tiles.

This time, we deal with the second row of Fig. 36.

First, we have the tiles 2-1..2-4 which describe the execution of an instruction when the head of the Turing machine arrives at a square for the first time. This is why the execution happens on the border of the tree. Accordingly, the counting of the tiles 2-1..2-4 is the same as that of the tile 1-5, as they happen at the same place. Now, as the tiles take into account which border of the tree is concerned, we only have to take 3 tiles of the mantilla into account. This defines 96 meta-tiles.

The tiles 2-5..2-8 deal with the standard execution of an instruction. This happens on a free row, and again 3 tiles of the mantilla are concerned. But they are not the same 3 tiles as in the previous case. Here, the three tiles are those which define a ray of **8**-centres. Accordingly, this again gives us 96 meta-tiles.

Now, we consider the tiles of the third row of Fig. 36.

The first two tiles of the row, the tiles 3-1 and 3-2, are also connected with the execution of an instruction: they concern the moment when the computing signal reaches a new free row where it will look for the expected vertical of the next square of the tape to be visited. The counting is exactly the same as before. As two tiles only are concerned, this gives 48 meta-tiles.

We now have to deal with the tiles 3-3 and 3-4. Here, the discussion is close to that on the tile 1-4. We have the same counting for the crossing with the basis and for the 16 passive rows of the mantilla, which gives us $96 + 732 = 828$ meta-tiles. The aperiodic part of the verticals initiated by the tiles 2-1..2-4 or by the vertex 1-1 gives us 18 new meta-tiles. But here, we have to take into account that the tiles coming from the vertex receive the scent. This gives exactly 4 new tiles and, as the vertex itself may be on any isocline 5 or 15, this gives 8 meta-tiles to append to the counting. And so, for these tiles, we get $828 + 2 \times (18 + 8) = 880$ meta-tiles.

At last, we arrive at the tiles 3-5 and 3-6. These tiles correspond to the interruption of the computation when meeting the basis of the red triangle. As we are inside the triangle, the basis is necessarily open. Now, on isocline 15, it may be accompanied by a green signal or by an orange one and, this time, the meeting with a join-tile is possible. We also have the possibility of an open red basis on isocline 5 where there are neither green nor orange signals. Looking at Table 16, we find 1 case with a green signal, 6 cases with an orange one and 4 cases for a red basis on an isocline 5, as a blue join-pattern is possible. Again, three tiles of the mantilla are possible, as we are on a vertical. This gives us 66 new meta-tiles.

At last, we consider the tiles of the fourth row of Fig. 36. These tiles deal with the halting of the Turing machine.

First, we have the case of a halting within a free row by the tiles 4-1 and 4-2. The counting is exactly the same as for the tiles 1-2 and 1-3 and so, we get 880 meta-tiles.

Then, we have the case of a halting on a vertical: this is the case when the halting occurs on a change of direction of the head of the Turing machine. This situation is implemented by the tiles 4-3 and 4-4. Now, by their constitution, as the concerned execution of the halting instruction occurs on an isocline 0 or 10, the tiles 4-3 and 4-4 occur on an isocline 1 or 11.

There is no basis on these isoclines and we only have to take into account the number of the isocline and the pattern of the tile of the mantilla. As we are on a vertical, there are three of them only. And so, we find 12 meta-tiles.

And so, we find exactly 3810 meta-tiles.

However, this number does not give us the exact number of prototiles which we need when we know the program of the Turing machine. The actual number depends on the number s of symbols on the tape of the Turing machine and on the number q of states of the Turing machine. Here, we assume that the number of symbols contains the blank but that the halting state is not taken into account in the number of states, as usual.

From this point of view, the tiles of Fig. 36 contain tiles with only a signal for the symbol on the tape, for example the tile 1-4, and tiles with only a signal for the state of the head, for instance the tile 1-2. Now, many tiles contain both symbols. If we consider the tiles of the second row of the figure, these tiles correspond exactly to the instructions of the Turing machine. But the number I of these instructions is not necessarily $q \times s$. In fact, we have $I \leq q \times s$. Now, a few tiles also depend on another parameter: the tiles of the third row only contain an entry of the table of the Turing machine: they contain the new symbol, the new state and the move to be performed by the head of the Turing machine. Now, the number X of different entries of the table is not necessarily the same as the number of instructions of the Turing machine. We simply have that $X \leq I$.

Let us count the number of tiles of each category:

- tiles depending on q only: 1-2 and 1-3 and so, 880 tiles;
- tiles depending on s only: 1-4, 1-5 and 4-3, 4-4 and so, 858 tiles;
- tiles depending on I only: 2-1..2-8 and so, 192 tiles;
- tiles depending on X only: 3-1..3-6 and so, 994 tiles;
- prototiles: 1-1, 4-1, 4-2 and so, 886 tiles.

This allows us to state the following result, taking into account the prototiles which we have counted in Section 6.2.1:

Proposition 6. *Let M be a Turing machine which starts its computation from an empty tape in state* 1*, goes to to the right and writes* 1 *on its first scanned cell. Denote the number of states of M by q, the number of its tape symbols by s, the number of its instructions by I and the number of different outputs produced by its instructions by X. Then, the set of tiles described in Section* 6.2.1 *defines* $858 \times s + 880 \times q + 192 \times I + 994 \times X + 18{,}870$ *prototiles.*

This completes the proof of Theorem 1.1.

7. A few corollaries for connected tiling problems

The construction leading to the proof of Theorem 1.1 allows to get a few results along the same line of problems.

As indicated in [3,4], there is a connection between the general tiling problem and the **Heesch number** of a tiling. This number is defined as the maximum number of **coronas** of a disc which can be formed with the tiles of a given set of tiles, see [11] for more information. As indicated in [4], and as our construction fits in the case of domino tilings, we have the following corollary of Theorem 1.1.

Theorem 7. *There is no computable function which bounds the Heesch number for the tilings of the hyperbolic plane.*

The construction of [15,17] gives the following result, see [19,23].

Theorem 8. *The finite tiling problem is undecidable for the hyperbolic plane.*

Indeed, when the Turing machine halts, the halting state triggers a signal which encloses the computation area and which compels the tiling to be completed by blank tiles only, see [23].

Combining the construction proving Theorem 8 and the partition theorem which is proved in [24], Chapter 4, Section 4.5.2 about the splitting of Fibonacci patchworks, also see [14], the construction of this paper allows us to establish the following result, see [20].

Theorem 9. *The periodic tiling problem is undecidable for the hyperbolic plane, also in its domino version.*

Note that the analog of Theorem 9 for the Euclidean plane was proved by Gurevich and Koriakov, see [5].

In the statement of Theorem 9, **periodic** means that there is a shift which leaves the tiling globally invariant. The construction mimics that of Theorem 8 in the fact that if the simulated Turing machine halts, we also enclose the computing area. But this time, we enlarge the notion of computing area and of triangles so as to also permit black trees to support interwoven triangles. In this way, we can define areas of the kind defined by Fibonacci patchworks and of the size dictated by the halting of the machine. We define colours for these surrounding signals in such a way that they entail a construction of a scaled Fibonacci tree, see [27]. Next, it is not difficult to construct a tiling of the hyperbolic plane in this way, periodically, applying the shifts already mentioned in [24], Chapter 4, Section 4.5.3, also see [14].

At last, in another direction, we may apply the arguments of Hanf and Myers, see [6,28], and prove the following result, see [18].

Theorem 10. *There is a finite set of tiles such that it generates only non-recursive tilings of the hyperbolic plane.*

The proof makes use of the construction of two incomparable recursively enumerable sets A and B of integers. The set of tiles defines the computation of these sets by a Turing machine. Moreover, the set of tiles tiles the plane if and only if there is a set to separate A from B. As such a set cannot be constructed by an algorithm, we obtain the result stated in Theorem 10.

7.1. Temporary conclusion

It seems to me that the construction of Section 5.1 could be applied to prove undecidability problems on cellular automata. Of course, the halting problem for cellular automata is undecidable, but this is a simple consequence of the undecidability of the same problem for Turing machines.

In fact, it is interesting to notice that the construction of Section 5.1 which is based on Algorithm 2 can be performed by a cellular automaton.

The working of the automaton could be devised as follows.

We consider that the automaton works on three layers. On the first one, it tries to construct the tiling. The initial configuration of this layer is a blank plane, except at a tile called central, which is an active seed. On the second layer, the cellular automaton updates a ball around the central tile which coincides with that of the first layer. The third layer is a 'working sheet' for intermediate computations performed by the automaton.

It is plain that if the Turing machine implemented in the set of tiles does not halt, the cellular automaton will tile the plane in infinite time. If the Turing machine halts, the cellular automaton will take notice that the construction has stopped at some point.

A last consequence of the construction of Section 5.1 leads us back to hyperbolic geometry.

Let us look at the lifting of the abstract brackets to the interwoven triangles. At first glance, this seems to be a Euclidean construction. Moreover, a whole sub-section is devoted to the Euclidean implementation of the interwoven triangles. The goal of the next sub-section is to prove that this construction can be transferred to the hyperbolic plane. It seems to me that the fact that this transfer is possible has an important meaning. From my humble point of view, it means that a construction which seems to be purely Euclidean has indeed a purely combinatoric character. It belongs to absolute geometry and it mainly requires Archimedes' axiom. Note that absolute geometry itself has no pure model. A realization is necessarily either Euclidean or hyperbolic. To conclude with this, we suggest that probably the extent of absolute geometry is somehow underestimated.

Acknowledgements

I am very pleased to acknowledge the interest of several colleagues and friends in the main result of this paper. Let me especially thank André Barbé, Jean-Paul Delahaye, Chaim Goodman-Strauss, Serge Grigorieff, Yuri Gurevich, Tero Harju, Oscar Ibarra, Hermann Maurer, Gheorghe Păun, Grzegorz Rozenberg and Klaus Sutner. I am specially in debt to Professor Chaim Goodman-Strauss for most valuable comments to improve the presentation of the proof.

References

[1] R. Berger, The undecidability of the domino problem, Memoirs of the American Mathematical Society 66 (1966) 1–72.
[2] K. Chelghoum, M. Margenstern, B. Martin, I. Pecci, Cellular automata in the hyperbolic plane: Proposal for a new environment, in: Lecture Notes in Computer Sciences, vol. 3305, 2004, pp. 678–687. Proceedings of ACRI'2004, Amsterdam, October, 25–27, 2004.
[3] Ch. Goodman-Strauss, A strongly aperiodic set of tiles in the hyperbolic plane, Inventiones Mathematicae 159 (1) (2005) 119–132.
[4] Ch. Goodman-Strauss, Growth, aperiodicity and undecidability, Invited Address at the AMS Meeting at Davidson, NC, March, 3–4, 2007.
[5] Yu. Gurevich, I. Koriakov, A remark on Berger's paper on the domino problem, Siberian Mathematical Journal 13 (1972) 459–463.
[6] W. Hanf, Nonrecursive tilings of the plane. I, Journal of Symbolic Logic 39 (1974) 283–285.
[7] J.E. Hopcroft, R. Motwani, J.D. Ullman, Introduction to Automata Theory, Languages, and Computation, Addison Wesley, Boston, San Francisco, New York, 2001.
[8] J. Kari, A new undecidability proof of the tiling problem: The tiling problem is undecidable both in the Euclidean and in the hyperbolic plane, AMS meeting at Davidson, NC, Special Session on Computational and Combinatorial Aspects of Tilings and Substitutions, March, 3–4, 2007.
[9] J. Kari, The Tiling Problem Revisited, Lecture Notes in Computer Science, vol. 4664, 2007, pp. 72–79.
[10] L.A. Levin, Aperiodic tilings: Breaking translational symmetry, The Computer Journal 48 (6) (2005) 642–645.
[11] C. Mann, Heesch's tiling problem, American Mathematical Monthly 111 (6) (2004) 509–517.
[12] M. Margenstern, New tools for cellular automata of the hyperbolic plane, Journal of Universal Computer Science 6 (12) (2000) 1226–1252.
[13] M. Margenstern, Cellular automata and combinatoric tilings in hyperbolic spaces, a survey, in: Lecture Notes in Computer Sciences, vol. 2731, 2003, pp. 48–72.
[14] M. Margenstern, A new way to implement cellular automata on the penta- and heptagrids, Journal of Cellular Automata 1 (1) (2006) 1–24.
[15] M. Margenstern, About the domino problem in the hyperbolic plane from an algorithmic point of view. arXiv:cs.CG/0603093 v1, 2006, 11p.
[16] M. Margenstern, About the domino problem in the hyperbolic plane, a new solution. arXiv:cs.CG/0701096, 2007, January, 60p.
[17] M. Margenstern, About the domino problem in the hyperbolic plane from an algorithmic point of view, Technical Report, 2006–101, LITA, Université Paul Verlaine – Metz, 2006, 100p. Available at: http://www.lita.sciences.univ-metz.fr/~margens/hyp_dominoes.ps.gzip.
[18] M. Margenstern, About the domino problem in the hyperbolic plane, a new solution, Technical Report, 2007–102, LITA, Université Paul Verlaine – Metz, 2007, 106p. Available at: http://www.lita.sciences.univ-metz.fr/~margens/new_hyp_dominoes.ps.gzip.
[19] M. Margenstern, The finite tiling problem is undecidable in the hyperbolic plane. arXiv:cs.CG/0703147v1, 2007, March, 8p.
[20] M. Margenstern, The periodic domino problem is undecidable in the hyperbolic plane. arXiv:cs.CG/0703153v1, 2007, March, 12p.
[21] M. Margenstern, About the domino problem in the hyperbolic plane, a new solution: Complement. arXiv:0705.0086v4, 2007, May, 20p.
[22] M. Margenstern, The domino problem of the hyperbolic plane is undecidable. arXiv:0706.4161, 2007, June, 18p.
[23] M. Margenstern, The finite tiling problem is undecidable in the hyperbolic plane, in: Workshop on Reachability Problems, RP07, July 2007, Turku, Finland.
[24] M. Margenstern, Cellular Automata in Hyperbolic Spaces, Volume 1, Theory, OCP, Philadelphia, (2007), 422p..
[25] M. Margenstern, The domino problem of the hyperbolic plane is undecidable, Bulletin of the EATCS 93 (2007) 220–237. October.
[26] M. Margenstern, About the domino problem in the hyperbolic plane from an algorithmic point of view, RAIRO-Theoretical Informatics and Applications 42 (1) (2008) 21–36.

[27] M. Margenstern, A uniform and intrinsic proof that there are universal cellular automata in hyperbolic spaces, Journal of Cellular Automata 3 (2) (2008) 157–180.
[28] D. Myers, Nonrecursive tilings of the plane. II, Journal of Symbolic Logic 39 (1974) 286–294.
[29] R.M. Robinson, Undecidability and nonperiodicity for tilings of the plane, Inventiones Mathematicae 12 (1971) 177–209.
[30] R.M. Robinson, Undecidable tiling problems in the hyperbolic plane, Inventiones Mathematicae 44 (1978) 259–264.
[31] A.M. Turing, On computable real numbers, with an application to the Entscheidungsproblem, Proceedings of the London Mathematical Society, Ser. 2 42 (1936) 230–265.
[32] H. Wang Proving, theorems by pattern recognition, Bell System Technical Journal 40 (1961) 1–41.